FORTA CORPORATION
THE FORTA® FAMILY OF FIBERS • EST. 1978
100 FORTA DRIVE • GROVE CITY, PENNSYLVANIA 16127-6399 U.S.A.
LOCAL 724-458-5221 TOLL FREE 1-800-245-0306 FAX 724-458-8331

Cover page to Report # 200903AT101

FORTA Corporation is pleased to offer the following report, "*Evaluation of FORTA Fiber-Reinforced Asphalt Mixtures Using Advanced Material Characterization Tests – Evergreen Drive, Tempe, Arizona.*" produced by Arizona State University. This comprehensive report was published in September 2008.

Since 1999, the Department of Civil and Environmental Engineering at Arizona State University (ASU) has been involved with several major asphalt mixtures characterization studies, research being conducted at the Advanced Pavements Laboratory. These studies include the nationally recognized National Cooperative Highway Research Program (NCHRP) 9-19 project (1), which dealt with the development of Simple Performance Tests (SPT) for permanent deformation and cracking potential evaluation of asphalt mixtures. The results from these advanced tests were utilized as input in the newly developed Mechanistic-Empirical Pavement Design Guide (MEPDG) (flexible pavement program developed at ASU). It is noteworthy that ASU has the largest database of HMA Mix engineering properties in the United States, which includes tests conducted on asphalt mixtures from national and international test sites.

Please note that some information or descriptions in this report have been redacted to preserve trade secrets, or other proprietary information. The redactions are blackened out, and appear like this [redacted]. These occurrences are very limited, and in no way alter any results or conclusions.

Tracy H. Lang
Manager Asphalt
Email: tlang@forta-fi.com

Evaluation of FORTA Fiber-Reinforced Asphalt Mixtures Using Advanced Material Characterization Tests – Evergreen Drive, Tempe, Arizona.

Prepared by

Kamil E. Kaloush, Ph.D., P.E.
Associate Professor

Krishna P. Biligiri, Waleed A. Zeiada, Carolina Rodezno, Smita Dwivedi, Jordan Reed, and Carlos Cary
Graduate Research Associates

Submitted to

FORTA Corporation
100 Forta Drive
Grove City, PA 16127-9990

September 2008

ARIZONA STATE UNIVERSITY

IRA A. FULTON SCHOOL OF ENGINEERING
Department of Civil and Environmental Engineering
Tempe, AZ 85287-5306

Report # 200903AT101

TABLE OF CONTENTS

Page

LIST OF TABLES

Page

LIST OF FIGURES

Page

Acknowledgements

The authors would like to acknowledge the invaluable assistance of many organizations and individuals for the successful completion the project:

- FORTA Corporation: Clifford MacDonald, John Lindh, Jeff Lovett, and George Sadowski; for their technical support through out the project.
- [redacted]: Jorg Willing for his technical support and input.
- City of Tempe engineering department and personnel: John Osgood, Denise Brewer, Toby Crooks and Derik Winkle for their invaluable assistance in providing the field test section at Evergreen Drive and for their help in coordinating the construction activities.
- CEMEX (formally Rinker West, Central Region): Donald Green for his coordination and assistance at the asphalt plant;
- MACTEC: Sam Huddleston and Brian Waterbury for their assistance in extracting the fibers from the asphalt mixture.
- ASU Supervisor of the Advanced Pavement Laboratory, Kenneth Witczak for the production and preparation of the laboratory test specimens; ASU faculty: Professors Matthew W. Witczak and Michael S. Mamlouk; and graduate students: Ravi Kantipudi and Atish Nadkarni.

The authors would like to acknowledge the financial support of FORTA Corporation [redacted]

1. Introduction

1.1. Background

FORTA fibers have been used to improve the performance of asphalt mixtures against permanent deformation and fatigue cracking. Previous outdated laboratory tests have been conducted to demonstrate performance benefits and to optimize the fiber content in the mixture. Recent development in materials characterization tests in the pavement community necessitated the re-evaluation of the FORTA reinforced asphalt mixtures using state-of-the art testing procedures to demonstrate these performance benefits. Figure 1 (a) shows typical FORTA fibers contained in one pound bag (~445 g). The fibers comprise two types: Aramid [redacted] and Polypropylene [redacted] Table 1 shows the main physical properties of both fibers used with Hot Mix Asphalt (HMA).

Since 1999, the Department of Civil and Environmental Engineering at Arizona State University (ASU) has been involved with several major asphalt mixtures characterization studies, research being conducted at the Advanced Pavements Laboratory (Figure 2). These studies include the nationally recognized National Cooperative Highway Research Program (NCHRP) 9-19 project (1), which dealt with the development of Simple Performance Tests (SPT) for permanent deformation and cracking potential evaluation of asphalt mixtures. The results from these advanced tests were utilized as input in the newly developed Mechanistic-Empirical Pavement Design Guide (MEPDG) (flexible pavement program developed at ASU). It is noteworthy that ASU has the largest database of HMA Mix engineering properties in the United States, which includes tests conducted on asphalt mixtures from national and international test sites.

(a)

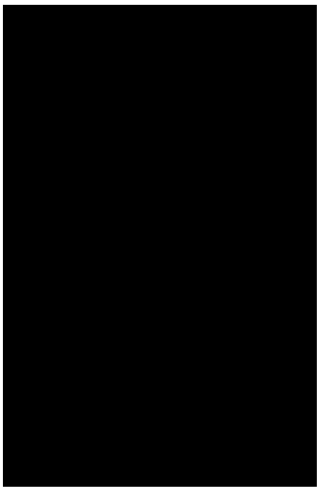

(b)

Figure 1 (a) FORTA Reinforced Fibers, (b) Separated FORTA Fibers – Aramid [redacted] and Polypropylene [redacted]

Table 1 Physical Characteristics of the FORTA Fibers

Materials	Polypropylene	Aramid
Form	Twisted Fibrillated Fiber	Monofilament Fiber
Specific Gravity	0.91	1.45
Tensile Strength (MPa)	483	3000
Length (mm)	19.05	19.05
Color	[redacted]	[redacted]
Acid/Alkali Resistance	inert	inert
Decomposition Temperature (°C)	157	>450

Figure 2 Advanced Pavements Laboratory, Arizona State University.

Furthermore, a long-range asphalt pavement research program is on-going with the Arizona Department of Transportation (ADOT); other studies included work completed for Ford Motor Company, Maricopa County Department of Transportation (MCDOT), Texas DOT, Alberta - Canada, and Sweden.

1.2. Study Objective

The objective of this study was to conduct an advanced laboratory experimental program to obtain typical engineering material properties for FORTA fiber-reinforced asphalt mixtures using the most current laboratory tests adopted by the pavement community. The results were compared with a control asphalt mixture to evaluate the value-added benefits for asphalt pavement containing FORTA fibers.

1.3. Scope of Work

In coordination with FORTA Corporation and the City of Tempe, Arizona, a City of Phoenix asphalt concrete conventional mixture designated as Type C-3/4 base and surface course was selected for paving on the Evergreen Drive (East of the Loop 101 and North of University Drive) in Tempe. The designated road section within the construction project had three main asphalt mixtures: a control mix with no fibers added; a mixture that contained 1-lb of fibers per ton of asphalt mixture; and a mixture that used 2-lbs of fibers per ton of asphalt mixture. Figures 3 and 4 show a map of Evergreen Drive where the three mixtures were laid. Figure 5 shows the road section condition before it was overlaid. Basically, no repair work was done and the 2-inch overlay was placed on a much deteriorated section of Evergreen Drive. Only the edge of the pavement was milled off to match the final overlay grade of the curb as shown in Figure 6. Figure 7 provides a schematic of Evergreen Drive that shows the different (multiple) sections of each mixture and where they were placed along the road. Half of the road shown, which is on the west side, is the pavement site of interest and that falls within the City of Tempe jurisdiction (the other half falls within the City of Mesa). Figure 7 shows that the 24 feet (2-lanes) wide pavement was constructed in three 8 feet passes. The overall length of the pavement section was 211 feet. The pavement sections were placed with staggered combinations to get an unbiased effect on pavement performance of the mixtures, including the evaluation of a section with a bus stop (about 186^{th} ft station). The addition of fibers was done in coordination and supervision of FORTA representative at Rinker's batch asphalt plant in Phoenix (Figure 8). Samples of the mixtures were brought back to the ASU laboratories. Preparation included compaction of 150 mm diameter gyratory specimens for triaxial testing (

Figure **9**). In addition, beam specimens were prepared and compacted according to AASHTO TP8 test protocols (2, 3).

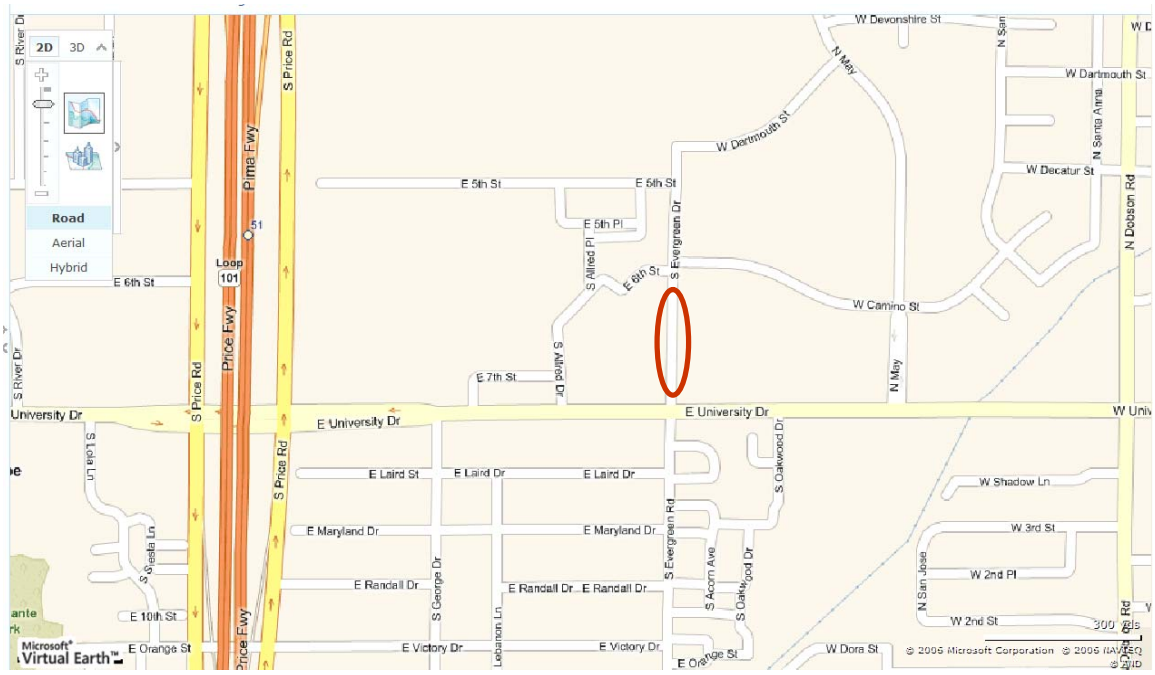

Figure 3 Location of Evergreen Drive, Tempe, Arizona

Figure 4 Areal Photo of Evergreen Drive, Tempe, Arizona.

Figure 5 Pavement Section before the Fiber-Reinforced Asphalt Concrete Mixture Overlay

Figure 6 Surface Preparation by Milling off the Edge of the Pavement

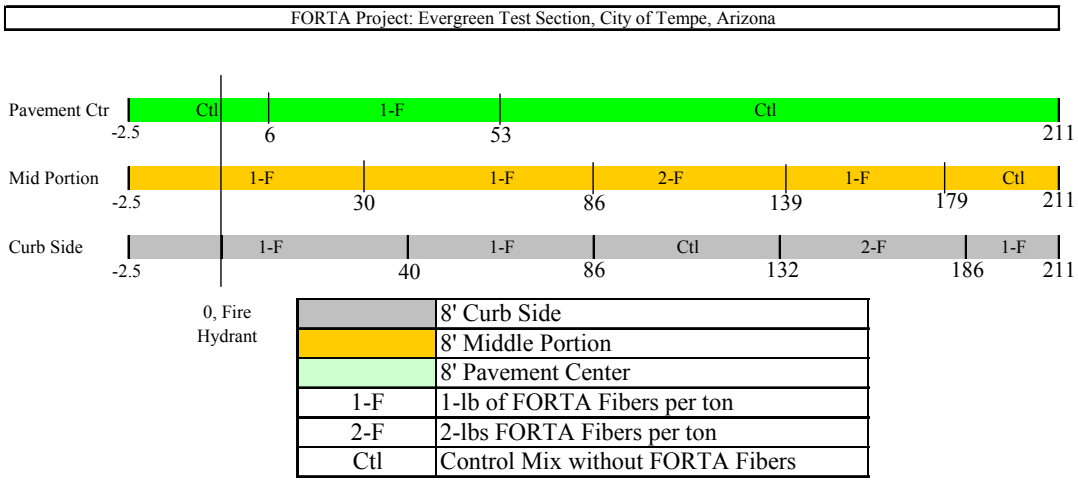

Figure 7 Schematic of Evergreen Drive and Location of the Different Tests Sections

Figure 8 FORTA Evergreen Mix Production at Rinker's Batch Asphalt Plant – Phoenix

The target air void level for the test specimens was 7% (typical field compaction). Rice gravities were determined. 100 mm diameter samples were cored from each gyratory plug and the sample ends were sawed to get final specimens of 100 mm in diameter and 150 mm in height (Figure 10).

Figure 9 Gyratory Compaction Equipment, Advanced Pavements Laboratory, ASU

Figure 10 Asphalt Concrete Plug Preparation Procedure

Thickness and bulk densities were measured and the samples were stored in plastic bags in preparation for the testing program. Data obtained from these mixtures were summarized in spreadsheets. The spreadsheet comprised of information such as binder information, aggregates, volumetric mix properties, and the results of the advanced dynamic material characterization tests. The tests included: triaxial shear strength, dynamic (complex) modulus, and repeated load for permanent deformation characterization; and flexural beam tests for fatigue and fracture cracking evaluation. The data were also used to establish a relative comparison of the mixtures according to their expected rutting or cracking potential.

Binder tests were conducted to develop information that will complement other mix material properties. The tests provided ASTM A_i-VTS_i consistency-temperature relationships. These tests were conducted for original conditions and included: penetration, ring and ball softening point, and rotational viscosities at selected temperature range.

1.4. Number of Tests

This section summarizes the testing program followed for this study for each mixture:

- Binder Tests
    - Penetration Test

      3 binders x 3 replicates x 5 readings = 45 tests

    - Softening Point Test

      3 binders x 2 replicates = 6 tests

    - Rotational Viscosity Test

      3 binders x 6 temperatures x 2 replicate = 36 tests

- Triaxial Shear Strength

3 confinement levels x 1 temperature (130 °F) x 2 replicate = 6 tests

- Repeated Load / Flow Number

Unconfined x 1 temperature (130 °F) x 3 replicates = 3 tests

- Dynamic Complex Modulus

Unconfined x 5 temperatures x 6 frequencies x 3 replicates = 90 tests

- Beam Fatigue

3 temperatures x 6 strain levels = 18 tests

- Beam Toughness

1 temperature (70 ^{o}F) x 2 loading x 2 replicates = 4 tests

- C* Integral Test

1 temperature (70 ^{o}F) x 5 displacement rates = 5 tests

1.5. Report Organization

This report has been divided into eleven chapters. Chapter 1 includes the introduction, objective of the study and scope of work. Chapter 2 summarizes the mixture properties, whereas Chapter 3 presents the binder characterization tests. Chapter 4 includes the results for the Triaxial Shear Strength tests; Chapter 5 contains the permanent deformation test results and analysis. Chapter 6 documents the Dynamic Modulus tests. Beam fatigue and toughness tests are included in Chapter 7. Chapter 8 discusses the test results of the low temperature Indirect Diametral Tensile tests. Chapter 9 provides a discussion on C* Integral crack propagation test results. Chapter 10 presents a methodology and test results of the fiber extraction from the asphalt mixtures. Chapter 11 presents the summary, conclusions and recommendations of the study.

2. MIXTURE CHARACTERISTICS

2.1. Introduction

As mentioned earlier, the objective of this study was to conduct a laboratory experimental program to obtain typical engineering material properties for the FORTA fiber-reinforced asphalt concrete mixtures placed on Evergreen Street in Tempe, Arizona. The reference air voids for the mix was 7.0%. This section provides information on the mixtures' characteristics. The asphalt binder used in the study was PG 70-10 (4). The HMA mixture was obtained as loose mix samples taken from the hauling trucks at the site of the asphalt plant. The mixture properties of the FORTA Evergreen project are reported in Table 2 including the maximum theoretical specific gravity that was determined at ASU. Table 3 shows the reported average aggregate gradations for the each mixture (4).

Table 2 Mixture Characteristics, FORTA Evergreen

Mix Type	Binder Mix Design Data			
	Binder Type	Design AC (%)	Target Va (%)	Gmm
PHX C-3/4 Control	PG 70-10	5.00	7	2.428
PHX C-3/4 1 lb/Ton	PG 70-10	5.00	7	2.458
PHX C-3/4 2 lb/Ton	PG 70-10	5.00	7	2.471

Table 3 Average Aggregate Gradations, FORTA Evergreen

Aggregate Gradation		FORTA Evergreen PHX C-3/4
Percent Passing	1 "	100
	0.75 "	95
	0.5 "	85
	0.375 "	75
	No. 4	58
	No. 8	44
	No. 30	24
	No. 200	4

Figure 11 shows a close up of the FORTA Evergreen asphalt mixture that was spread on the table for preparation of the Rice gravity test. Figure 12 presents microscopic views of FORTA fibers.

Figure 11 FORTA Fiber Reinforced Asphalt Mix

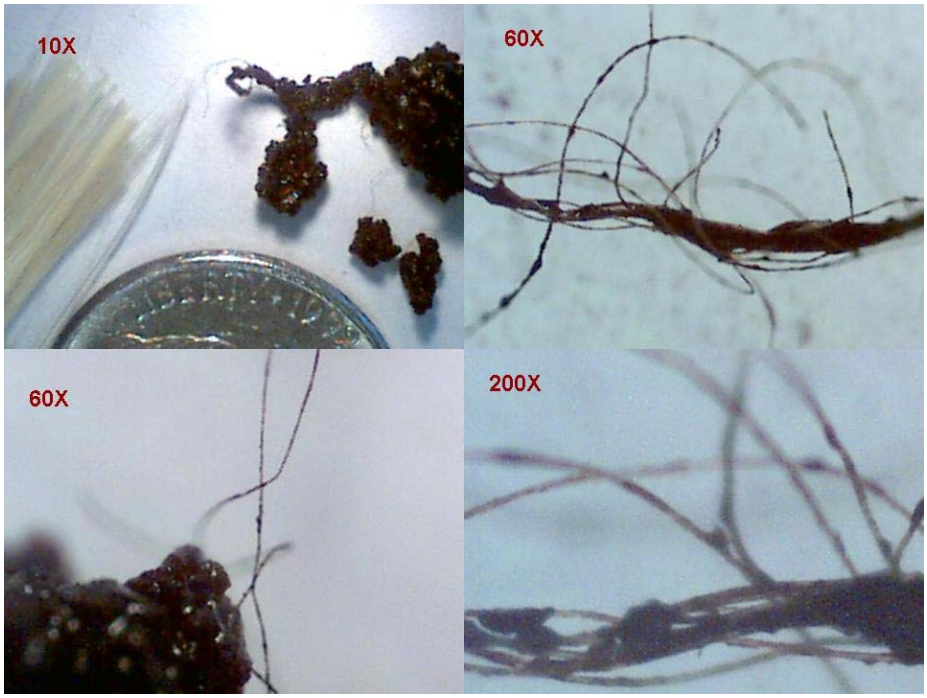

Figure 12 Observations of FORTA Fibers with Asphalt Mix through an Electronic Microscope

2.3. Preparation of Polypropylene Modified FORTA Asphalt Binder

The calculation of the amount of Polypropylene fibers added to the virgin binder is described in Appendix A. The mix time for the preparation was 30 minutes and the mixing temperature ranged between 329 and 365 °F (165-185 °C). Figure 13 shows the process of the adding the Polypropylene fibers. The pavement material testing program comprised of three different asphalt concrete mixtures: conventional (no fibers) as well as fiber-modified asphalt concrete mixtures with 1 and 2 pound amount of fibers per one ton of the mix. Therefore, three different binders similar to the available three mixes were prepared for testing: virgin binder, and the equivalent of 1 and 2 pounds of fiber modified binders per ton of mix to investigate the effect of fibers on the binder characterization.

Figure 13 Preparation of Polypropylene Modified Binder

3. BINDER CHARACTERIZATION

3.1. Introduction

The objective of binder testing was to compare the effect of soluble polypropylene fibers on the binder, if any. Conventional consistency tests (penetration, softening point and viscosity) were conducted on the extracted binders to determine whether there are any unique characteristics or difficulties in handling the material. Consistency tests across a wide range of temperatures were conducted according to the accepted American Society for Testing and Materials (ASTM) practices. Test results and analysis conducted in this task provided the viscosity-temperature susceptibility of the original (virgin) and polypropylene modified asphalt cements.

3.2. Binder Consistency Test – Viscosity Temperature Relationship

ASU's experience in regard to applying conventional / standard binder consistency tests to modified asphalt cements had been positive. It has been shown in earlier studies that these test methods can be rational and can be used as a general guide; especially when these consistency tests are being used for descriptive comparative purposes and not for specification control.

Most refined asphalt cements, with the exception of heavily air blown or high wax content crudes, exhibit a linear relationship when plotted on a log-log viscosity (centipoises, cP) versus log temperature (in degree Rankine: $R = F + 459.7\ ^{o}F$) scale. In this study, centipoise (cP) was selected for this type of plots because the test results are reported in these units. The approach uses only viscosity units (cP) to define the viscosity-temperature relationship. In order to make use of all consistency tests variables over a wide range of temperatures, it was necessary to convert all penetration (pen) and softening point (T_{RB}) measurements into viscosity units.

Penetration data was converted to viscosity units by the following model developed at the University of Maryland as a part of a Strategic Highway Research Program (SHRP) study. It should be noted that the following equation is applicable over a very wide range of penetration from 3 to 300.

$$\log \eta = 10.5012 - 2.2601 \times \log(pen) + 0.00389 \times (\log(pen))^2 \quad (3.1)$$

The viscosity obtained from the above equation is in poise (P). The second consistency variable point defined by the softening point (T_{RB}) is converted to viscosity units by the approach suggested by Shell Oil researchers. It states that all asphalts at their softening point (T_{RB}) will yield a penetration of approximately 800 and a viscosity of 13,000 poises. The third group of viscosity values at high temperature was obtained by use of the Brookfield Viscometer.

Using the above three methods, all penetration and softening point results can be shown or converted to viscosity units, which along with the Brookfield test results can then be used as direct viscosity measurements to obtain a viscosity (η) - temperature (T_R) relationship from the following regression equation:

$$\log\log \eta(\text{centipoise}) = A_i + VTS_i \times \log T_R \quad (3.2)$$

In Equation (3.2), A_i and VTS_i represents regression coefficients, which describe the unique consistency-temperature relationship of any blend. The VTS term in this equation represents the slope of the regression equation, which is also interpreted as the Viscosity- Temperature

Susceptibility parameter. For example, a larger (negative) slope value defines a higher temperature susceptibility of the binder (5, 6).

3.3. Testing Program

The testing program comprised of the tests on three different types of binder: virgin, fiber-modified binders equivalent to 1 and 2 lb/ton of polypropylene fibers. Penetration, Ring & Ball, and Brookfield Viscosity binder consistency tests were performed. Table 4 summarizes the binder tests conducted at ASU.

Table 4 Summary of Binder Tests

Age	Test	Properties Tested	Method	Test Conditions
Tank	Penetration	Penetration	AASHTO T49-93	77 °F
Tank	Ring and Ball	Softening point	AASHTO T53-92	Measured Temp.
Tank	Brookfield Viscosity	Rotational viscosity	AASHTO TP-48	275, 300, 350, 400, 450 & 500 °F

3.3.1. Penetration Test

This test covers the determination of the penetration of semi-solid and solid asphalt binders. The penetration of an asphalt binder is the distance in tenths of a millimeter that a standard needle penetrates vertically into a sample of the material under fixed conditions of temperature, load and time. This test is commonly used as a measure of consistency. Higher values of penetration indicate softer consistency. The binder sample was heated and cooled under controlled conditions. The penetration was measured with a penetrometer using a standard needle under a specified condition. Penetration tests were conducted at 25 °C (77 ^{o}F) using a 100 g load for 5 second. Penetrations were converted to viscosity using Equation 3.1.

3.3.2. Softening Point Test

This test covers the determination of the softening point of asphalt binders using the ring-and-ball apparatus. Two horizontal disks of binder, cast in shouldered brass rings, are heated at controlled rate in a liquid bath while each supports a steel ball. The softening point is reported as the mean of the temperatures at which the two disks softens enough to allow each ball, enveloped in asphalt binder, to fall a vertical distance of 25 mm. The softening point is used in the classification of asphalt binders and as one of the elements in establishing the uniformity of shipments or sources of supply. The softening point is indicative of the tendency of the binder to flow at elevated temperatures encountered in service. For most asphalt binders, the ring and ball softening point corresponds to a viscosity of 13,000 Poise.

3.3.3. Brookfield^{TM} Viscosity Test

This test determines the viscosity i.e. flow characteristics of asphalt binders at higher temperatures. A Brookfield^{TM} rotational coaxial viscometer was used with a Thermosel^{TM} temperature control system. The rotational viscometer automatically calculates the viscosity at the test temperature. The rotational viscosity is determined by measuring the torque required to maintain a constant rotational speed of a cylindrical spindle while submerged in a binder at a constant temperature. This torque is directly related to the binder viscosity. A rotational viscometer can measure viscosity of asphalt binder both at Newtonian and non-Newtonian binder conditions. Unlike capillary tube viscometers, the rotational viscometers have larger clearances between the components and, therefore, are applicable to modified as well as unmodified asphalt binders. The viscosity at different shear rates at different temperatures can be used to determine the viscosity-temperature susceptibility of asphalt binders.

3.4. Results and Analysis

3.4.1. FORTA Evergreen Virgin Binder

Table 5 shows results from three consistency tests performed on the FORTA virgin binder.

Table 5 Summary of Viscosity-Consistency Tests Results, Virgin Binder

Test	Temp (C)	Temp (F)	Temp (R)	Log Temp (R)	Penetration (.1mm)	Viscosity (Poise)	Viscosity (cP)	Log Log Visc (cP)
Penetration	25.0	77	536.7	2.73	*30.10*	1.47E+07	1.47E+09	0.962
Softening Point	55.5	131.9	591.6	2.77	---	13000	1.30E+06	0.786
Brookfield	80.0	176	635.7	2.80	---	---	*4.50E+04*	0.668
Brookfield	121.1	250	709.7	2.85	---	---	*1.39E+03*	0.497
Brookfield	135.0	275	734.7	2.87	---	---	*6.12E+02*	0.445
Brookfield	148.9	300	759.7	2.88	---	---	*3.14E+02*	0.397
Brookfield	177.2	351	810.7	2.91	---	---	*1.06E+02*	0.306

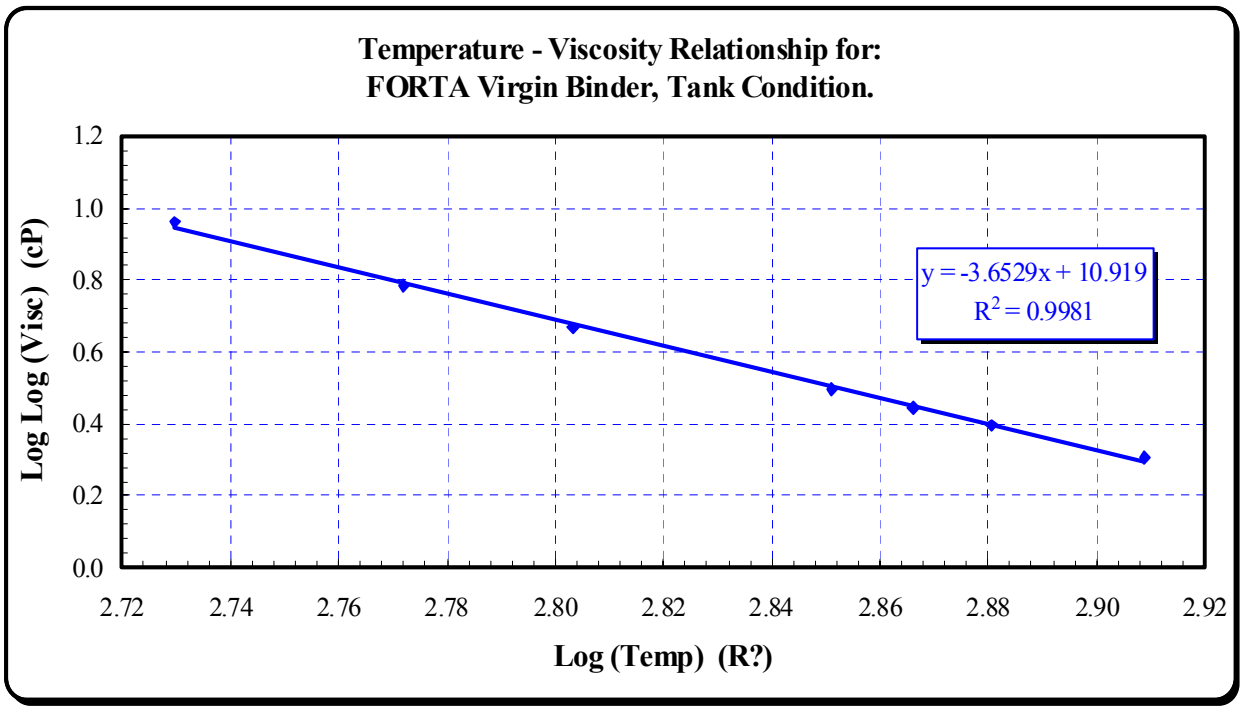

Ai =	**10.9189**
VTSi =	**-3.6529**
R^2 =	**0.9981**

3.4.2. FORTA Fiber-Modified Binders

Tables 6 and 7 show results from three consistency tests performed on two FORTA Evergreen modified binders: the equivalent of 1 and 2 lb/Ton modification.

Table 6 Summary of Viscosity-Consistency Tests Results, FORTA Evergreen 1 lb/Ton Binder

Test	Temp (C)	Temp (F)	Temp (R)	Log Temp (R)	Penetration (.1mm)	Viscosity (Poise)	Viscosity (cP)	Log Log Visc (cP)
Penetration	25.0	77	536.7	2.73	*23.40*	2.59E+07	2.59E+09	0.974
Softening Point	61.0	141.8	601.5	2.78	---	13000	1.30E+06	0.786
Brookfield	80.0	176	635.7	2.80	---	---	*4.70E+04*	0.670
Brookfield	99.4	211	670.7	2.83	---	---		
Brookfield	121.1	250	709.7	2.85	---	---	*1.59E+03*	0.505
Brookfield	135.0	275	734.7	2.87	---	---	*7.49E+02*	0.459
Brookfield	148.9	300	759.7	2.88	---	---	*3.75E+02*	0.411
Brookfield	177.2	351	810.7	2.91	---	---	*1.26E+02*	0.322

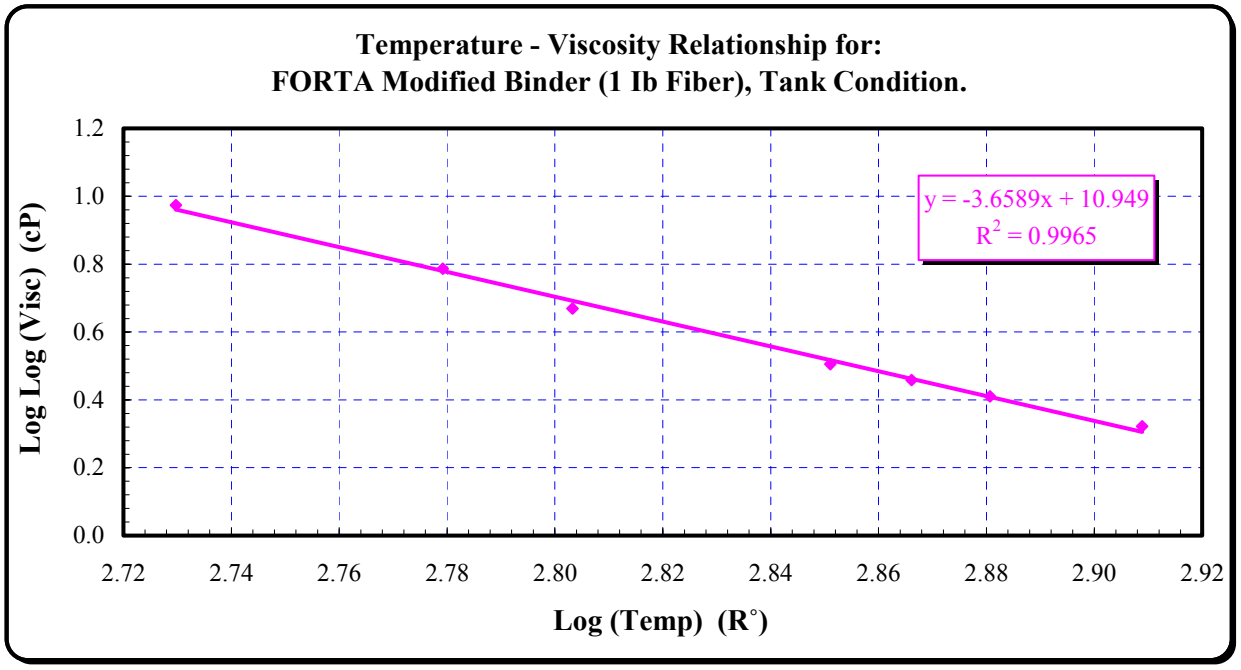

Ai =	**10.9489**
VTSi =	**-3.6589**
R^2 =	**0.9965**

Table 7 Summary of Viscosity-Consistency Tests Results, FORTA Evergreen 2 lb/Ton Binder

Test	Temp (C)	Temp (F)	Temp (R)	Log Temp (R)	Penetration (.1mm)	Viscosity (Poise)	Viscosity (cP)	Log Log Visc (cP)
Penetration	25.0	77	536.7	2.73	*22.70*	2.78E+07	2.78E+09	0.975
Softening Point	60.5	140.9	600.6	2.78	---	13000	1.30E+06	0.786
Brookfield	80.0	176	635.7	2.80	---	---	*4.06E+04*	0.664
Brookfield	99.4	211	670.7	2.83	---	---	*1.09E+04*	0.606
Brookfield	121.1	250	709.7	2.85	---	---	*2.21E+03*	0.524
Brookfield	135.0	275	734.7	2.87	---	---	*9.21E+02*	0.472
Brookfield	148.9	300	759.7	2.88	---	---	*5.75E+02*	0.441
Brookfield	177.2	351	810.7	2.91	---	---	*2.27E+02*	0.372

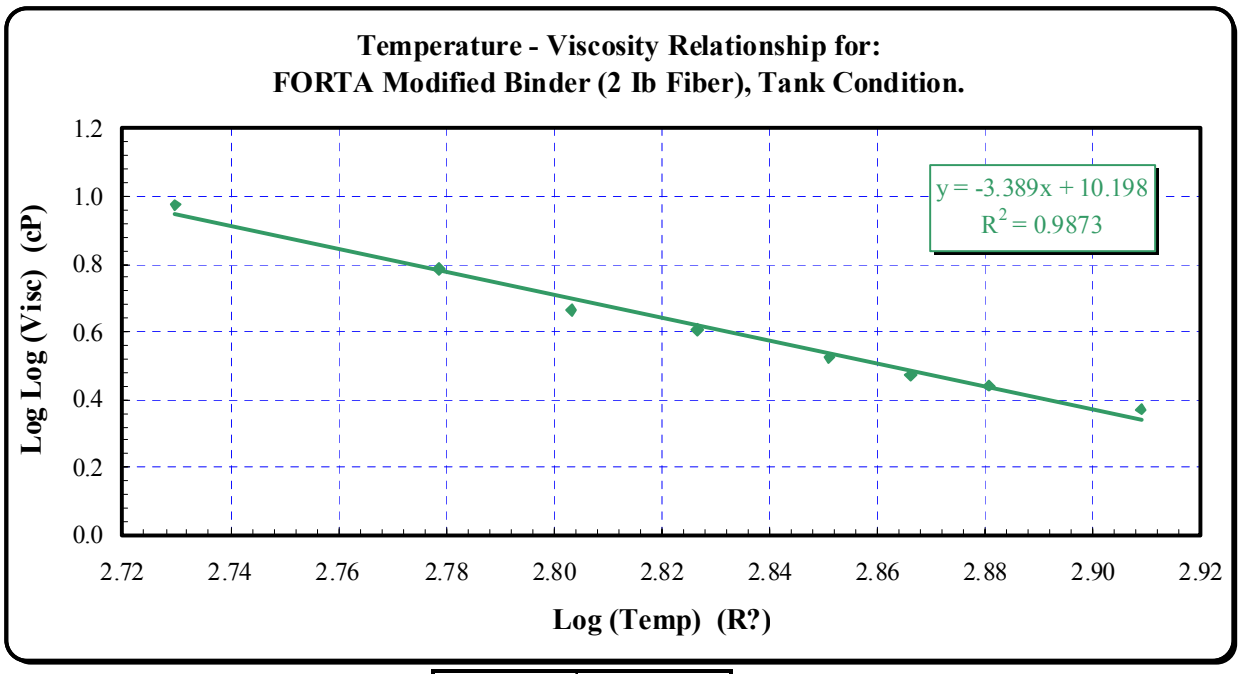

Ai =	**10.1979**
VTSi =	**-3.3890**
R^2 =	**0.9873**

3.5. Comparison of FORTA Binders

Figure 14 presents the viscosity – temperature relationship for the three FORTA binders. The very high coefficients of determinations for the three binders clearly establish the fact that the conducted conventional binder tests were adequate to define the viscosity-temperature susceptibility of the binders. This plot indicates that at lower temperatures, the FORTA modified binder has equal or similar viscosity when compared with the virgin binder. At higher

temperatures, the FORTA modified binder has higher viscosity, especially for 2 lb fiber-modified binder than the other two binders.

Also, when comparing the 1 and 2 lb/Ton fiber-modified binders, it was noticed that at higher temperatures, the higher the amount of fibers in the binder, the higher is the viscosity of the binder. One obvious reason for this behavior is the increase in the fiber content in the binder, and the saturation of the non-dissolved fibers producing a mat within the binder. This leads to an increase in the binder viscosity. In conclusions, at higher temperatures, the FORTA modified binder has higher viscosity, indicating higher stiffness and lower susceptibility to temperature change.

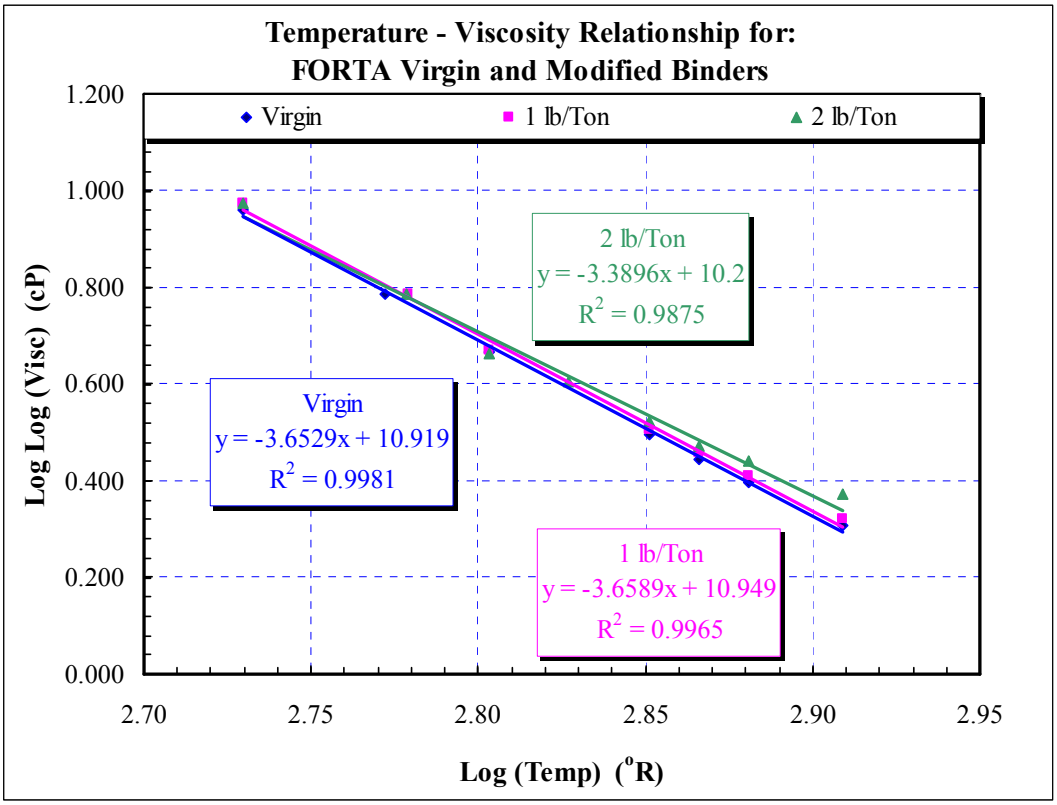

Figure 14 Viscosity – Temperature Relationship of FORTA Binders

3.6 Summary of Binder Consistency Test Results

- Binder consistency tests were conducted to develop information that will complement other mixture material properties such as fatigue cracking and permanent deformation.
- The conventional consistency tests (penetration, softening point and viscosity) were conducted on the virgin binder as well as two FORTA modified binders (the equivalent of 1 and 2 lb of fibers per ton of asphalt mix) to determine whether there were any unique characteristics or difficulties in handling the material.
- The modification process was only done using the Polypropylene fibers. Consistency tests across a wide range of temperatures were conducted according to the accepted American Society for Testing and Materials (ASTM) practices.
- There were no handling problems or difficulties in adding and mixing the Polypropylene fibers. Based on the test results and analysis, the viscosity-temperature susceptibility relationship at lower temperatures showed no changes from the original virgin binder, which is positive and desirable.
- At high temperatures, improved properties were observed in having higher viscosities; therefore, the modified binder is less susceptible to viscosity change with increased temperatures.

4. TRIAXIAL SHEAR STRENGTH TEST

4.1. Background for the Triaxial Shear Strength Test

The Triaxial Shear Strength Test has been recognized as the standard test for determining the strength of materials for over 50 years (7). The results from these tests provide a fundamental basis, which can be employed in analyzing the stability of asphalt mixtures. This is because the stresses acting on the laboratory specimen during the test truly simulate the state of stresses existing in the pavement provided certain specimen boundary and geometry conditions are met. In general, there has been reluctance to adopt this test as a routine test procedure because of the degree of difficulty in performing the test. However, with the improvement in testing equipment and computerized data acquisition systems, an increased interest in the use of the triaxial strength test has been extended to more than just a research tool.

The shear strength of an asphalt mixture is developed mainly from two sources:

1) The cementing action of the binder, which is commonly referred to as “cohesion” from Mohr plots;
2) Strength developed by the aggregate matrix interlock from the applied loads, commonly referred to as “ϕ” or the angle of internal friction.

The major role and interaction of both of these terms varies substantially with rate of loading, temperature, and the volumetric properties of the mixture.

Triaxial tests are run at different confining pressures to obtain the Mohr-Coulomb failure envelope. The Mohr-Coulomb failure envelope is defined by:

$$\tau_{ff} = c + \sigma_{ff} \tan \phi \qquad (4.1)$$

where,

τ_{ff} = shear stress at failure on failure plane

σ_{ff} = normal stress at failure on failure plane

c = intercept parameter, cohesion

tan ϕ = slope of the failure envelope (ϕ is the angle of internal friction)

Typical "c" values for conventional AC mixtures are in the range of 5 and 35 psi; whereas typical "ϕ" values range between 35 and 48^o.

Typical triaxial tests require testing specimens at three or more levels of lateral confinement to accurately develop the failure envelope. Although each test may be run on a single specimen, replicate specimens are desired if higher reliability is required. Specimen size and preparation are also important factors needed to be considered in the testing protocols. Normally, a sample with a height to diameter ratio of 2 is used in order to eliminate the effects of friction against the loading platens and interference of shear cones within the specimen. According to the modified sample preparation protocols used in NCHRP Report 465 (1) (sawed specimen ends and the use of thin lubricated membranes), a sample size of 100 mm (4 inches) in diameter and 150 mm (6 inches) in height was recommended. This size was judged sufficient in providing representative (reproducible) material properties provided the ends are parallel and well lubricated.

4.2. Test Conditions for the Triaxial Shear Strength Test

Three triaxial strength tests, one unconfined and two confined were conducted for the three FORTA Evergreen mixtures: Control, fiber-reinforced asphalt concrete mixtures with 1 and 2 lb of fibers per ton of the mix. These tests provided the standard cohesion "c" and the angle of internal friction "ϕ" parameters. The test was carried out on cylindrical specimens, 100 mm (4 inches) in diameter and 150mm (6 inches) in height, prepared as described previously. The tests were conducted at 130 ^{o}F (54.4 ^{o}C). In addition to the unconfined test, two additional confining pressures were used: 138 and 276 kPa (20 and 40 psi). The specimens were loaded axially to failure, at the selected constant confining pressure, and at a strain rate of 0.05 in/in/min (1.27 mm/mm/min). An IPC Universal Testing Machine (UTM 100) electro- hydraulic system was used to load the specimens. The machine was equipped to apply up to 100 psi (690 kPa) confining pressure and 22,000 lbs (100 kN) maximum vertical load. The load was measured through the load cell, whereas, the deformations were measured through the actuator Linear Variable Differential Transducer (LVDT). Thin and fully lubricated membranes at the sample ends were used to reduce end friction. All tests were conducted within an environmentally controlled chamber throughout the testing sequence, controlled within ±1 ^{o}F throughout the entire test.

4.3. Test Results and Analysis for the Triaxial Shear Strength Test

The results for the triaxial strength tests for the FORTA Evergreen mixtures are summarized and reported in Tables 8, 9 and 10. The maximum deviator stress, normal stress and percent strain at failure are summarized for each test condition along with Shear strength parameters, "c" and "ϕ", as well as failure envelopes.

Table 8 Triaxial Shear Strength Results for FORTA Evergreen Control Mix

Mix: FORTA Evergreen Control Mix - FEC00
Project: FORTA Evergreen Project
Test Temp: 54.4^{0}C 130^{0}F

Binder: Control
Air Voids Content: 7%
Test Machine: UTM100
Binder Content: 5.00%

Replicate Data

σ_3 (kPa)	σ_3 (PSI)		(KPa)	(PSI)	Air Voids	Sample	Strain*	Time Sec
0	0	σ_{D1}	811	117.5	7.37	FEC14	3.4	253
		σ_{D2}	1062	153.9	7.11	FEC15	2.4	183
138	20	σ_{D1}	1671	242.2	7.08	FEC16	2.7	202
		σ_{D2}	1946	282.0	7.43	FEC17	3.7	276
276	40	σ_{D1}	2648	383.8	7.25	FEC18	4.7	347
		σ_{D2}	2262	327.8	7.41	FEC19	4.8	362

* Strain at Maximum Deviator Stress

Stress Data

σ_3 (PSI)	Maximum Deviator Stress (PSI)			Radius	Center Point	σ_1 (PSI)
	σ_{D1}	σ_{D2}	$\sigma_{DAverage}$			
0	117.5	153.9	135.7	67.9	67.9	135.72
20	242.2	282.0	262.1	131.1	151.1	282.10
40	383.8	327.8	355.8	177.9	217.9	395.80

Cohesion & Angle of Friction

Test points	C	ϕ
0-20	25.1	49.4
0-40	26.6	47.2
20-40	35.3	44.5

Tangent Line

σ_3	Normal Stress (PSI)		Shear Stress τ (PSI)	
	Tangent Points	Average	Tangent Points	Average
0	16.3	18.2	44.1	46.2
	18.1		46.1	
	20.3		48.4	
20	51.5	55.2	85.2	89.3
	54.9		89.1	
	59.2		93.5	
40	82.8	87.8	115.7	121.2
	87.4		120.9	
	93.2		126.9	

Results

$\tau = c + \sigma_n \tan\phi$

c = 27.5 $\phi = 47.2$

τ = 27.5 + σ_n tan (47.2)

Mohrs Circles

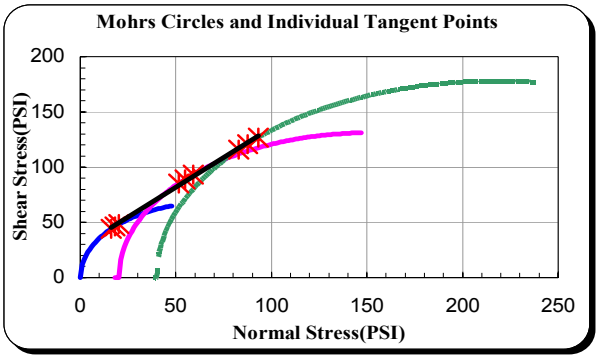

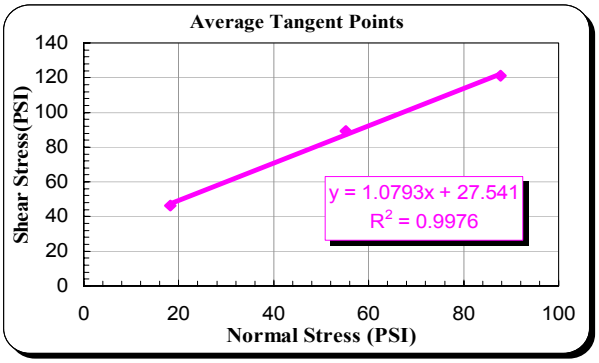

Table 9 Triaxial Shear Strength Results for FORTA Evergreen 1 lb/Ton Mix

Mix: FORTA 1 lb per Ton Mix - FE100
Project: FORTA Evergreen Project
Test Temp: 54.4^{0}C 130^{0}F

Binder: 1 lb per Ton
Air Voids Content: 7%
Test Machine: UTM100
Binder Content: 5.00%

eplicate Data

σ_3 (kPa)	σ_3 (PSI)		(KPa)	(PSI)	Air Voids	Sample	Strain*	Time Sec
0	0	σ_{D1}	1244	180.3	6.94	FE124	1.3	99
		σ_{D2}	1240	179.8	6.82	FE125	1.6	122
138	20	σ_{D1}	1964	284.6	7.12	FE117	3.0	227
		σ_{D2}	2214	320.9	6.86	FE118	2.8	205
276	40	σ_{D1}	2890	418.8	6.71	FE119	4.2	315
		σ_{D2}	2844	412.2	7.11	FE123	3.7	279

* Strain at Maximum Deviator Stress

Stress Data

σ_3 (PSI)	Maximum Deviator Stress (PSI)			Radius	Center Point	σ_1 (PSI)
	σ_{D1}	σ_{D2}	$\sigma_{DAverage}$			
0	180.3	179.8	180.0	90.0	90.0	180.03
20	284.6	320.9	302.8	151.4	171.4	322.75
40	418.8	412.2	415.5	207.8	247.8	455.51

Cohesion & Angle of Friction

Test points	C	ϕ
0-20	33.7	49.0
0-40	34.3	48.3
20-40	36.9	47.6

Tangent Line

σ_3	Normal Stress (PSI)		Shear Stress τ (PSI)	
	Tangent Points	Average	Tangent Points	Average
0	22.1	22.8	59.1	59.9
	22.8		59.9	
	23.6		60.7	
20	57.2	58.4	99.4	100.8
	58.4		100.7	
	59.6		102.1	
40	91.1	92.7	136.4	138.3
	92.7		138.3	
	94.4		140.2	

Results

$$\tau = c + \sigma_n \tan\phi$$

c = 34.6 $\phi = 48.3$

τ = 34.6 + σ_n tan (48.3)

Mohrs Circles

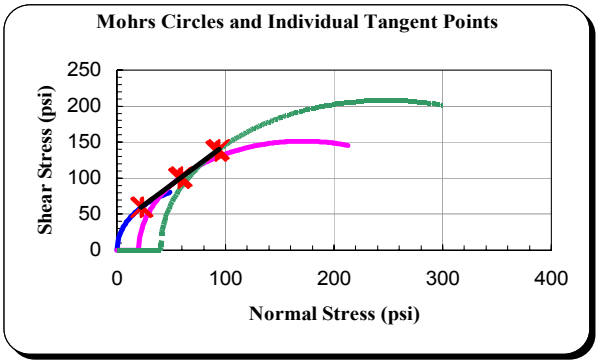

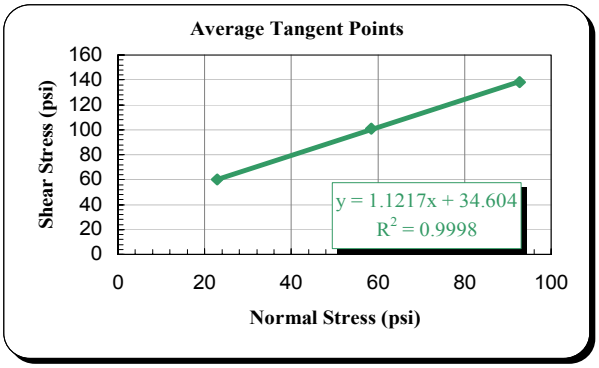

Table 10 Triaxial Shear Strength Results for FORTA Evergreen 2 lb/Ton Mix

Mix: FORTA Evergreen 2 lb per Ton Mix - FE200 **Binder:** FORTA 2 lb per Ton
Project: FORTA Evergreen Project **Air Voids Content:** **7%**
Test Temp: 54.4^{0}C 130^{0}F **Test Machine:** UTM100
Binder Content: 5.00%

Replicate Data

σ_3	σ_3 (PSI)		(KPa)	(PSI)	Air Voids	Sample	Strain*	Time Sec
0	0	σ_{D1}	1651	239.3	6.99	FE210	2.4	175
		σ_{D2}	1597	231.4	6.86	FE215	1.9	138
138	20	σ_{D1}	2132	309.0	6.82	FE216	2.6	195
		σ_{D2}	1695	245.7	6.74	FE217	2.0	148
276	40	σ_{D1}	2881	417.5	6.99	FE218	4.8	361
		σ_{D2}	2876	416.8	6.91	FE219	3.3	251

Strain at Maximum Deviator Stress

Stress Data

σ_3 (PSI)	Maximum Deviator Stress (PSI)			Radius	Center Point	σ_1 (PSI)
	σD_1	σD_2	$\sigma D_{Average}$			
0	239.3	231.4	235.4	117.7	117.7	235.36
20	309.0	245.7	277.3	138.7	158.7	297.32
40	417.5	416.8	417.2	208.6	248.6	457.17

Cohesion & Angle of Friction

Test points	C	ϕ
0-20	66.9	30.8
0-40	50.0	44.0
20-40	24.3	51.0

Tangent Line

σ_3	Normal Stress (PSI)		Shear Stress τ (PSI)	
	Tangent Points	Average	Tangent Points	Average
0	57.4	39.9	101.1	86.6
	36.0		84.7	
	26.2		74.0	
20	87.7	67.0	119.1	102.0
	62.4		99.8	
	50.8		87.2	
40	141.8	110.6	179.2	153.5
	103.7		150.1	
	86.4		131.2	

Results

$\tau = c + \sigma_n \tan\phi$

c = 43.9 $\phi = 44.0$

τ = 43.9 + σ_n tan (44)

Mohrs Circles

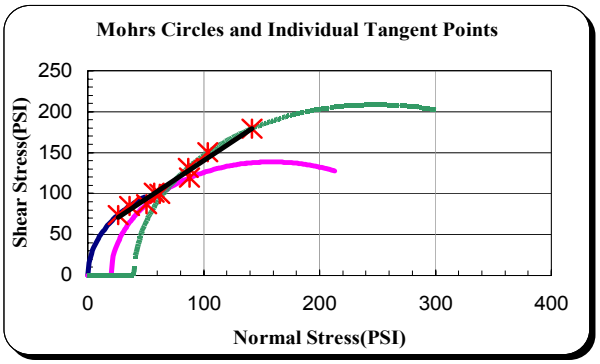

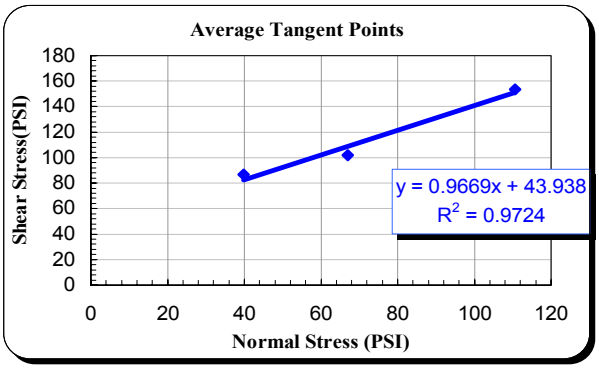

4.4. Mohr-Coulomb Failure Envelope for FORTA Evergreen Mixtures

The above tables also show plots of the Mohr-Coulomb failure envelopes represented by the cohesion "c" and angle of internal friction "ϕ" for the tested mixtures (2 samples for each confinement: 0, 20 and 40 psi). The parameters "c" and "ϕ" are the strength indicators of the mix. The larger the "c" value, the larger the mix resistance to shearing stresses. In addition, the larger the value of "ϕ", the larger is the capacity of the asphalt mixture to develop strength from the applied loads, and hence, the smaller the potential for permanent deformation. Typical "c" values for conventional AC mixtures have been found to be in the range of 5 to 35 psi and typical "ϕ" values have been found to be in the range between 35 and 48^{o}.

Figure 15 shows plots of the Mohr-Coulomb failure envelope for the three FORTA Evergreen mixtures. When the three mixes were compared, fiber-modified mixes show a higher value of "c" compared to the control mix. Interestingly, the 2 lb/Ton fiber-reinforced asphalt mix has the highest cohesion value owing to the reinforcing effect of the fibers. The 1 lb/Ton fiber-reinforced asphalt mix has slightly higher "ϕ" value.

In essence, the mix with higher values of "c" and "ϕ" would resist permanent deformation better, which is being indicated by both fiber-reinforced asphalt concrete mixes. The 1 lb/Ton fiber-reinforced asphalt mix would yield the best performance in this case and based on triaxial shear laboratory tests.

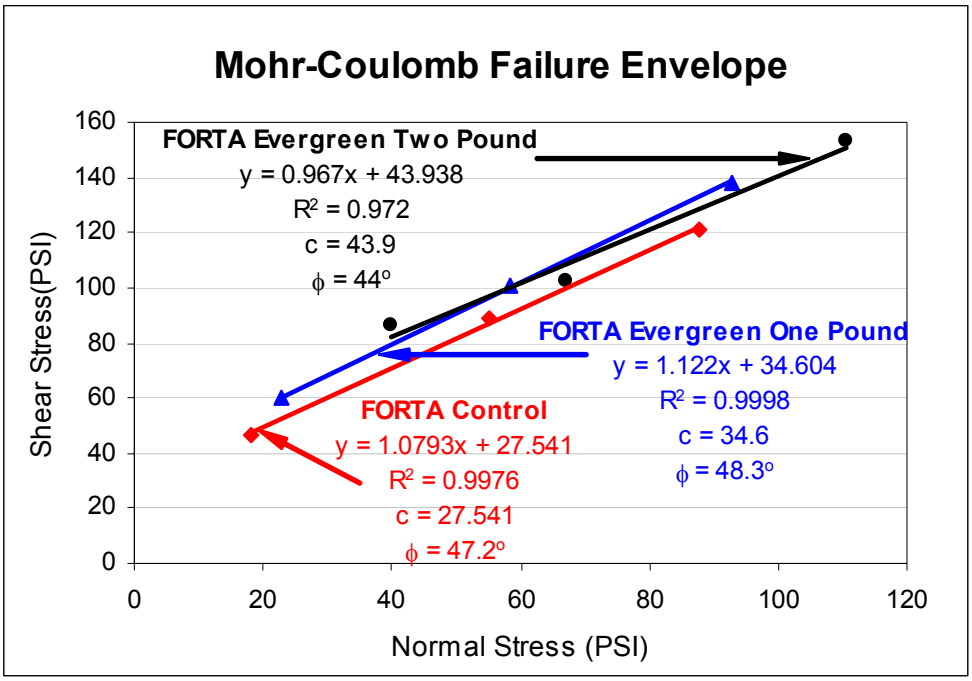

Figure 15 Comparisons of Results for FORTA Evergreen Mixtures

4.5. Residual Energy Analysis Approach

The research team also investigated the importance of dissipated energy of the mixture. This was studied using residual energy approach. Figure 16 shows plots of the cumulative area under the Load – Deformation curve for the three tested mixtures. The value of this area is an indicator of the mix to resist the propagation of the cracks after they begin to appear. The higher the area under the curve, the better is the crack propagation resistance of the mix. When comparing the three mixes, the fiber-reinforced asphalt concrete mixtures show a higher value of cumulative area compared to the control conventional dense graded mix. Effectively, it can be stated that the fibers show higher resistance against crack propagation than the mixes without fibers.

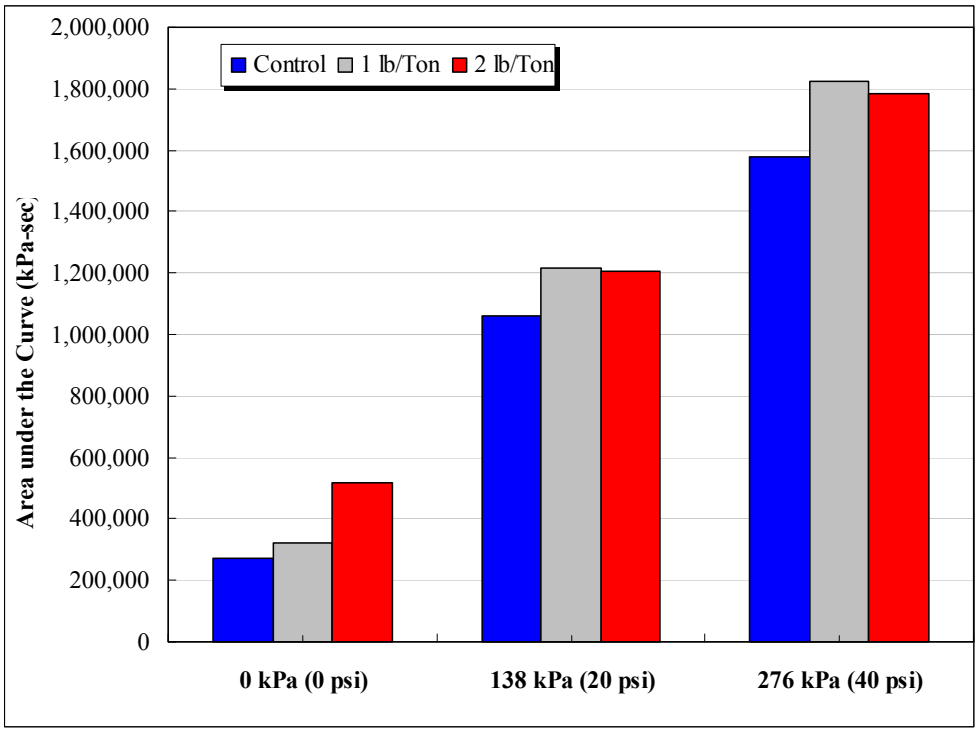

Figure 16 Comparison of Cumulative Areas under the Curve, FORTA Evergreen Mixtures

4.6 Summary of Triaxial Shear Strength Tests

- Triaxial Shear Strength tests were conducted at 130 ^{o}F (54.4 ^{o}C). These tests provided the standard cohesion and the angle of internal friction parameters of the mixtures.
- When the three mixes were compared, the fiber-modified mixes showed higher values of "c" compared to the control mix. The 2 lb/Ton fiber-reinforced asphalt mix had the highest cohesion value owing to the reinforcing effect of the fibers.
- The 1 lb/Ton fiber-reinforced asphalt mix would yield the best performance based on triaxial shear strength laboratory tests.
- Both fiber-reinforced asphalt concrete mixtures showed higher residual energy compared to the control mix. This indicated that the fiber-reinforced mixes show higher resistance against crack propagation than the mixes without fibers.

5. PERMANENT DEFORMATION TESTS

5.1. Background for the Static Creep /Flow Time Tests

In a static creep / flow time test, a total strain – time relationship for a mixture is obtained experimentally in the lab (8). The static creep is a fundamental test because the rate of cumulative strain and the time at which tertiary deformation occurs for an asphalt mixture was found to be dependent on the temperature, deviator and confining stresses applied, and mix quality (10). While the creep test has been used in the pavement community for many decades; the starting point of tertiary deformation, or flow time, concept also obtained from a creep test, had been evaluated for asphalt mixtures by Witczak et al at the University of Maryland (UMd) and later on at Arizona State University (8, 9).

The static creep test, using either one cycle load/unload or cyclic loading is capable of providing much information concerning the material response characteristics. The interpretation of the strain/time response of a material undergoing a static creep test provides significant parameters, which describe the instantaneous elastic/plastic and viscoelastic/plastic components of the material response.

5.1.1. Modulus/Compliance Components

In mechanics, the term "modulus" represents the ratio of stress to strain on a deformable body. In creep testing, several unique moduli can be defined dependent upon the particular strain value used. The "resilient" modulus is:

$$E_R = \frac{\sigma_d}{\varepsilon_r} \qquad (5.1)$$

The "pure" elastic (instantaneous) modulus is:

$$E_e = \frac{\sigma_d}{\varepsilon_e} \tag{5.2}$$

The "creep" or time dependent modulus is:

$$E_c = \frac{\sigma_d}{\varepsilon(t)} \tag{5.3}$$

Where ε_ρ, ε_ε, $\varepsilon(t)$ are the resilient, elastic and total strains. The "modulus" of a material is a very important property that relates stress to strain. However, for viscoelastic materials, it is more advantageous to use the term "compliance" or D (t). Compliance is the reciprocal of the modulus and is expressed by:

$$D(t) = E(t)^{-1} = \frac{\varepsilon(t)}{\sigma_d} \tag{5.4}$$

The main advantage of its use in viscoelasticity / plasticity is that it allows for the separation of the various strain components (e.g., ε_e, ε_p, ε_{ve}, and ε_{vp}) at a constant stress level. Thus, the time dependent strain $\varepsilon(t)$ can be simply expressed by:

$$\varepsilon(t) = \sigma_d * D(t)$$
$$= \sigma_d (D_e + D_p + D_{ve}(t) + D_{vp}(t)) \tag{5.5}$$

The stress used to calculate compliance in the above equations is defined as the following:

$$\sigma_d = \sigma_1 - \sigma_3 \tag{5.6}$$

where:

σ_d = deviator stress (psi)

σ_1 = vertical stress (psi)

σ_3 = confining pressure (psi)

The creep test can be conducted at unconfined and triaxial / confined conditions. For the unconfined condition, $\sigma_d = \sigma_1$ (σ_3=0) while for the triaxial / confined condition, $\sigma_d = \sigma_1 - \sigma_3$. The vertical stress ($\sigma_1$) is calculated by the following equation:

$$\sigma_1 = \frac{P}{A} \qquad (5.7)$$

where:

σ_1 = vertical stress (psi)

P = vertical load applied (lb)

A = area of cross section of specimen (in^2)

Therefore, compliance values calculated in the above equations are "true" compliance values as both stress and strain computed are in the same axis or direction.

5.2. Background for the Repeated Load Permanent Deformation Test

Another approach to determine the permanent deformation characteristics of paving materials is to employ a repeated dynamic load test for several thousand repetitions and record the cumulative permanent deformation as a function of the number of cycles (repetitions) over the test period. This approach was employed by Monismith et al. in the mid 1970's using uniaxial compression tests (7). Several research studies conducted by Witczak et al, used a temperature of 100 or 130 ^oF, and at 10, 20, or 30 psi unconfined deviator stress level (9). A haversine pulse load of 0.1 sec and 0.9 sec dwell (rest time) is applied for the test duration of approximately 3 hours. This approach results in approximately 10,000 cycles applied to the specimen.

A number of parameters describing the accumulated permanent deformation response can be obtained from the test. Figure 17 illustrates the typical relationship between the total cumulative plastic strain and number of load cycles. The cumulative permanent strain curve is generally defined by three zones: primary, secondary, and tertiary. In the primary zone, permanent deformations accumulate rapidly. The incremental permanent deformations decrease reaching a constant value in the secondary zone. Finally, the incremental permanent deformations again increase and permanent deformations accumulate rapidly in the tertiary zone. The starting point, or cycle number, at which tertiary flow occurs, is referred to as the "Flow Number" (1, 8, 9).

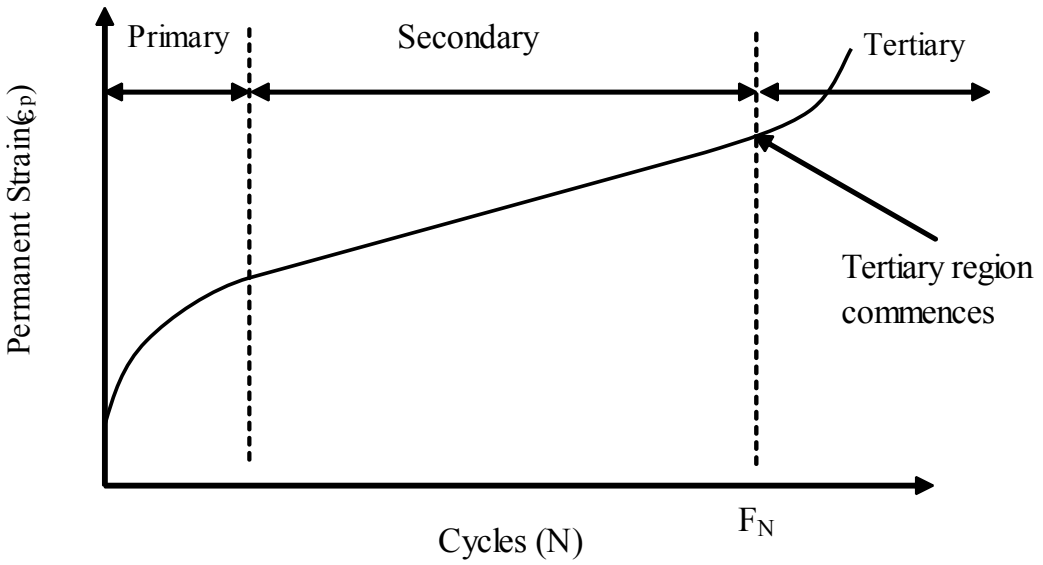

Figure 17 Typical Relationship between Total Cumulative Plastic Strain and Number of Load Cycles

5.3. Evaluation of Flow Time / Flow Number

The development of models to estimate the Flow Time / Flow Number is accomplished using statistical techniques. The best suited mathematical modeling for all three stages of permanent deformation was provided by the Francken model. The Francken model developed in 1977 was

found to be the most comprehensive representation of the permanent deformation test data. The model structure was selected because it combines both a power model, which characterizes the primary and secondary stages of the permanent deformation plot, and an exponential model that fits the tertiary stage. The Francken model was also used to fit the permanent strain test data obtained from the laboratory testing (9, 10).

The steps that were used to determine the Flow Time (FT) / Flow Number (FN) values using this model were as follows (10):

Step 1: The mathematical model for the regression analysis was:

$$\varepsilon_p(N) = A(N)^B + C(e^{D(N)}-1) \qquad (5.8)$$

Where:

ε_p (T or N) = Permanent deformation or permanent strain

T or N = Number of Loading Time / Cycles

A, B, C and D = Regression constants

Step 2: Using any statistical package software, the model's coefficients were estimated through non linear regression techniques for the test files.

Step 3: The first derivative of Equation (5.8) with respect to N is found, which gives the strain rate of change as follows:

$$\frac{d\varepsilon_p}{dN} = ABN^{(B-1)} + (CDe^{DN}) \qquad (5.9)$$

Step 4: The method of estimating the FT/FN for the strain slope curve for this model was done by taking the lowest point of the strain slope against number of cycles. This is where the strain slope starts to increase from a constant value to a higher value.

5.4. Test Conditions for the Static Creep and Repeated Load Tests

Static creep and repeated load tests were conducted at unconfined test conditions only using at least two replicate test specimens for each mixture. All tests were carried out on cylindrical specimens, 100 mm (4 inches) in diameter and 150 mm (6 inches) in height.

For the static creep tests, a static constant load was applied until tertiary flow occurred. For the repeated load tests, a haversine pulse load of 0.1 sec and 0.9 sec dwell (rest time) was applied for a target of 300,000 cycles. This number was bigger if the test specimen failed under tertiary flow before reaching this target level.

An IPC Universal Testing Machine (UTM 25) electro- pneumatic system was used to load the specimens. The machine is equipped to apply up to 90 psi (620 kPa) confining pressure and 5,500 lb (24.9 kN) maximum vertical load. The load was measured through the load cell, whereas, the deformations were measured through six spring-loaded LVDTs. Two axial LVDTs were mounted vertically on diametrically opposite specimen sides. Parallel studs, mounted on the test specimen, placed 100 mm (4 inches) apart and located at the center of the specimen were used to secure the LVDTs in place. The studs were glued using a commercial 5-minute epoxy. An alignment rod with a frictionless bushing was used to keep the studs aligned at extreme failure conditions.

Figure 18 shows a photograph of an actual specimen set-up for unconfined test. For radial deformations, four externally mounted LVDTs aligned on diametrical and perpendicular lines were located at the center of the specimen and along opposite specimen sides. The radial LVDTs set-up is also shown in the figure. Thin and fully lubricated membranes at the test specimen ends were used to warrant frictionless surface conditions. The tests were conducted within an environmentally controlled chamber throughout the testing sequence (i.e., temperature was held constant within the chamber to ±1 ^{o}F throughout the entire test). The figure shows typical unconfined test set up for the repeated load test. A complete matrix of the stress level / temperature combinations used for the Static Creep and Repeated Load tests for FORTA Evergreen project is shown in Table 11.

Table 11 Stress Level / Temperature Combination used for the Static Creep and Repeated Load Tests, FORTA Evergreen

Test Type	Stress Type *		Test Temperature
			54.4 ^{o}C (130 ^{o}F)
			UC
Static Creep/ Flow Time	σ_3	(kPa)	0
		(psi)	0
	σ_d	(kPa)	105
		(psi)	15
Repeated Load/ Flow Number	σ_3	(kPa)	0
		(psi)	0
	σ_d	(kPa)	105
		(psi)	15

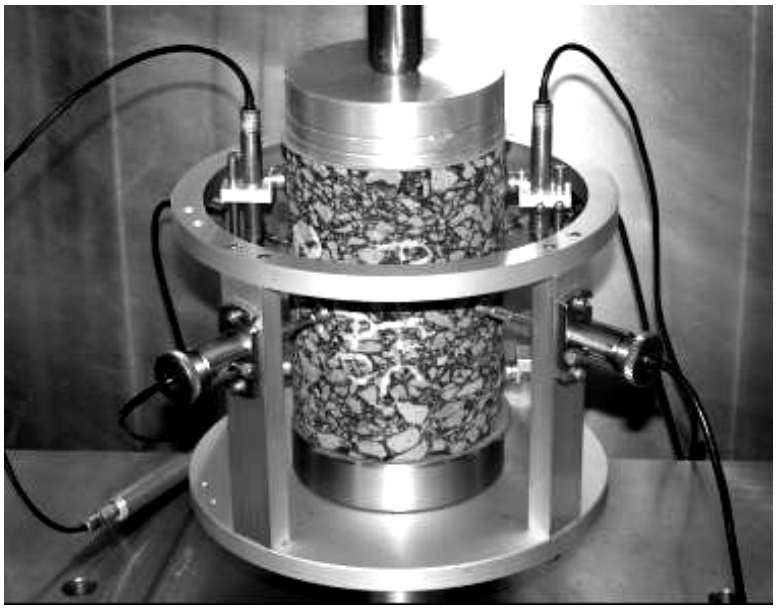

Figure 18 Vertical and Radial LVDTs' Set Up for an Unconfined Repeated Load Permanent Deformation Test

5.5. Static Creep/Flow Time (FT) Test Results and Analysis

5.5.1. Static Creep Results

The results for the static creep unconfined tests for all the mixtures of FORTA Evergreen Project are summarized in this section**.** As mentioned previously, the test results were analyzed using Francken model. The regression coefficients found by non-linear regression are shown in Table 12.

Table 12 Francken Model Coefficients for FORTA Evergreen Mixtures, Flow Time

Mix Type	Specimen ID	Regression Coefficients				R^2
		A	B	C	D	
Control	FECO5	0.02106401	0.65433238	0.00000093	0.02692150	0.992
	FECO7	0.07790790	0.36399030	0.00928751	0.00355209	0.994
1 lb/Ton	FE111	0.17976223	0.13990080	8.41675E-06	0.00088326	0.975
	FE126	0.15318386	0.22093798	0.000716826	0.00302539	0.994
2 lb/Ton	FE208	0.14177432	0.18638008	0.000430447	0.00271346	0.997
	FE209	0.16115691	0.1397934	2.64811E-05	0.00145960	0.997

A master summary table of test results for all the three FORTA Evergreen mixtures from the FT tests for control and fiber-reinforced mixes are summarized and reported in Table 13. The average values used in comparison analysis of the control and two fiber-reinforced mixes are reported in Table 14. These tables include the FT, axial strain at FT (%), Creep Modulus at FT, and Slope of Creep Compliance, m.

Table 13 Master Summary of Static Creep Flow Time Test Results

Mix Type	Specimen ID	Temp °F	σ_d (psi)	Flow Time (sec)	Axial Strain at Failure %	Creep Modulus at Failure (psi)	Inst. Comp. at Failure $D_o \times 10^{-3}$ (psi)	Slope m
Control	FECO5	130	15.0	301	0.8433	1410.15	0.7091	1.70
	FECO7	130	15.0	501	0.7605	1550.54	0.6449	0.60
1 lb/Ton	FE111	130	15.0	6375	0.5974	1825.38	0.5478	0.02
	FE126	130	15.0	980	0.7151	1587.96	0.6297	0.30
2 lb/Ton	FE208	130	15.0	1114	0.5240	2183.18	0.4580	0.10
	FE209	130	15.0	3195	0.4832	2309.06	0.4331	0.01

Table 14 Master Summary of Average Static Creep Flow Time Test Results

Mix Type	σ_d (psi)	Flow Time (sec)	Axial Strain at Failure %	Creep Modulus at Failure (psi)	Inst. Comp. at Failure $D_o * 10^{-3}$ (psi)	Slope m
Control	15.0	401.0	0.802	10.207	0.6770	1.150
1 lb/Ton	15.0	3677.5	0.656	11.768	0.5888	0.160
2 lb/Ton	15.0	2154.5	0.504	15.487	0.4456	0.055

5.5.2. Analysis of Static Creep Tests

Figures 19 and 20 represent typical load/strain plots of FORTA control and fiber-reinforced asphalt concrete samples. Two important characteristics were observed for fiber-reinforced

mixes when compared to the control mix. One was the endurance of the secondary stage and the second gradual (less) accumulation of permanent strain beyond tertiary flow for fiber-reinforced asphalt mix. Both were attributed to the presence of the Aramid fibers in the mix, as this behavior is not typically observed in conventional mixes.

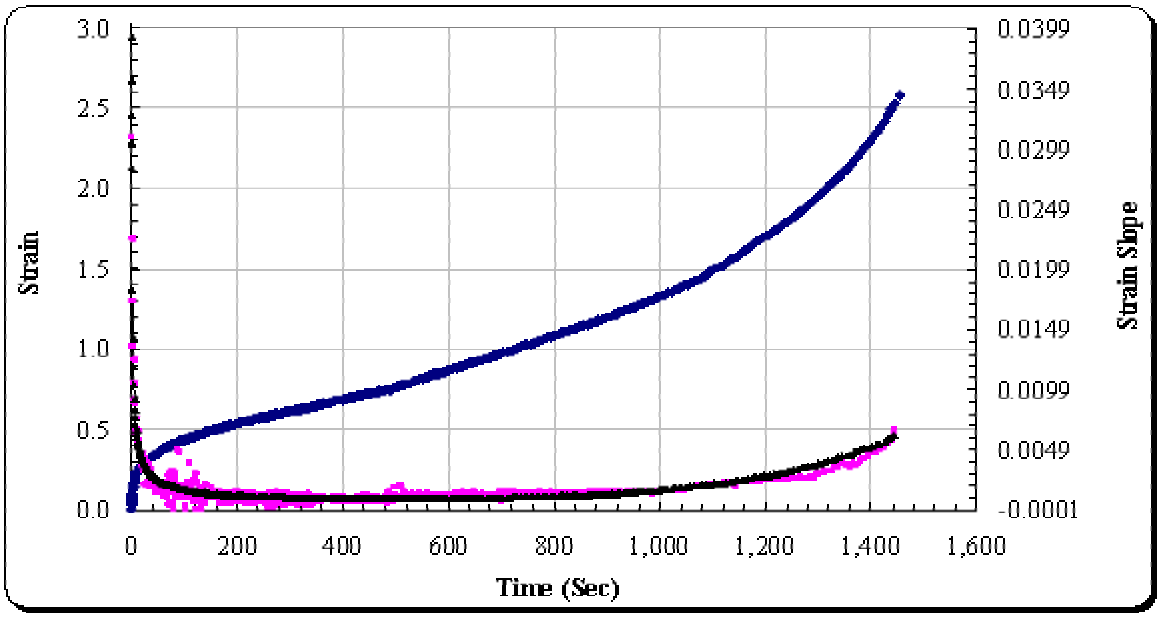

Figure 19 Static Creep / Flow Time Results for FORTA Evergreen Control Mixture

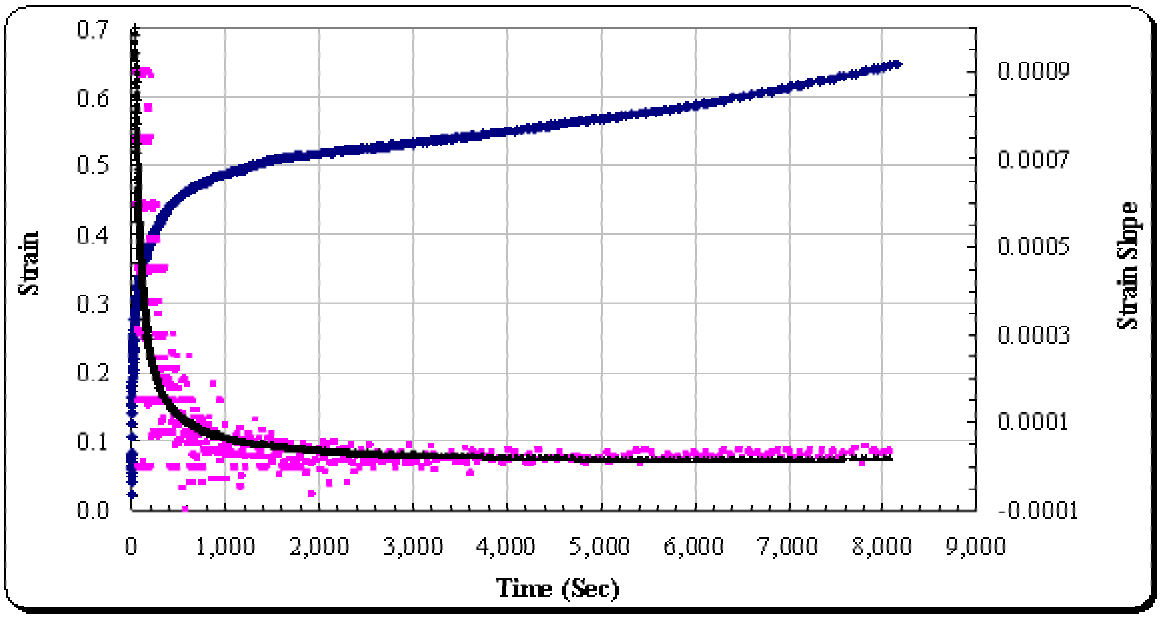

Figure 20 Static Creep / Flow Time Results for FORTA Evergreen Fiber-Reinforced Mixture

Figure 21 shows a comparison plot of FT for the three mixes. It is noticed that the fiber-reinforced mixes have higher FT values than the control mix (over 9 times for 1 lb/Ton mix and 5 times for 2 lb/Ton mix higher than the control mix). This indicates that fiber-reinforced mixes have the potential to resist permanent deformation better than the control mix. However, a lot of variability was observed between the FT values within the same fiber reinforced mixture as represented by error bars. The reason for this variability was attributed, possibly, to the inhomogeneous distribution and orientation of the fibers in the mixtures.

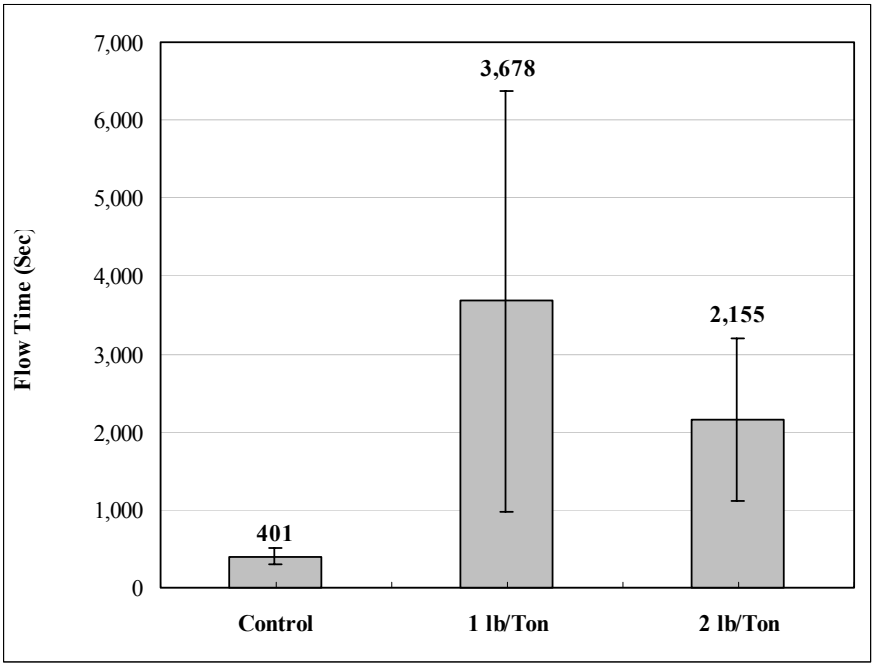

Figure 21 Flow Time at Failure for FORTA Control and Fiber-Reinforced Mixtures

Figure 22 shows the axial strain at failure values for the three mixtures under investigation. It is observed that the control mixes have higher axial strain values at failure compared to the fiber-reinforced mixes (20% higher than 1 lb/Ton and 60% higher than 2 lb/Ton mix).

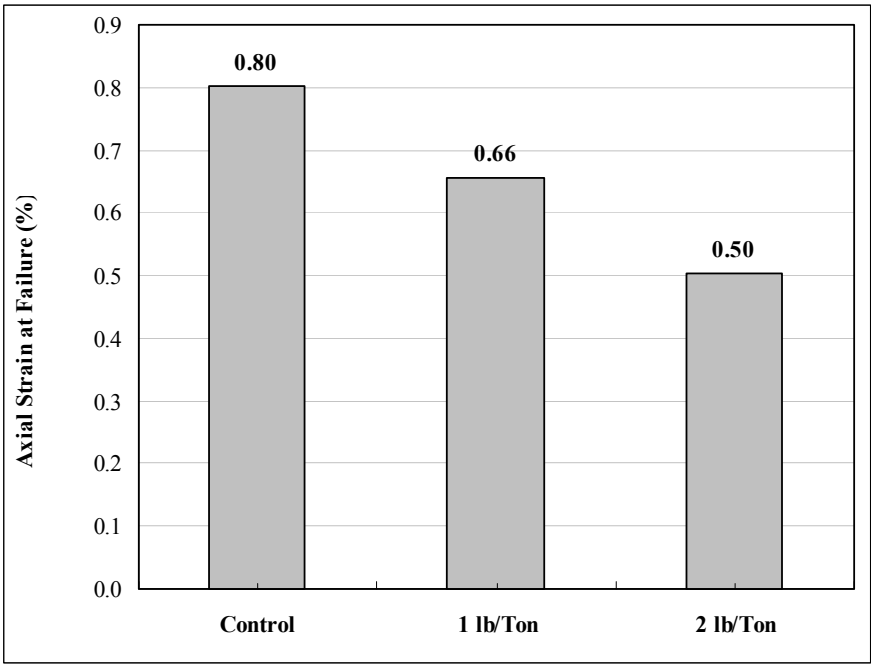

Figure 22 Axial Strains at FT for FORTA Control and Fiber-Reinforced Mixtures

Figures 23 and 24 show creep moduli and slope of the creep compliance curves for the three FORTA mixtures under study. Creep moduli values at failure indicate that that the control mix has higher values than the fiber-reinforced mixtures (15% higher than 1 lb/Ton and 50% higher than 2 lb/Ton). The results of the slope parameter of the compliance curve for the unconfined tests at 130 ^{o}F showed that the control mix had 7 times higher slope than the 1 lb/Ton mix and 3 times than the 2 lb/Ton fiber-reinforced mix. Higher slope values are indicative of susceptibility of the mixture to permanent deformation.

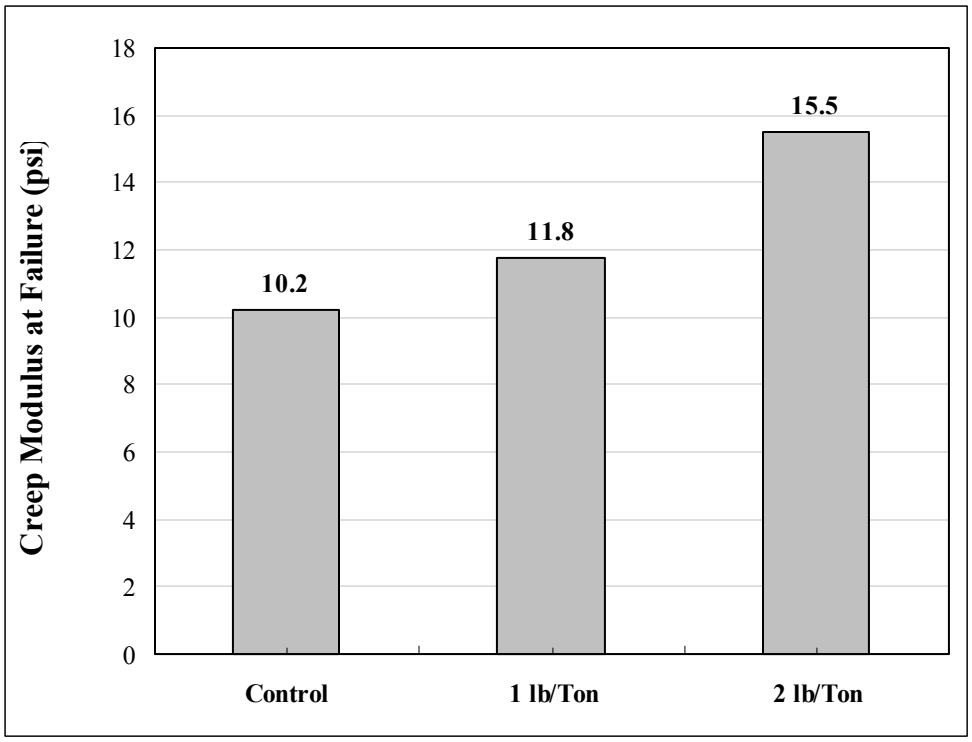

Figure 23 Creep Modulus at FT for FORTA Control and Fiber-Reinforced Mixtures

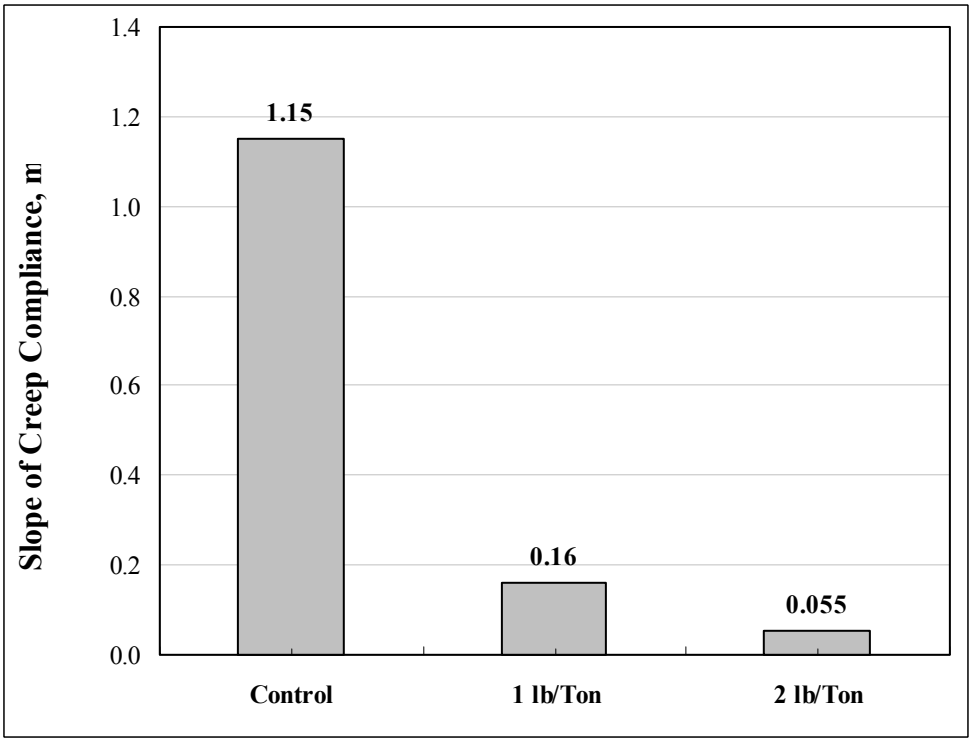

Figure 24 m, Slope of the Creep Compliance for FORTA Control and Fiber-Reinforced Mixtures

5.6. Repeated Load / Flow Number Test Results and Analysis

5.6.1. Repeated Load Results

The results for the repeated load unconfined tests for the three FORTA Evergreen mixtures are summarized in this section. As it was mentioned before, for the analysis of the test results, the Francken model was used to fit the permanent strain results. The model regression coefficients that were found by non-linear regression are summarized in Table 15.

Table 15 Francken Model Coefficients for Repeated Load Test, FORTA Evergreen Mixtures

Mix Type	Specimen ID	Regression Coefficients				S_e	S_y	S_e/S_y	R^2
		A	B	C	D				
Conv. Mix	FECO2	0.047276	0.08543	1.6556	0.0516	0.08543	1.6556	0.0516	0.997
	FECO3	0.032957	0.04823	1.5787	0.0306	0.04823	1.5787	0.0306	0.999
	FECO4	0.0644621	0.01775	1.2416	0.0143	0.01775	1.2416	0.0143	0.999
1 lb/Ton Mix	FE101	0.007610	0.09270	1.0655	0.0870	0.09270	1.0655	0.0870	1.000
	FE102	0.020764	0.08951	1.1806	0.0758	0.08951	1.1806	0.0758	0.995
	FE103	0.000443	0.12629	1.8170	0.0695	0.12629	1.8170	0.0695	0.995
	FE104	0.019648	0.08784	1.1597	0.0758	0.08784	1.1597	0.0758	0.999
	FE106	0.058636	0.00245	0.0157	0.1318	0.00245	0.0157	0.1318	0.999
	FE107	0.034359	0.01059	0.1629	0.0650	0.01059	0.1629	0.0650	1.000
2 lb/Ton Mix	FE201	0.013189	0.05253	0.8036	0.0654	0.05253	0.8036	0.0654	0.994
	FE202	0.003600	0.0790	0.8484	0.0931	0.0790	0.8484	0.0931	1.000
	FE203	0.017023	0.07726	0.9274	0.0834	0.07726	0.9274	0.0834	1.000
	FE204	0.003308	0.01279	0.2717	0.0471	0.01279	0.2717	0.0471	1.000
	FE206	0.039176	0.08889	0.94886	0.0937	0.08889	0.94886	0.0937	1.000
	FE207	0.032908	0.05585	1.0279	0.0543	0.05585	1.0279	0.0543	1.000

The FN test results for FORTA control and fiber-reinforced mixtures are summarized and reported in Tables 16, 17 and 18. The tables include the FN, axial strain at flow (%), resilient modulus at flow.

Table 16 Master Summary of Flow Number Test Results for FORTA Evergreen Control Mix

Mix Type	Specimen ID	Flow Number (cycles)	Axial Strain at Failure (%)	Resilient Modulus at Failure (psi)
Control Mix	FECO2	436	0.84	2137
	FECO3	241	0.56	1058
	FECO4	166	0.95	1053
Range		166 - 436	0.56 – 0.95	1058 - 2137
Average		281	0.78	1416
Standard Deviation		139	0.20	625
% Coefficient of Variation		49.60	25.76	44.11

Table 17 Master Summary of Flow Number Test Results for FORTA Evergreen 1 lb/Ton Mix

Mix Type	Specimen ID	Flow Number (cycles)	Axial Strain at Failure (%)	Resilient Modulus at Failure (psi)
1 lb/Ton Mix	FE101	5916	0.46	1160
	FE102	3336	0.47	1096
	FE103	3466	0.60	1273
	FE104	3836	0.90	948
	FE106	70076	0.26	899
	FE107	105916	0.65	1280
Range		3336 - 105916	0.26 – 0.9	899 - 1280
Average		32091	0.56	1109
Standard Deviation		44772	0.22	161
% Coefficient of Variation		139.52	38.91	14.48

Table 18 Master Summary of Flow Number Test Results for FORTA Evergreen 2 lb/Ton Mix

Mix Type	Specimen ID	Flow Number (cycles)	Axial Strain at Failure (%)	Resilient Modulus at Failure (psi)
2 lb/Ton Mix	FE201	4416	0.48	1213
	FE202	10716	0.47	1285
	FE203	9116	0.52	1129
	FE204	4656	0.23	2708
	FE206	3176	0.75	1046
	FE207	2096	0.63	1103
Range		2096 - 10716	0.23 – 0.75	1046 - 2708
Average		5696	0.51	1414
Standard Deviation		3433	0.17	640
% Coefficient of Variation		60.27	33.86	45.24

Table 19 presents the results of permanent to the resilient strain ratio ($\varepsilon_p/ \varepsilon_r$) for the three FORTA Evergreen mixtures. This has been found to be an important property for its future use in the Mechanistic-Empirical Pavement Design Guide (MEPDG). The Design Guide uses this ratio in the model that predicts permanent deformation in the asphalt layer.

Table 19 Summary of $\varepsilon_p/\varepsilon_r$ Ratio at Failure for Flow Number Test, FORTA Evergreen Mixtures

Mix Type	Specimen ID	σ_3 (psi)	σ_d (psi)	Flow Number	ε_p [%] at Failure	ε_r [%] at Failure	$\varepsilon_p/\varepsilon_r$ at Failure
Conv. Mix	FECO2	0.0	15.0	436	0.8470	0.007	121
	FECO3	0.0	15.0	241	0.5620	0.014	40
	FECO4	0.0	15.0	166	0.9550	0.02	48
1 lb Fiber Mix	FE101	0.0	15.0	5916	0.4640	0.007	66
	FE102	0.0	15.0	3336	0.4770	0.01	48
	FE103	0.0	15.0	3466	0.6080	0.013	47
	FE104	0.0	15.0	3836	0.9090	0.012	76
	FE106	0.0	15.0	70076	0.2600	0.004	65
	FE107	0.0	15.0	105916	0.6550	0.006	109
2 lb Fiber Mix	FE201	0.0	15.0	4416	0.4830	0.006	81
	FE202	0.0	15.0	10716	0.4690	0.011	43
	FE203	0.0	15.0	9116	0.5190	0.009	58
	FE204	0.0	15.0	4656	0.2310	0.009	26
	FE206	0.0	15.0	3176	0.7480	0.008	94
	FE207	0.0	15.0	2096	0.6280	0.012	52

Figures 25 and 26 represent typical repeated load/strain plots of FORTA control and fiber-reinforced asphalt concrete samples. Two important characteristics were observed for fiber-reinforced mixes when compared to the control mix. One was the endurance of the secondary stage and the second gradual (less) accumulation of permanent strain beyond tertiary flow for fiber-reinforced asphalt mix. Both were attributed to the presence of the Aramid fibers in the mix, as this behavior is not typically observed in conventional mixes.

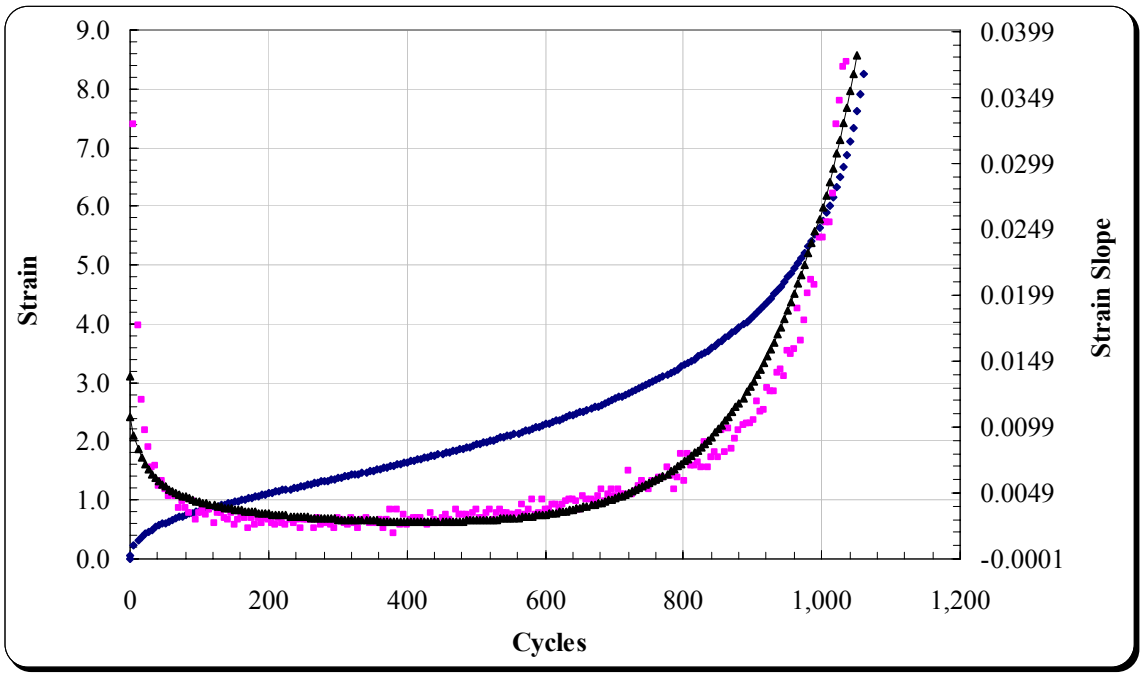

Figure 25 Repeated Load / Flow Number Results for FORTA Evergreen Control Mixture

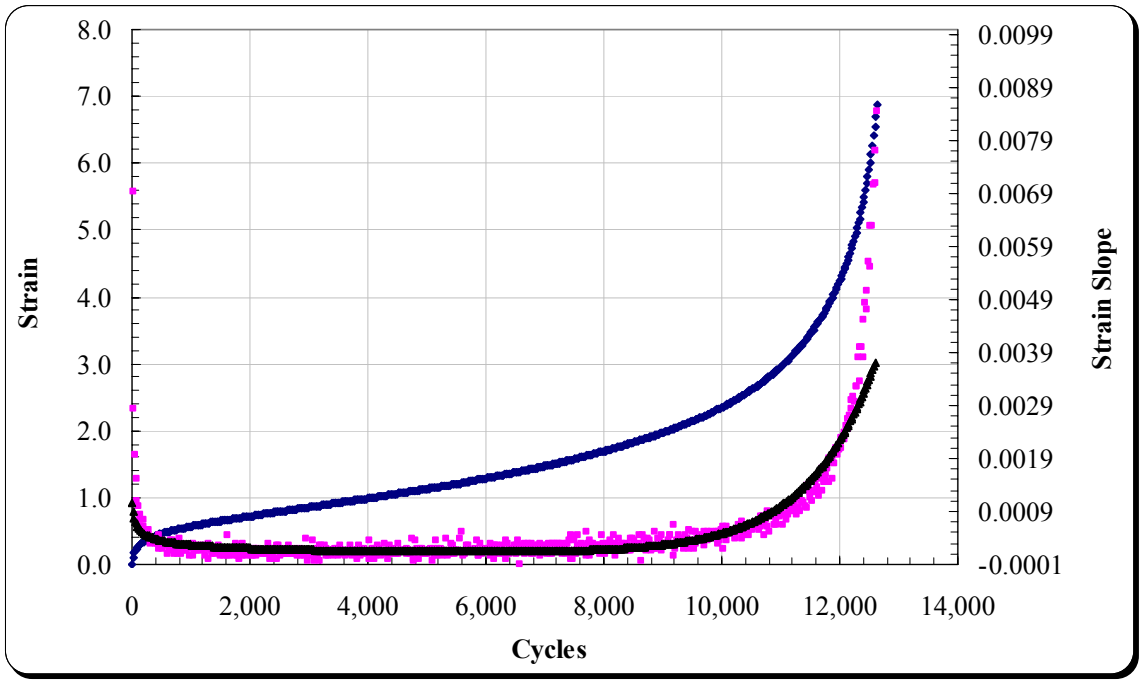

Figure 26 Repeated Load / Flow Number Results for FORTA Evergreen Fiber-Reinforced Mixture

Figure 27 shows a comparison of flow number for control and fiber-reinforced mixtures. As can be observed, the FN for fiber-reinforced mixtures are higher than the control mixture. The FN for 1 lb/Ton mix was 115 times higher than the control mix and 2 lb/Ton was 20 times higher than control mix. Also, between the fiber-reinforced mixtures, 1 lb/Ton mix had about 6 times higher FN than the 2 lb/Ton mix.

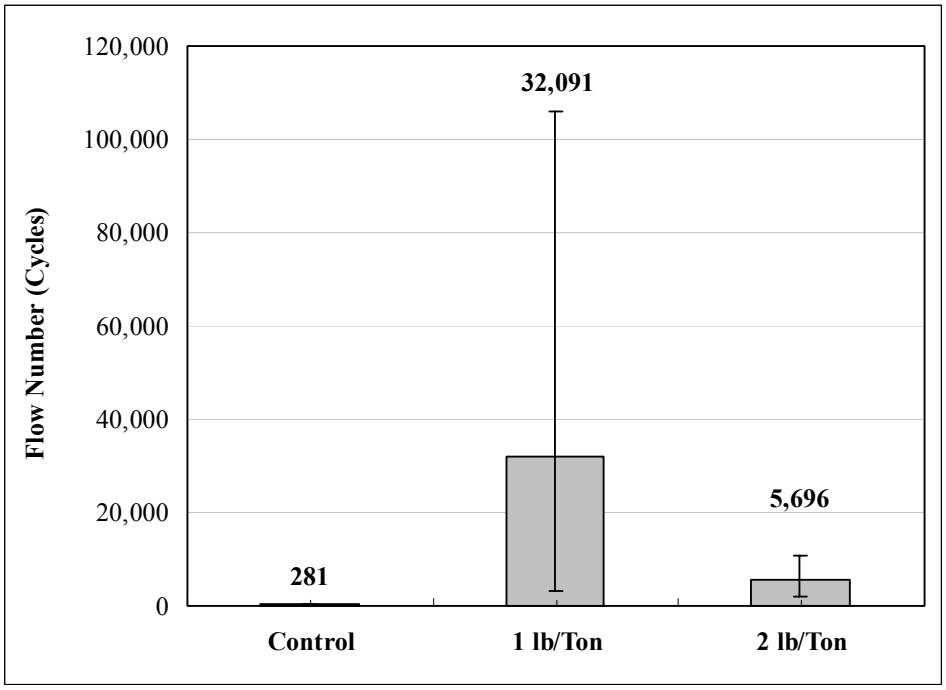

Figure 27 Axial Flow Number for FORTA Control and Fiber-Reinforced Mixtures

Figure 28 shows the range of FN for the three tested mixtures. It is noticed that the fiber-reinforced mixtures show higher variability in the test results than the control mixtures and this perhaps may be due to the inhomogeneous distribution of the fibers in the mix. This random distribution could be a function on how the fibers were added and mixed at the at the HMA production facility, and later on compacted in the laboratory. However, the FN values of fiber-reinforced mixtures were found to be higher than the control mixture.

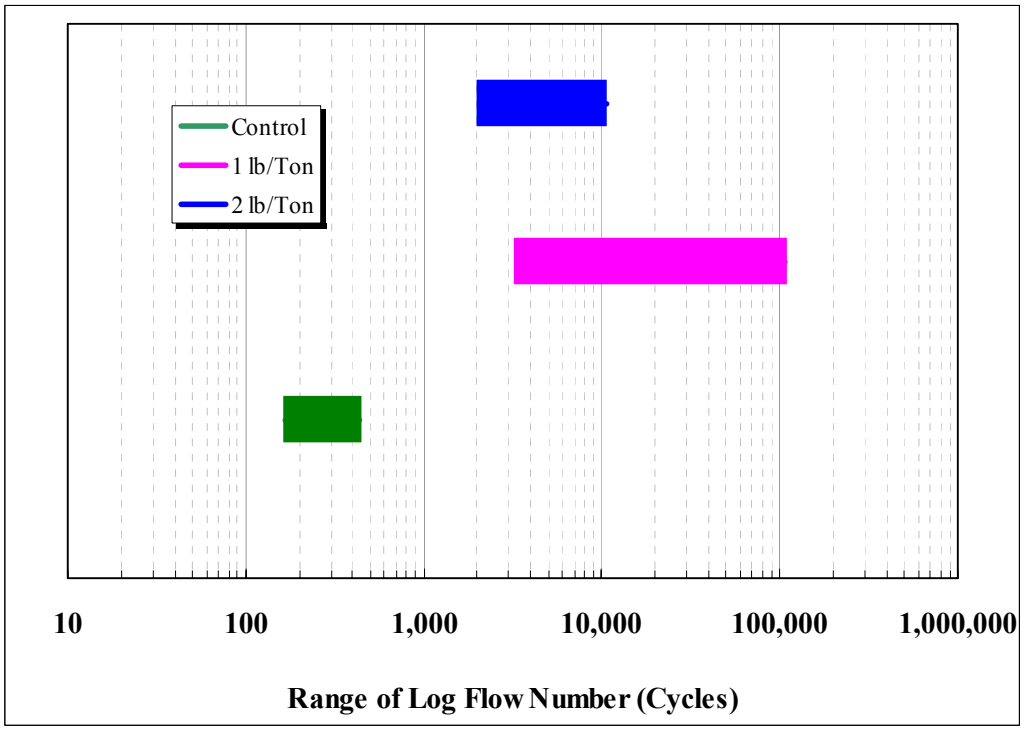

Figure 28 Flow Number Ranges at Failure for FORTA Evergreen Control and Fiber-Reinforced Mixtures

Figure 29 shows different values of axial strain at failure for FORTA Evergreen control and fiber-reinforced mixtures. It is noticed that the control mix has a higher axial strain values at failure when compared with the fiber-reinforced mixtures (40% higher than 1 lb/Ton mix and 55% higher than 2 lb/Ton mix). Also, the 1 lb/Ton mix has a slightly higher axial strain values at failure than 2 lb/Ton mix (~10% higher).

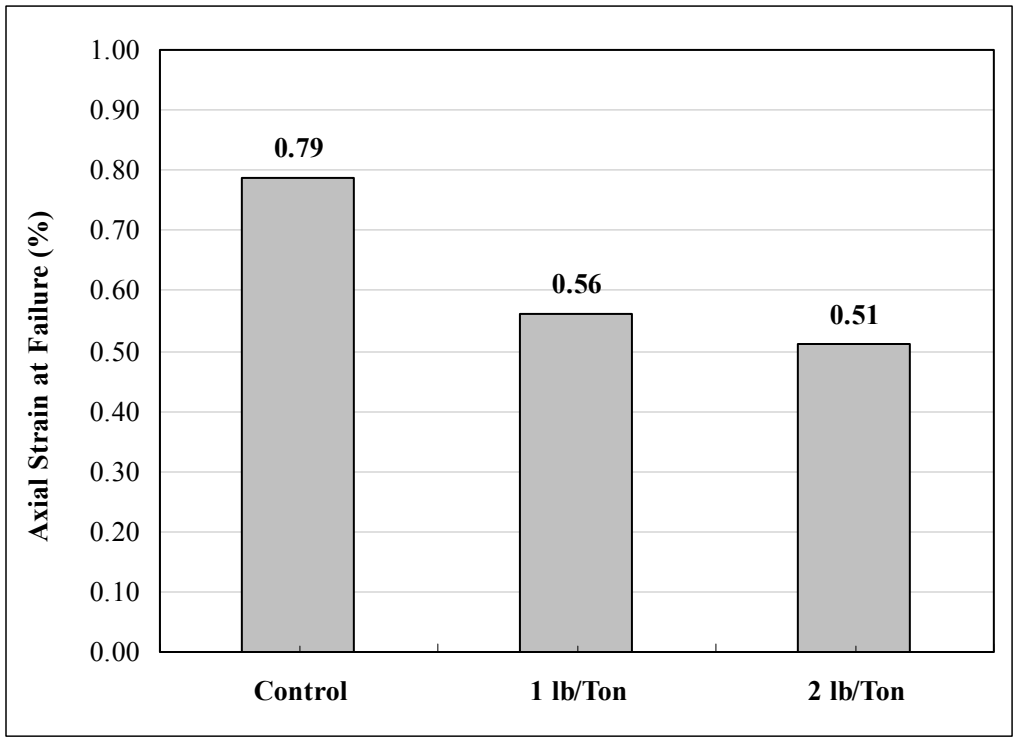

Figure 29 Axial Strain at Failure (%) for FORTA Control and Fiber-Reinforced Mixtures

The unconfined resilient modulus at flow results showed that there is no difference among the FORTA Evergreen mixtures (Figure 30); however, 1 lb/Ton has slightly lower values than the other two mixtures. The results of the slope of the permanent strain curve for the unconfined tests showed that the slope of the control mix is higher than the fiber-reinforced mixtures (Figure 31). Higher slope values are indicative of susceptibility of the mixture to permanent deformation. It is also noticed that both the 1 lb/Ton and 2 lb/Ton fiber-reinforced mixtures have about the same value of the slope parameters.

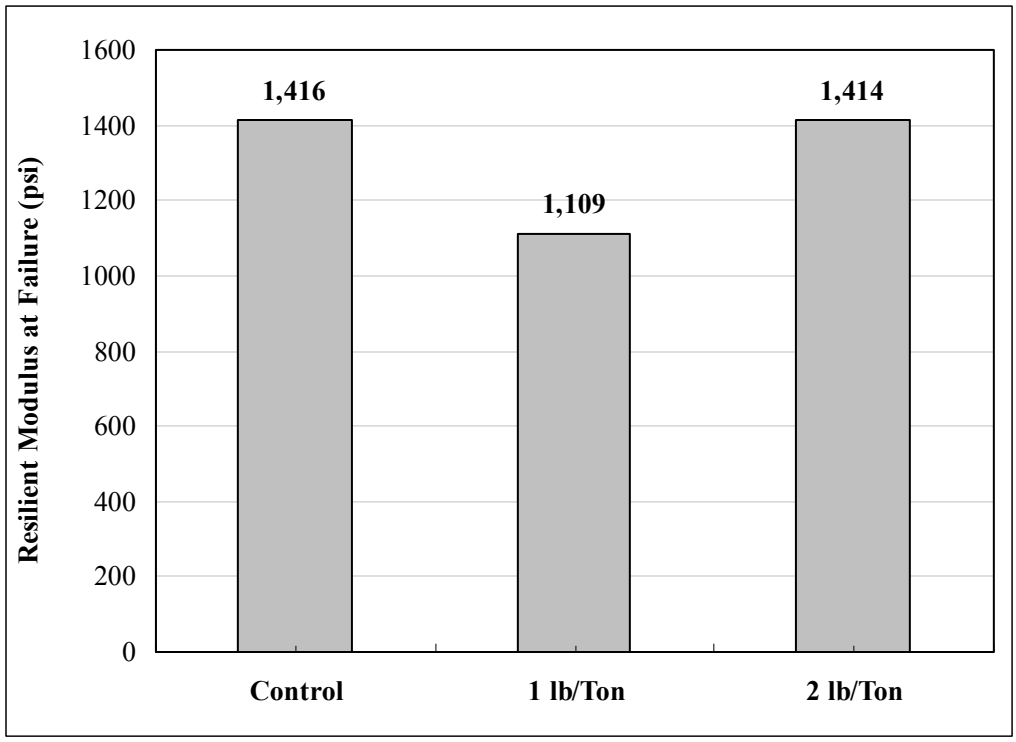

Figure 30 Resilient Modulus at Failure (%) for FORTA Control and Fiber-Reinforced Mixtures

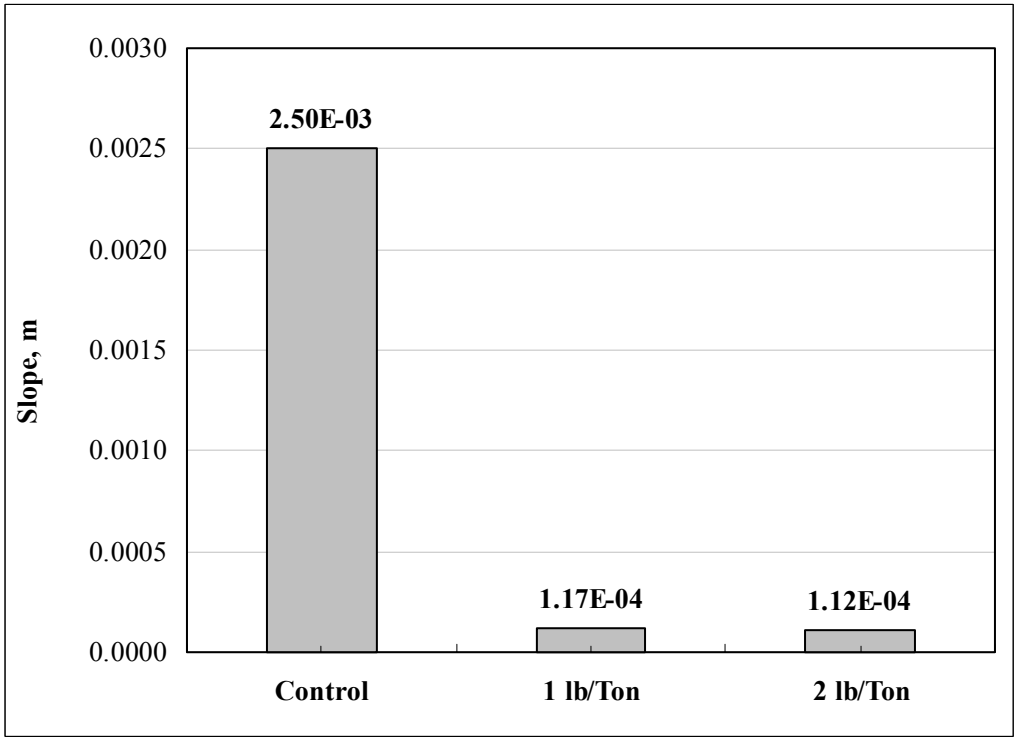

Figure 31 m, Slope for FORTA Control and Fiber-Reinforced Mixtures

Figure 32 shows the values of strain slope for FORTA Evergreen mixtures during the tertiary stage. It is noticed that the control mix has a higher strain slope compared to the fiber-reinforced mixtures. Also the 1 lb/Ton mix has a higher strain slope than the 2 lb/Ton mix. Lower values of strain slope during the tertiary stage (when the sample has already failed due to higher shear stress) means that the mix has higher potential to resist this shear failure and shows a lower rate of permanent deformation and rutting during this stage. Therefore, the fiber-reinforced mixes will show higher resistance to permanent deformation than the control mix. Furthermore, the presence of the Aramid fiber that imparts more resistance to the mix against shear failure by its reinforcing effect can hold the mix together even after failure, which is evident from the fiber-reinforced mixtures. With lower strain slopes of fiber-reinforced mixes, the mixes are capable to store more energy than conventional mixes before failure in the tertiary flow.

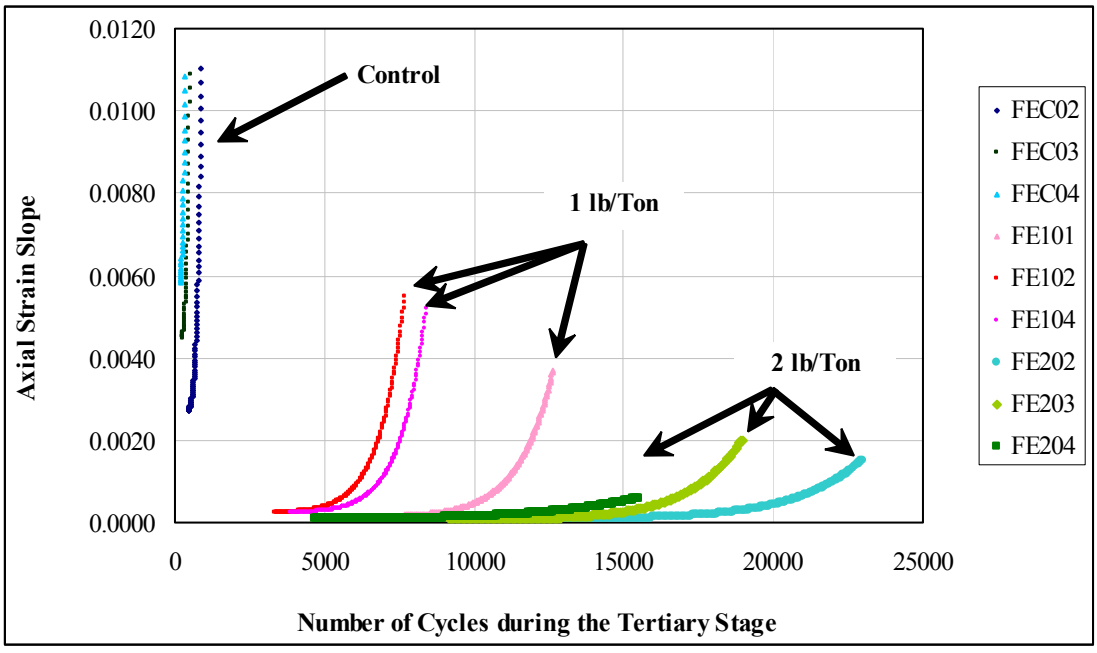

Figure 32 Axial Strain Slope during the Tertiary Stage for FORTA Evergreen Control and Fiber-Reinforced Mixtures

5.7 Summary of Static Creep / Flow Time Test

- Static creep tests were conducted at unconfined test conditions only using at least two replicate test specimens for each mixture. The deviator stress used for loading was 15-psi (105 kPa) for all the test samples. The tests were carried out at 130 ^{o}F (54.4 ^{o}C).
- All tests were carried out on cylindrical specimens, 100 mm (4 inches) in diameter and 150 mm (6 inches) in height.
- Two important characteristics were observed for fiber-reinforced mixes when compared to the control mix. One was the endurance of the secondary stage and the second gradual (less) accumulation of permanent strain beyond tertiary flow for fiber-reinforced asphalt mix. Both were attributed to the presence of the Aramid fibers in the mix, as this behavior is not typically observed in conventional mixes.
- Fiber-reinforced mixes had higher Flow Time values than the control mix (over 9 times for 1 lb/Ton mix and 5 times for 2 lb/Ton mix higher than the control mix). This indicates that fiber-reinforced mixes have the potential to resist permanent deformation better than the control mix. However, a lot of variability was observed between the FT values of fiber-reinforced mixtures within the same mixture. The reason for this variability perhaps could be due to inhomogeneous distribution and orientation of the fibers in the mixtures.
- The results of the slope parameter of the compliance curve showed that the control mix had 7 times higher slope than the 1 lb/Ton mix and 3 times than the 2 lb/Ton fiber-reinforced mix. Higher slope values are indicative of susceptibility of the mixture to permanent deformation.

5.8 Summary of Repeated Load / Flow Number Tests

- Repeated load / Flow Number tests were conducted at unconfined test conditions only using at least three replicate test specimens for each mixture. The deviator stress used for loading was 15-psi (105 kPa) for all the test samples. The tests were carried out at 130 ^{o}F (54.4 ^{o}C).
- All tests were carried out on cylindrical specimens, 100 mm (4 inches) in diameter and 150 mm (6 inches) in height.
- Similar to Flow Time tests, in the Flow Number tests, fiber-reinforced mixes when compared to the control mix showed an endurance of the secondary stage and a gradual (less) accumulation of permanent strain beyond tertiary flow. Both were attributed to the presence of the Aramid fibers in the mix, as this behavior is not typically observed in conventional mixes.
- The FN for 1 lb/Ton mix was 115 times higher than the control mix and 2 lb/Ton was 20 times higher than control mix. Also, between the fiber-reinforced mixtures, 1 lb/Ton mix had about 6 times higher FN than the 2 lb/Ton mix. But, the fiber-reinforced mixtures showed higher variability in the test results than the control mixtures and this perhaps may be due to the inhomogeneous distribution of the fibers in the mix.
- The results of the slope of the permanent strain curve showed that the slope of the control mix is higher than the fiber-reinforced mixtures. Higher slope values are indicative of susceptibility of the mixture to permanent deformation. Both the 1 lb/Ton and 2 lb/Ton fiber-reinforced mixtures had about the same value of the slope parameters.

- The control mix had a higher strain slope compared to the fiber-reinforced mixtures. Also the 1 lb/Ton mix had a higher strain slope than the 2 lb/Ton mix. Lower values of strain slope during the tertiary stage (when the sample has already failed due to higher shear stress) means that the mix has higher potential to resist this shear failure and shows a lower rate of permanent deformation and rutting during this stage.
- The fiber reinforcement, and in particular the Aramid fibers, provide unique resistance to the mix against shear failure beyond the tertiary flow point. This was evident from the monitoring the behavior of the fiber-reinforced mixtures in the tertiary stage of permanent deformation. With lower strain slopes of the fiber-reinforced mixes, the mixes are capable to store more energy than conventional mixes before and during tertiary flow.

6. DYNAMIC MODULUS TEST

6.1. Introduction

The main objective of this section is to summarize test data and master curve parameters obtained from the E* testing and analysis conducted for the FORTA Evergreen Project mixes.

6.2. Theory of Dynamic Modulus

For linear viscoelastic materials such as AC mixes, the stress-to-strain relationship under a continuous sinusoidal loading is defined by its complex dynamic modulus (E*). This is a complex number that relates stress to strain for linear viscoelastic materials subjected to continuously applied sinusoidal loading in the frequency domain. The complex modulus is defined as the ratio of the amplitude of the sinusoidal stress (at any given time, t, and angular load frequency, ω), $\sigma = \sigma_0 \sin(\omega t)$ and the amplitude of the sinusoidal strain $\varepsilon = \varepsilon_0 \sin(\omega t - \phi)$, at the same time and frequency, that results in a steady state response (Figure 33):

$$E^* = \frac{\sigma}{\varepsilon} = \frac{\sigma_0 e^{i\omega t}}{\varepsilon_0 e^{i(\omega t - \phi)}} = \frac{\sigma_0 \sin \omega t}{\varepsilon_0 \sin(\omega t - \phi)} \quad (6.1)$$

Where,

σ_0 = peak (maximum) stress

ε_0 = peak (maximum) strain

ϕ = phase angle, degrees

ω = angular velocity

t = time, seconds

Mathematically, the dynamic modulus is defined as the absolute value of the complex modulus, or:

$$|E^*| = \frac{\sigma_o}{\varepsilon_o} \qquad (6.2)$$

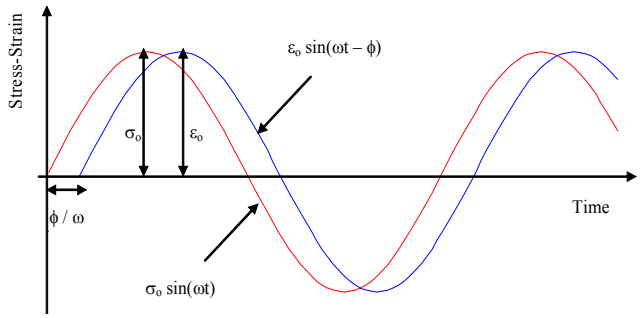

Figure 33 Dynamic (Complex) Modulus Test

For a pure elastic material, $\phi = 0$, and it is observed that the complex modulus (E*) is equal to the absolute value, or dynamic modulus. For pure viscous materials, $\phi = 90°$. The dynamic modulus testing of asphaltic materials is normally conducted using a uniaxially applied sinusoidal stress pattern as shown in the above figure.

6.3. Master Curve

In the Mechanistic Empirical Pavement Design Guide (MEPDG), the modulus of the asphalt concrete at all analysis levels of temperature and time rate of load is determined from a master curve constructed at a reference temperature (generally taken as 70 °F) (1). Master curves are constructed using the principle of time-temperature superposition. The data at various temperatures are shifted with respect to time until the curves merge into single smooth function. The master curve of the modulus, as a function of time, formed in this manner describes the time dependency of the material. The amount of shifting at each temperature required to form the

master curve describes the temperature dependency of the material. In general, the master modulus curve can be mathematically modeled by a sigmoidal function described as:

$$\text{Log}\,|E^*| = \delta + \frac{\alpha}{1 + e^{\beta + \gamma(\log t_r)}} \tag{6.3}$$

Where,

t_r = reduced time of loading at reference temperature

δ = minimum value of E*

$\delta+\alpha$ = maximum value of E*

β, γ = parameters describing the shape of the sigmoidal function

The shift factor can be shown in the following form:

$$a(T) = \frac{t}{t_r} \tag{6.4}$$

Where,

a (T) = shift factor as a function of temperature

t = time of loading at desired temperature

t_r = time of loading at reference temperature

T = temperature

While classical viscoelastic fundamentals suggest a linear relationship between log a(T) and T (in degrees Fahrenheit); years of testing by the researchers at ASU have shown that for precision, a second order polynomial relationship between the logarithm of the shift factor i.e. log $a(T_i)$ and the temperature in degrees Fahrenheit (T_i) should be used. The relationship can be expressed as follows:

$$\text{Log}\, a(T_i) = aT_i^2 + bT_i + c \tag{6.5}$$

Where,

$a(T_i)$ = shift factor as a function of temperature T_i

T_i = temperature of interest, °F

a, b and c = coefficients of the second order polynomial

It should be recognized that if the value of "a" approaches zero; the shift factor equation collapses to the classic linear form.

6.4. Summary of the Test Method

The NCHRP 1-37A Test Method DM-1 was followed for E* testing. For each mix, generally three replicates were prepared for testing (1). For each specimen, E* tests were generally conducted at 14, 40, 70, 100 and 130 °F for 25, 10, 5, 1, 0.5 and 0.1 Hz loading frequencies. A 60 second rest period was used between each frequency to allow some specimen recovery before applying the new loading at a lower frequency. Table 20 presents the E* test conditions.

Table 20 Test Conditions of the Dynamic Modulus (E*) Test

Test Temp. (°F)	Freq. (Hz)	Cycles	Rest Period (Sec)	Cycles to Compute E*
14, 40, 70, 100, 130 (Unless otherwise specified)	25	200	-	196 to 200
	10	100	60	196 to 200
	5	50	60	96 to 100
	1	20	60	16 to 20
	0.5	15	60	11 to 15
	0.1	15	60	11 to 15

The E* tests were done using a controlled stress mode, which produced strains smaller than 150 micro-strain. This ensured, to the best possible degree, that the response of the material was linear across the temperature used in the study. The dynamic stress levels were 10 to 100 psi for colder temperatures (14 to 70 °F) and 2 to 10 psi for higher temperatures (100 to 130 °F). All E*

tests were conducted in a temperature-controlled chamber capable of holding temperatures from 3.2 to 140 °F (–16 to 60 °C). The mixes were tested in unconfined mode only.

The axial deformations of the specimens were measured through two spring-loaded Linear Variable Differential Transducers (LVDTs) placed vertically on diametrically opposite sides of the specimen. Parallel brass studs were used to secure the LVDTs in place. Two pairs of studs were glued on the two opposite cylindrical surfaces of a specimen; each stud in a pair, being 100-mm (4 inch) apart and located at approximately the same distance from the top and bottom of the specimen. Top and bottom surface friction is a very practical problem for compressive type testing. In order to eliminate the possibility of having shear stresses on the specimen ends during testing, pairs of rubber membranes, with vacuum grease within the pairs, were placed on the top and bottom of each specimen during testing. Figure 34 shows the schematic presentation of the instrumentation of the test samples used in the dynamic modulus testing.

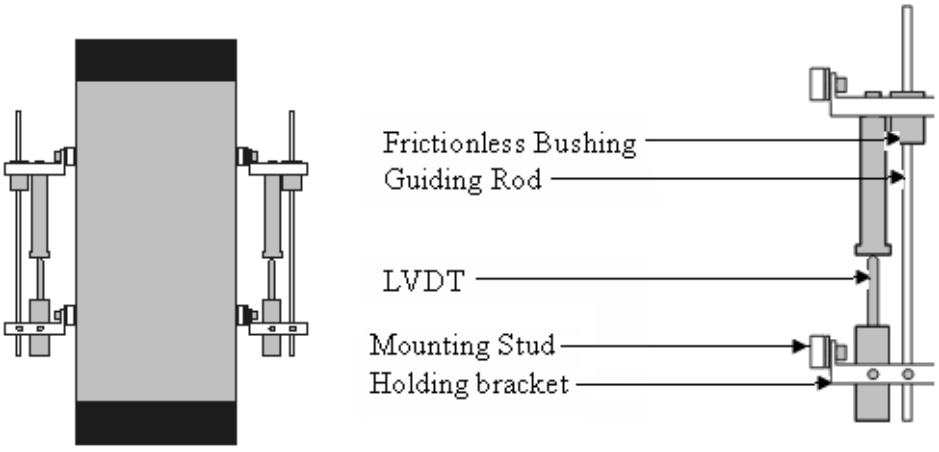

a. Sample Assembly b. Lateral View

Figure 34 Specimen Instrumentation of E* Testing

6.5. Test Data

The quality of the E* test data was checked by Black Space diagrams (E* versus ϕ), Cole-Cole Plane plots (E* sinϕ versus E* cosϕ) and E* versus loading frequency plots. Similar to the new MEPDG's input Level-1 approach, E* master curves of all mixtures were constructed for a reference temperature of 70 °F using the principle of time-temperature superposition. The time-temperature superposition was done by simultaneously solving for the four coefficients of the sigmoidal function (δ, α, β, and γ) as described in equation 6.3 and the three coefficients of the second order polynomial (a, b, and c) as described in equation 6.5. The "Solver" function of the Microsoft™ Excel was used to conduct the nonlinear optimization for simultaneously solving these 7 parameters.

For each mixture, the set of master curve parameters were obtained for: (i) average E* of all replicates, (ii) E* of all replicates, and (iii) each replicate. The E* of each mix at five test temperatures and six test loading frequencies were also computed using the 7 master curve and shift coefficients. The E* data obtained from laboratory for the three tested FORTA mixtures are summarized in Tables 21, 22 and 23. The Master Curve parameters are summarized in Tables 24, 25 and 26. Figures 35, 36 and 37 show the Master Curves for the three FORTA Evergreen mixes: Control, 1 lb/Ton and 2 lb/Ton mixtures using the equations 6.3, 6.4 and 6.5, the corresponding shift factors as well as Master curve for a typical replicate.

Table 21 Summary of E* and Phase Angle values for Unconfined FORTA Evergreen Control Mix

Mix	Temp.	Freq.	Dynamic Modulus, E* (ksi)					Phase Angle, ϕ (degrees)				
Control	°F	Hz	Rep1	Rep2	Rep3	Avg. E*	%C.V.	Rep1	Rep2	Rep3	Avg. ϕ	%C.V.
	14	25	6,154	5,862	6,161	6,059	3	3	4	8	5	45
		10	6,102	5,767	4,892	5,587	11	6	6	14	9	54
		5	6,050	5,634	4,816	5,500	11	7	7	16	10	51
		1	5,508	5,127	4,314	4,983	12	7	8	17	11	50
		0.5	5,290	4,883	4,154	4,775	12	8	8	17	11	47
		0.1	4,744	4,373	3,517	4,211	15	9	9	17	12	40
	40	25	3,904	4,180	4,489	4,191	7	9	9	8	9	7
		10	3,771	3,953	4,358	4,027	7	12	10	10	11	8
		5	3,579	3,703	4,096	3,793	7	13	10	13	12	13
		1	3,009	3,141	3,461	3,204	7	13	13	14	13	4
		0.5	2,771	2,893	3,156	2,940	7	14	13	14	14	5
		0.1	2,225	2,353	2,492	2,357	6	16	16	17	17	2
	70	25	1,979	2,562	2,232	2,258	13	16	13	19	16	18
		10	1,708	2,283	1,911	1,967	15	18	16	22	18	16
		5	1,517	2,067	1,696	1,760	16	20	18	25	21	16
		1	1,122	1,561	1,176	1,286	19	24	23	30	26	14
		0.5	970	1,362	991	1,108	20	26	26	33	28	14
		0.1	681	962	632	759	23	30	33	37	33	11
	100	25	941	1,363	725	1,010	32	22	19	28	23	19
		10	760	1,142	552	818	37	26	24	32	27	14
		5	631	986	438	685	41	28	26	32	29	10
		1	408	657	261	442	45	34	33	34	34	3
		0.5	332	540	208	360	46	36	35	35	35	2
		0.1	207	368	131	235	52	40	36	34	37	9
	130	25	339	578	244	387	44	29	26	31	29	9
		10	260	440	181	294	45	30	25	28	27	9
		5	198	380	163	247	47	30	25	26	27	11
		1	124	273	122	173	50	31	25	24	27	14
		0.5	103	247	118	156	51	31	26	25	28	12
		0.1	72	200	116	129	50	33	31	39	34	12

Table 22 Summary of E* and Phase Angle values for Unconfined FORTA Evergreen 1 lb/Ton Mix

Mix	Temp.	Freq.	Dynamic Modulus, E* (ksi)					Phase Angle, ϕ (degrees)				
1 lb/Ton	°F	Hz	Rep1	Rep2	Rep3	Avg. E*	%C.V.	Rep1	Rep2	Rep3	Avg. ϕ	%C.V.
	14	25	7,506	3,328	10,252	7,029	50	5	3	3	4	24
		10	6,411	2,880	10,242	6,511	57	7	3	4	5	36
		5	5,837	2,848	10,153	6,279	58	7	6	4	6	21
		1	5,191	2,740	9,513	5,815	59	9	10	5	8	37
		0.5	4,716	2,742	9,272	5,577	60	7	14	5	9	54
		0.1	4,019	2,570	8,372	4,987	61	7	17	5	10	64
	40	25	5,638	2,600	7,686	5,308	48	8	8	7	8	6
		10	5,500	2,358	7,539	5,132	51	9	8	9	9	9
		5	5,161	2,194	7,081	4,812	51	11	10	10	10	10
		1	4,480	1,972	6,262	4,238	51	12	10	11	11	9
		0.5	4,137	1,881	5,856	3,958	50	12	9	12	11	13
		0.1	3,415	1,545	5,017	3,325	52	14	12	14	13	11
	70	25	3,692	2,000	3,900	3,197	33	14	12	13	13	7
		10	3,202	1,900	3,669	2,924	31	18	15	16	16	7
		5	2,844	1,800	3,363	2,669	30	17	18	19	18	4
		1	2,137	1,633	2,587	2,119	23	21	22	23	22	4
		0.5	1,839	1,443	2,276	1,853	23	24	24	26	25	4
		0.1	1,243	1,022	1,617	1,294	23	30	29	31	30	4
	100	25	1,854	1,430	2,072	1,786	18	18	21	23	21	13
		10	1,531	1,223	1,745	1,500	18	23	25	26	24	6
		5	1,264	1,034	1,439	1,246	16	25	26	28	26	6
		1	839	678	924	814	15	31	33	34	32	5
		0.5	655	556	713	641	12	33	33	36	34	5
		0.1	309	357	280	315	12	41	36	44	40	10
	130	25	585	524	740	616	18	29	29	29	29	1
		10	439	392	567	466	19	29	29	31	29	3
		5	351	322	449	374	18	29	30	31	30	2
		1	221	205	269	231	14	30	30	31	30	3
		0.5	182	175	224	194	14	30	29	30	30	1
		0.1	123	124	165	138	17	29	27	30	28	5

Table 23 Summary of E* and Phase Angle values for Unconfined FORTA Evergreen 2 lb/Ton Mix

Mix	Temp.	Freq.	Dynamic Modulus, E* (ksi)					Phase Angle, ϕ (degrees)				
2 lb/Ton	°F	Hz	Rep1	Rep2	Rep3	Avg. E*	%C.V.	Rep1	Rep2	Rep3	Avg. ϕ	%C.V.
	14	25	3,843	6,223	5,288	5,118	23	7	6	4	6	33
		10	2,939	6,027	4,663	4,543	34	7	8	4	6	36
		5	2,805	5,825	4,414	4,348	35	8	8	5	7	22
		1	2,570	5,295	4,018	3,961	34	9	9	7	8	15
		0.5	2,452	5,061	3,788	3,767	35	8	9	7	8	13
		0.1	2,465	4,429	3,362	3,419	29	20	9	8	12	52
	40	25	2,545	4,449	3,460	3,485	27	7	8	10	8	24
		10	1,858	4,164	2,923	2,981	39	7	10	13	10	33
		5	1,751	3,867	2,708	2,775	38	11	12	14	12	10
		1	1,477	3,230	2,286	2,331	38	14	14	14	14	3
		0.5	1,362	2,927	2,079	2,122	37	15	15	16	15	2
		0.1	1,071	2,260	1,622	1,651	36	21	19	18	19	7
	70	25	2,323	2,378	2,300	2,334	2	19	17	18	18	5
		10	2,087	1,935	1,818	1,947	7	22	21	20	21	4
		5	1,850	1,629	1,550	1,676	9	24	24	23	24	2
		1	1,322	1,113	1,053	1,162	12	31	29	29	30	3
		0.5	1,119	921	877	972	13	34	32	32	33	3
		0.1	724	584	565	624	14	39	36	37	37	3
	100	25	1,368	822	826	1,005	31	24	25	28	26	7
		10	1,114	637	658	803	34	28	30	30	29	5
		5	901	511	540	650	33	29	31	32	31	6
		1	556	302	305	388	38	33	35	37	35	6
		0.5	423	237	240	300	35	36	36	37	36	3
		0.1	192	143	152	162	16	43	34	36	38	12
	130	25	421	226	272	306	33	33	31	31	32	3
		10	279	161	188	209	30	31	32	30	31	4
		5	217	125	151	164	29	30	28	27	28	5
		1	139	82	101	107	27	28	26	27	27	2
		0.5	118	72	92	94	25	27	26	26	26	2
		0.1	102	59	84	81	27	26	25	25	26	2

Table 24 E* Master Curve Parameters of FORTA Evergreen Control Mix

Mix	MC Parameter	Parameter Values Based On:				
		Avg. of Replicates	All data	Replicate-1	Replicate-2	Replicate-3
Control	δ	4.6375	4.6031	3.1309	4.6442	4.8958
	α	2.2064	2.2250	3.8666	2.2559	1.8056
	β	-0.6983	-0.7262	-1.1555	-0.7823	-0.5884
	γ	0.4547	0.4625	0.2967	0.3911	0.7031
	a	1.39E-04	1.57E-04	1.95E-04	9.14E-05	1.88E-04
	b	-0.0879	-0.0920	-0.1004	-0.0764	-0.1003
	c	5.4715	5.6671	6.0733	4.8987	6.0997

Table 25 E* Master Curve Parameters of FORTA Evergreen 1 lb/Ton Mix

Mix	MC Parameter	Parameter Values Based On:				
		Avg. of Replicates	All data	Replicate-1	Replicate-2	Replicate-3
1 lb/Ton	δ	4.2038	4.4335	4.5830	4.2562	4.1741
	α	2.6856	2.3829	2.2978	2.2665	2.8837
	β	-1.3240	-1.3149	-1.1945	-1.6875	-1.2548
	γ	0.4512	0.5053	0.5582	0.4949	0.4408
	a	7.80E-05	2.87E-05	-6.75E-05	-1.07E-04	2.61E-04
	b	-0.0740	-0.0634	-0.0437	-0.0389	-0.1084
	c	4.7941	4.2933	3.3912	3.2465	6.3048

Table 26 E* Master Curve Parameters of FORTA Evergreen 2 lb/Ton Mix

Mix	MC Parameter	Parameter Values Based On:				
		Avg. of Replicates	All data	Replicate-1	Replicate-2	Replicate-3
2 lb/Ton	δ	4.4383	4.4373	4.7174	4.2562	4.5471
	α	2.3090	2.2903	1.7685	2.6168	2.2051
	β	-0.8701	-0.8810	-1.3005	-0.8001	-0.6862
	γ	0.5434	0.5457	0.7990	0.4801	0.5533
	a	-2.67E-05	-3.26E-05	-1.64E-04	7.73E-05	4.07E-06
	b	-0.0517	-0.0511	-0.0172	-0.0790	-0.0590
	c	3.7498	3.7324	2.0035	5.1532	4.1061

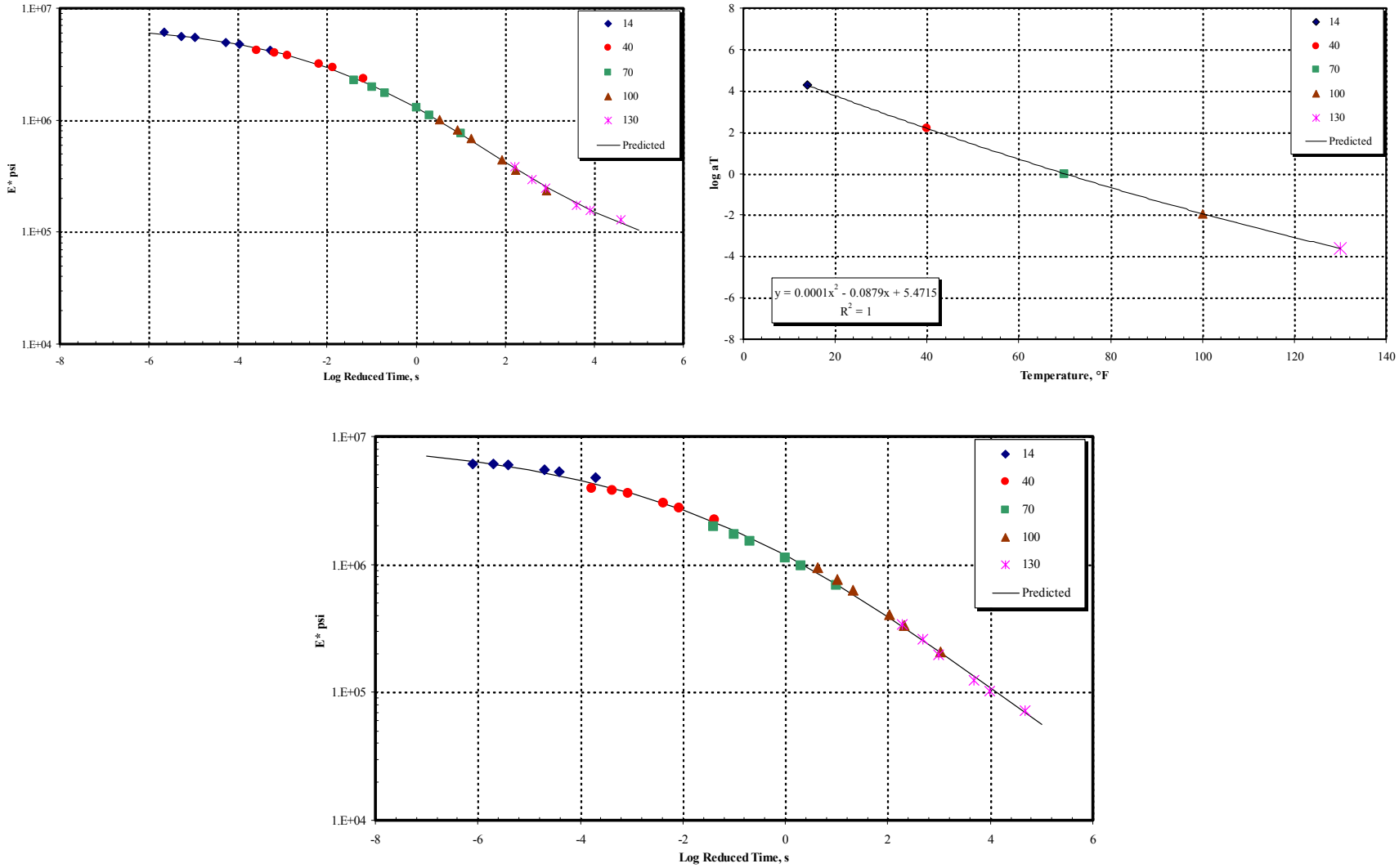

Figure 35 FORTA Evergreen Control Mix at Unconfined Condition (a) Master Curve based on Average of Three Replicates (b) Shift Factors based on Average of Three Replicates (c) Master Curve of a Typical Replicate

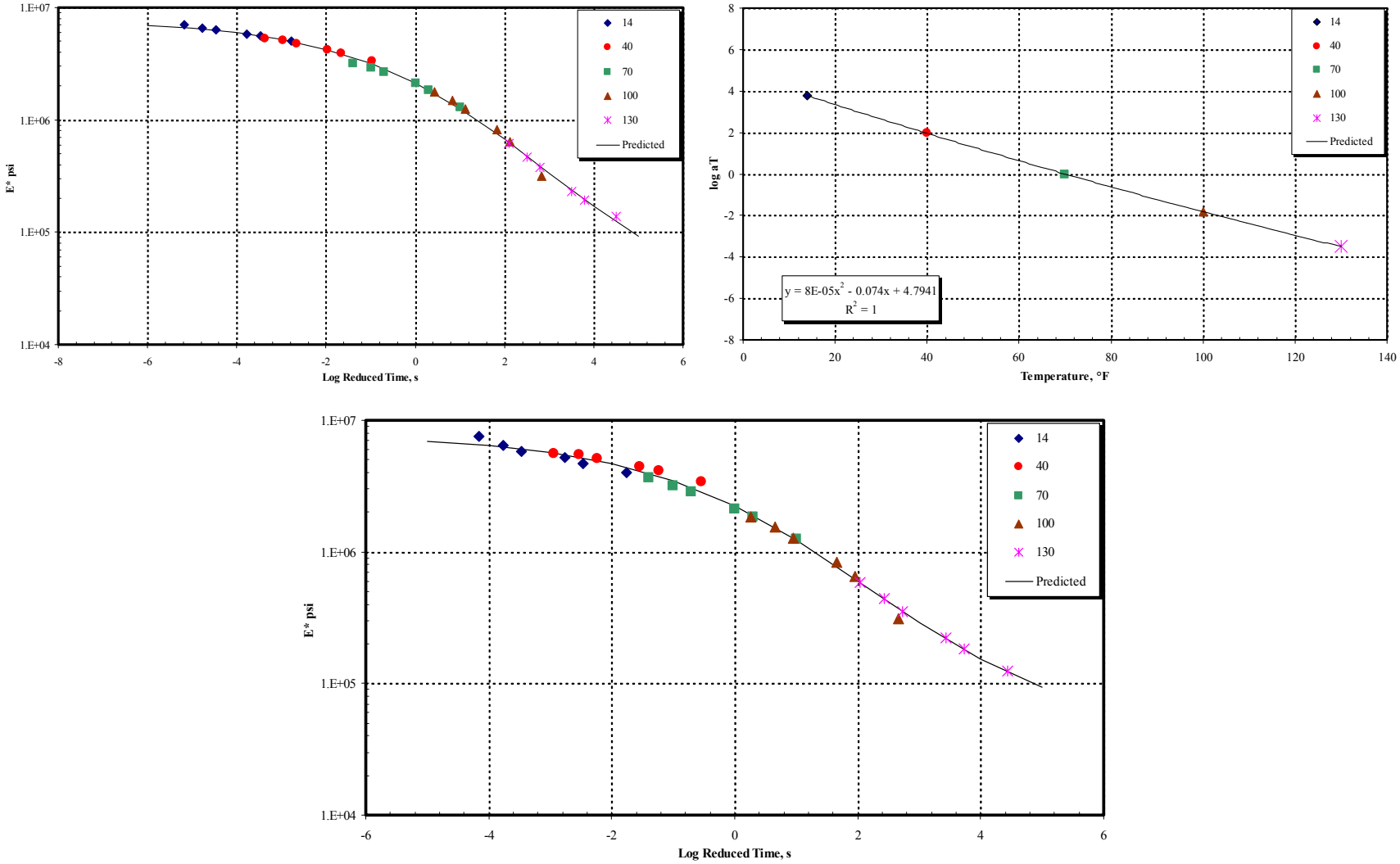

Figure 36 FORTA Evergreen 1 lb/Ton Mix at Unconfined Condition (a) Master Curve based on Average of Three Replicates (b) Shift Factors based on Average of Three Replicates (c) Master Curve of a Typical Replicate

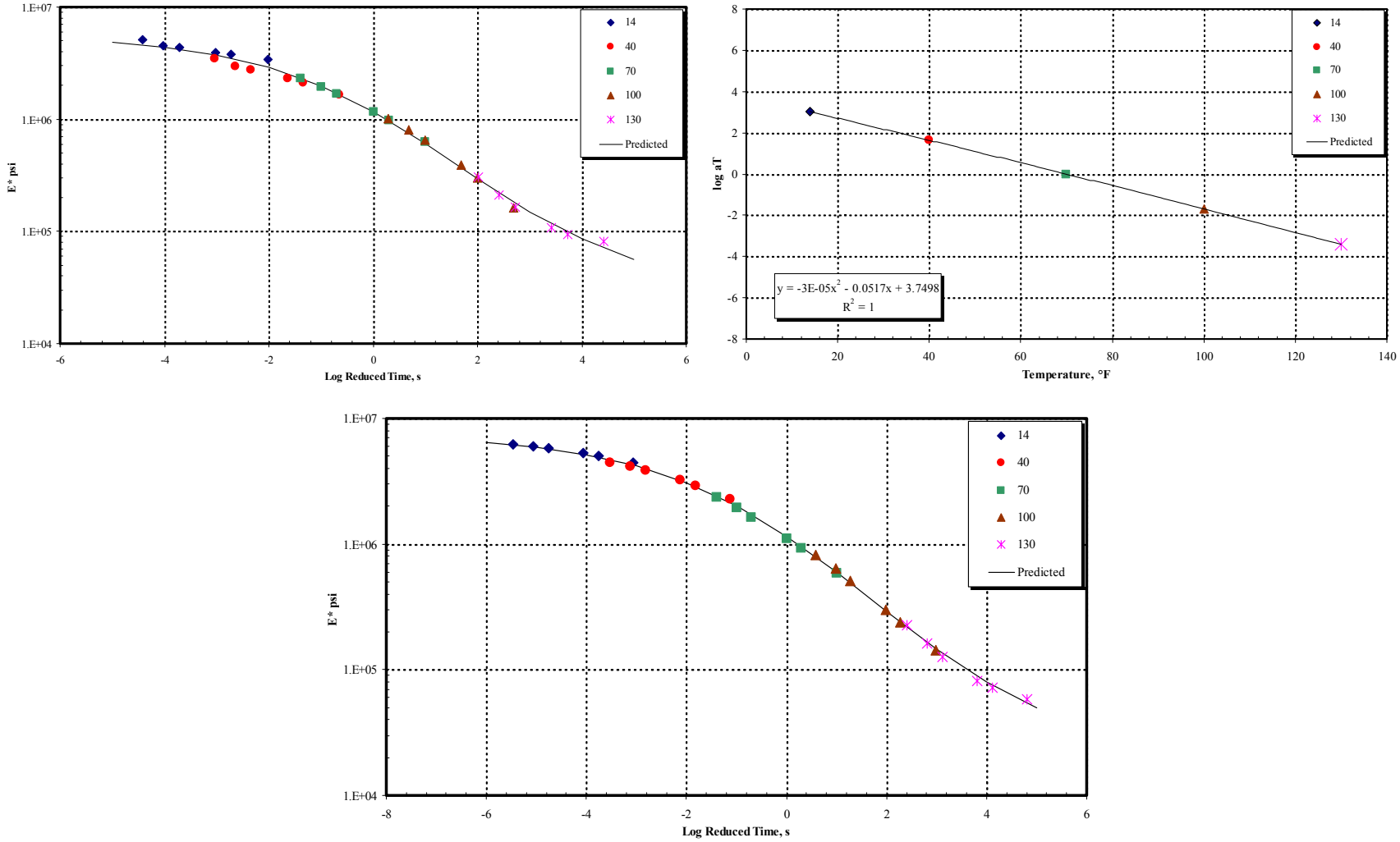

Figure 37 FORTA Evergreen 2 lb/Ton Mix at Unconfined Condition (a) Master Curve based on Average of Three Replicates (b) Shift Factors based on Average of Three Replicates (c) Master Curve of a Typical Replicate

6.6. Comparison of FORTA Evergreen Control Mix with Fiber-Reinforced Mixtures

This section provides the comparison of Dynamic Moduli between FORTA Evergreen Control mix without fiber-modification and two fiber-reinforced asphalt mixtures (1 lb/Ton and 2 lb/Ton mixtures). Figure 38 shows the average E* master curves for the three FORTA Evergreen mixtures under comparison. The figure can be used for general comparison of the mixtures, but specific temperature-frequency combination values need to be evaluated separately.

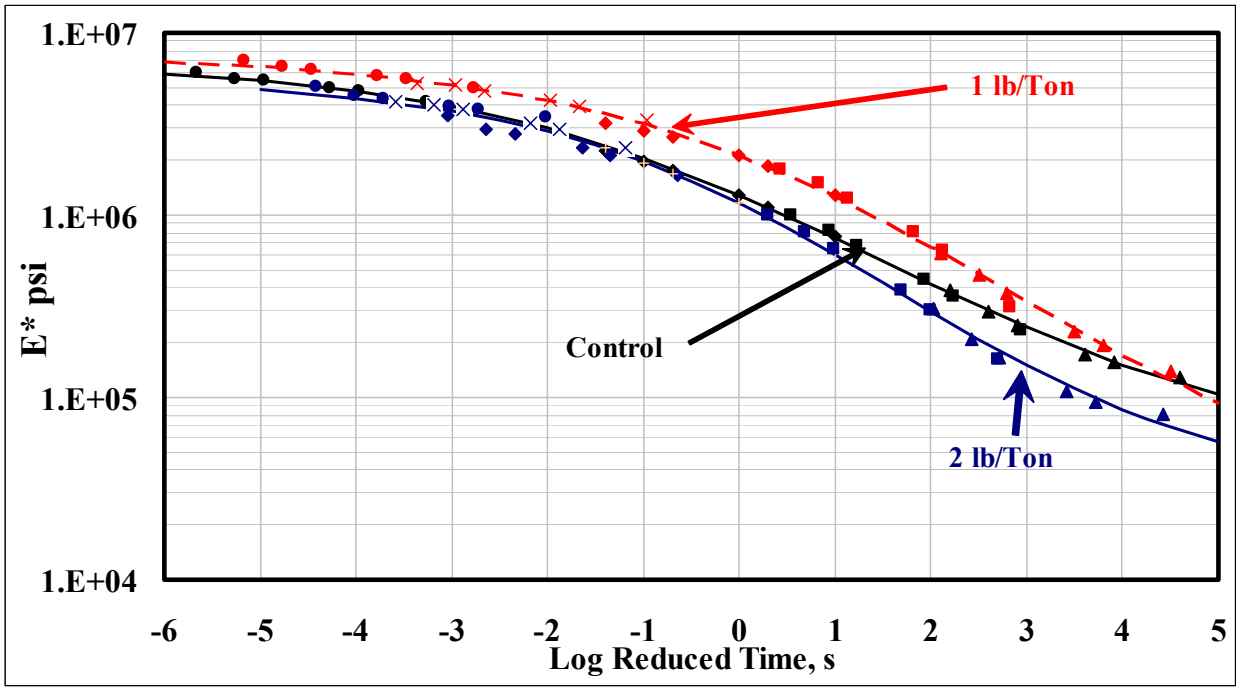

Figure 38 Unconfined Dynamic Modulus Master Curves for FORTA Evergreen Control, 1 lb/Ton and 2 lb/Ton Mixtures

As it is shown, FORTA 1 lb/Ton mixture shows, generally, the highest moduli values. This indicates that the fibers enhance the modulus of the mix and therefore its resistance to permanent deformation. However, the 2 lb/Ton mix test results did not show any improvement over control the mix. These result may indicate that the 1 lb/Ton mixture would be best, or optimum, for improved moduli properties.

The evaluation of modular ratios (R) of fiber-reinforced asphalt mixtures in contrast to the control mixes are described below. Modular Ratio (R) of a mix is represented by the following equation.

$$R = \frac{E^*_{MIX}}{E^*_{REFERENCE}} \quad (6.6)$$

Where:

R = Modular Ratio

E^*_{MIX} = Dynamic Complex Modulus value for a given mixture

$E^*_{REFERENCE}$ = Dynamic Complex Modulus value for the reference mixture

In this study, the temperature and frequency conditions used for the comparison were 40 ^oF for lower temperatures and 100 and 130 °F representing higher temperatures, at 10 Hz representing vehicle speed on an actual arterial street and 0.5 Hz which is the a lower test frequency analogous to the vehicle speed at parking lots or intersections. At cold temperatures, cracking is the most important consideration for an AC mixture. If the mix is too stiff, it will crack easily. Thus, to minimize cracking of an AC layer at cold temperatures, a lower stiffness is desirable for the mix.

Therefore, for E* values at 40 ^oF, the best performance will be that for the mix with the lowest E* value or lowest R. Conversely, at high temperatures, permanent deformation (rutting) is the most important distress that the AC mixture is affected by. Thus, the desired behavior of any mix at high temperatures is to have as stiff a layer as possible. Therefore, the best mix is the one that has the highest E* or R at 100 or 130 ^oF. Modular ratios translate the performance of fiber-

reinforced asphalt mixtures in comparison to the control mixtures into numbers that confirm if fiber modification provides any additional advantage on mixes' moduli. Table 27 shows ratios of dynamic modulus for fiber-reinforced mixes relative to the modulus of the control mix.

Table 27 Comparison of Modular Ratios (R) of FORTA Evergreen Fiber-Reinforced and Control Asphalt Concrete Mixes

Conditions	Temperature (°F)	Frequency (Hz)	R = E (1 lb/Ton)/ E (Control)	R = E (2 lb/Ton)/ E (Control)
High Temperatures at Moderate speed	130	10	1.59	0.71
	100	10	1.83	0.98
High Temperatures at Low Speed	130	0.5	1.24	0.60
	100	0.5	1.78	0.83
Low Temperature at Moderate speed	40	10	1.27	0.74
Low Temperature at Low Speed	40	0.5	1.35	0.72

As can be observed, the modular ratios of 1 lb/Ton mix with respect to the control mix was greater than 1 at all temperatures and frequency, a desirable characteristic especially for rutting resistance at higher temperatures and for all types of loading conditions. The modular ratios of 2 lb/Ton mix with respect to the control mix were all lower. The application of such dosage (2 lb/Ton) may be desirable for low temperature conditions, but it may not provide any additional advantage at the high temperature performance.

Figures 39 and 40 show a comparison for selected values of test temperatures (40, 100 and 130 ^{o}F) and loading frequencies (10 and 0.5 Hz). At high temperatures and selected frequency, the FORTA 1 lb/Ton mixture had the highest modulus than both the control and 2 lb/Ton mixtures (~1.8 times higher).

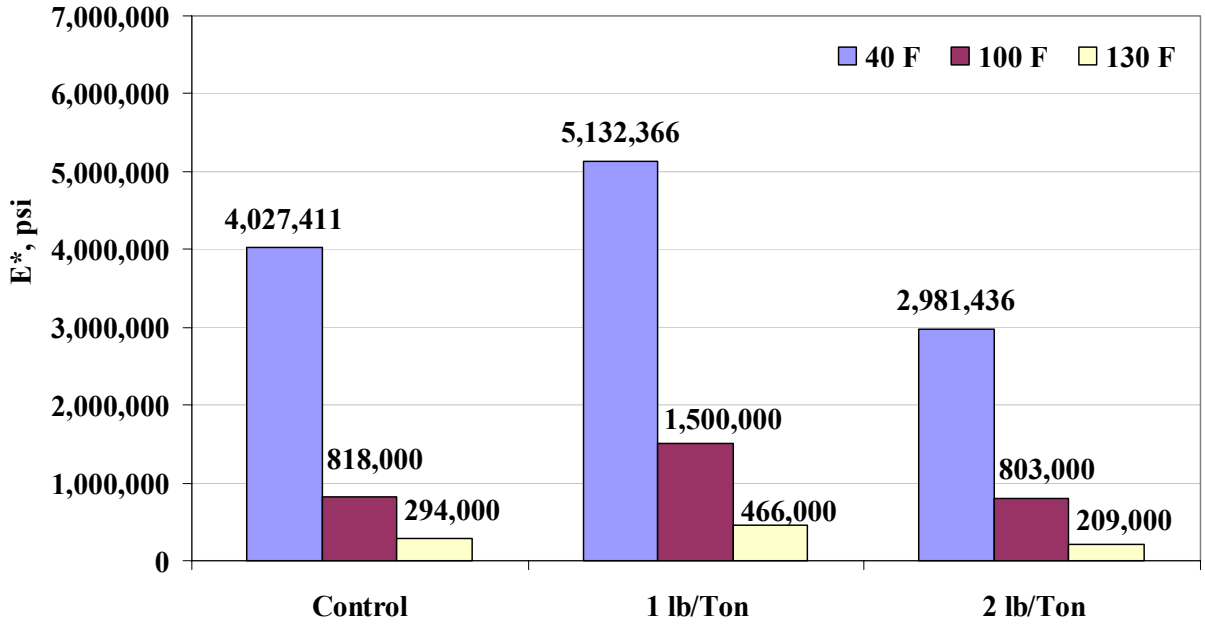

Figure 39 Comparison of Measured Dynamic Modulus E* values at 10 Hz for the FORTA Evergreen Control Mix and the Fiber-Reinforced Asphalt Mixtures at Selected Temperatures

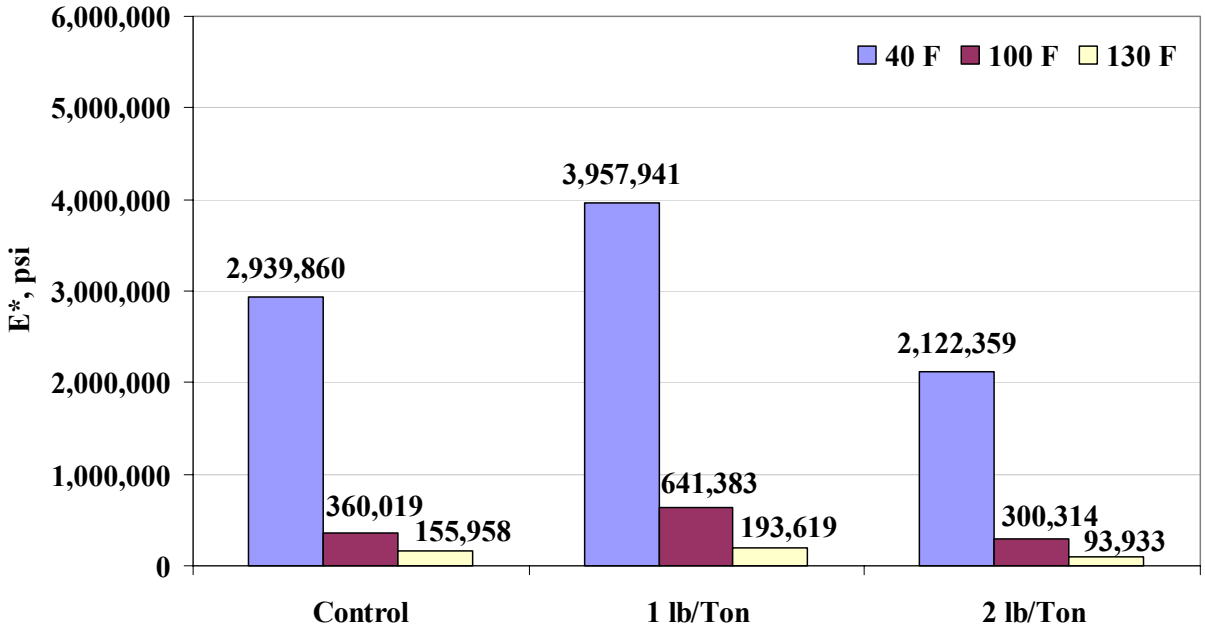

Figure 40 Comparison of Measured Dynamic Modulus E* values at 0.5 Hz for the FORTA Evergreen Control Mix and the Fiber-Reinforced Asphalt Mixtures at Selected Temperatures

6.7 Summary of E* Dynamic Modulus Test

- The NCHRP 1-37A Test Method was followed for E* testing. For each mix, at least three replicates were prepared for testing. For each specimen, E* tests were conducted at 14, 40, 70, 100 and 130 °F for 25, 10, 5, 1, 0.5 and 0.1 Hz loading frequencies.
- E* master curves of all mixtures were constructed for a reference temperature of 70 °F using the principle of time-temperature superposition.
- The moduli of the 1 lb/Ton mix was higher than the control mix which indicates that fibers enhance the modulus of the mix and therefore its resistance to permanent deformation. However, the 2 lb/Ton mix test results did not show any improvement over control the mix. These results may indicate that the 1 lb/Ton mixture would be best, or optimum, for improved moduli properties.
- The modular ratios of 2 lb/Ton mix with respect to the control mix were all lower. The application of such dosage (2 lb/Ton) may be desirable for low temperature conditions, but it may not provide any additional advantage at the high temperature performance.

7. FATIGUE CRACKING TESTS

7.1. Background of the Flexural Beam Fatigue Test

Load associated fatigue cracking is one of the major distress types occurring in flexible pavement systems. The action of repeated loading caused by traffic induced tensile and shear stresses in the bound layers, which will eventually lead to a loss in the structural integrity of a stabilized layer material. Fatigue initiated cracks at points where critical tensile strains and stresses occur. Additionally, the critical strain is also a function of the stiffness of the mix. Since the stiffness of an asphalt mix in a pavement layered system varies with depth; these changes will eventually effect the location of the critical strain that varies with depth; these changes will eventually effect the location of the critical strain that causes fatigue damage. Once the damage initiates at the critical location, the action of traffic eventually causes these cracks to propagate through the entire bound layer.

Over the last 3 to 4 decades of pavement technology, it has been common to assume that fatigue cracking normally initiates at the bottom of the asphalt layer and propagates to the surface (bottom-up cracking). This is due to the bending action of the pavement layer that results in flexural stresses to develop at the bottom of the bound layer. However, numerous recent worldwide studies have also clearly demonstrated that fatigue cracking may also be initiated from the top and propagates down (top-down cracking). This type of fatigue is not as well defined from a mechanistic viewpoint as the more classical “bottom-up” fatigue. In general, it is hypothesized that critical tensile and/or shear stresses develop at the surface and cause extremely large contact pressures at the tire edges-pavement interface this, coupled with highly aged (stiff) thin surface layer that have become oxidized is felt to be responsible for the surface cracking that

develops. In order to characterize fatigue in asphalt layers, numerous model forms can be found in the existing literature. The most common model form used to predict the number of load repetitions to fatigue cracking is a function of the tensile strain and mix stiffness (modulus). The basic structure for almost every fatigue model developed and presented in the literature for fatigue characterization is of the following form (11):

$$N_f = K_1\left(\frac{1}{\varepsilon_t}\right)^{k_2}\left(\frac{1}{E}\right)^{k_3} = K_1(\varepsilon_t)^{-k_2}(E)^{-k_3} \qquad (7.1)$$

Where:

N_f = number of repetitions to fatigue cracking

ε_t = tensile strain at the critical location

E = stiffness of the material

K_1, K_2, K_3 = laboratory calibration parameters

In the laboratory, two types of controlled loading are generally applied for fatigue characterization: constant stress and constant strain. In constant stress testing, the applied stress during the fatigue testing remains constant. As the repetitive load causes damage in the test specimen the strain increases resulting in a lower stiffness with time. In case of constant strain test, the strain remains constant with the number of repetitions. Because of the damage due to repetitive loading, the stress must be reduced resulting in a reduced stiffness as a function of repetitions. The constant stress type of loading is considered applicable to thicker pavement layers usually more than 8 inches. For AC thicknesses between these extremes, fatigue behavior is governed by a mixed mode of loading, mathematically expressed as some model yielding intermediate fatigue prediction to the constant strain and stress conditions.

7.2. Testing Equipment

Flexural fatigue tests are performed according to the AASHTO T321 (2), and SHRP M-009 (3). The flexural fatigue test has been used by various researchers to evaluate the fatigue performance of pavements (11-14). Figure 41 shows the flexural fatigue apparatus. The device is typically placed inside an environmental chamber to control the temperature during the test.

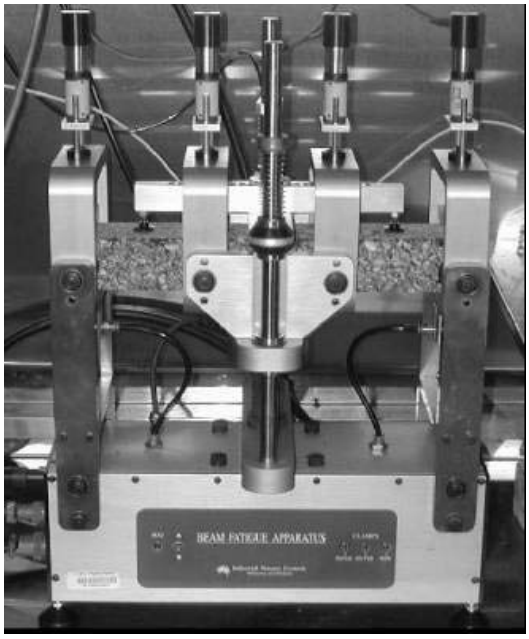

Figure 41 Flexural Fatigue Apparatus

The cradle mechanism allows for free translation and rotation of the clamps and provides loading at the third points as shown in Figure 42. Pneumatic actuators at the ends of the beam center it laterally and clamp it. Servomotor driven clamps secure the beam at four points with a pre-determined clamping force. Haversine or sinusoidal loading may be applied to the beam via the built-in digital servo-controlled pneumatic actuator. The innovative "floating" on-specimen transducer measures and controls the true beam deflection irrespective of loading frame compliance. The test is run under either a controlled strain or a controlled stress loading.

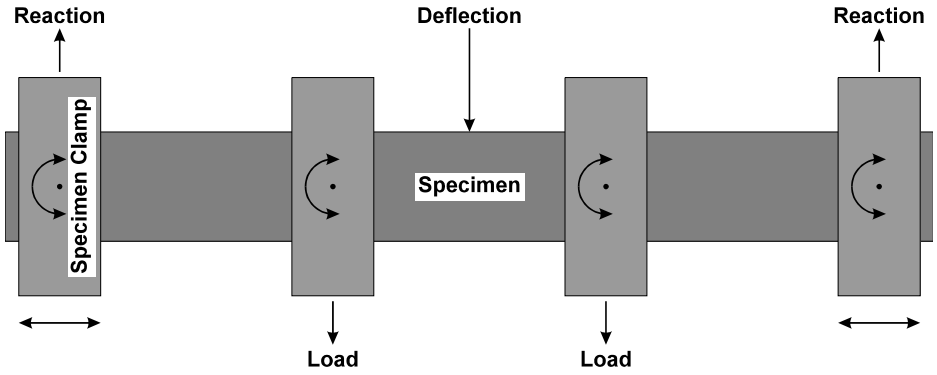

Figure 42 Loading Characteristics of the Flexural Fatigue Apparatus

In the constant stress mode, the stress remains constant but the strain increases with the number of load repetitions. In the constant strain test, the strain is kept constant and the stress decreases with the number of load repetitions. In either case, the initial deflection level is adjusted so that the specimen will undergo a minimum of 10,000 load cycles before its stiffness is reduced to 50 percent or less of the initial stiffness. In this study, all tests were conducted in the control strain type of loading.

7.3. Test Procedure and Calculations

The test utilized in this study applied repeated third-point loading cycles as was shown in above figure. The sinusoidal load was applied at a frequency of 10 Hz. The maximum tensile stress and maximum tensile strain were calculated as:

$$\sigma_t = 0.357\ P / b\ h^2 \qquad (7.2)$$

$$\varepsilon_t = 12\ \delta\ h / (3\ L^2 - 4\ a^2) \qquad (7.3)$$

where,

σ_t = Maximum Tensile stress, Pa

ε_t = Maximum Tensile strain, m/m

P = Applied load, N

b = Average specimen width, m

h = Average specimen height, m

δ = Maximum deflection at the center of the beam, m

a = Space between inside clamps, 0.357/3 m (0.119 m)

L = Length of beam between outside clamps, 0.357 m

The flexural stiffness was calculated as follow.

$$E = \sigma_t / \varepsilon_t \tag{7.4}$$

where,

E = Flexural stiffness, Pa

The phase angle (ϕ) in degrees was determined as follow.

$$\phi = 360\ f\ s \tag{7.5}$$

where,

f = Load frequency, Hz

s = Time lag between P_{max} and δ_{max}, seconds

The dissipated energy per cycle and the cumulative dissipated energy were computed using Equations 7.6 and 7.7, respectively.

$$w = \pi\ \sigma_t\ \varepsilon_t \sin\phi \tag{7.6}$$

$$\text{Cumulative Dissipated Energy} = \sum_{i=1}^{i=N} w_i \tag{7.7}$$

where,

w = Dissipated energy per cycle, J/m^3

w_i = w for the i^{th} load cycle

During the test the flexural stiffness of the beam specimen was reduced after each load cycle. The stiffness of the beam was plotted against the load cycles; the data was best fitted to an exponential function as follow.

$$E = E_i e^{bN} \quad (7.8)$$

where,

E = Flexural stiffness after n load cycles, Pa

E_i = Initial flexural stiffness, Pa

e = Natural logarithm to the base e

b = Constant

N = Number of load cycles

Once Equation 7.8 was formulated, the initial stiffness S_i can be obtained. Failure was defined as the point at which the specimen stiffness is reduced to 50 percent of the initial stiffness. The number of load cycles at which failure occurred was computed by solving Equation 7.8 for N, or simply:

$$N_{f,50} = [\ln (E_{f,50} / E_i)] / b \quad (7.9)$$

where,

$N_{f,50}$ = Number of load cycles to failure

$E_{f,50}$ = Stiffness at failure, Pa

7.4. Materials and Specimen Preparation

7.4.1. Materials

All beam specimens were prepared using the reheated hot mix asphalt Evergreen mixes that was obtained during construction.

7.4.2. Mold Assembly

The AASHTO TP8-94, and SHRP M-009, flexural fatigue testing protocol, require preparation of oversize beams that later have to be sawed to the required dimensions. The final required dimensions are 15 ± 1/4 in. (380 ± 6 mm) in length, 2 ± 1/4 in. (50 ± 6 mm) in height, and 2.5 ± 1/4 in. (63 ± 6 mm) in width. The procedure does not specify a specific method for preparation. Several methods have been used to prepare beam molds in the laboratory including full scale rolling wheel compaction, miniature rolling wheel compaction, and vibratory loading.

In this study beams were prepared using vibratory loading applied by a servo-hydraulic loading machine. A beam mold was manufactured at ASU with structural steel that is not hardened. The mold consists of a cradle and two side plates as shown in Figure 43 The inside dimensions of the mold are 1/2 inch (12 mm) larger than the required dimensions of the beam after sawing in each direction to allow for a 1/4 inch (6 mm) sawing from each face. A top loading platen was originally connected to the loading shaft assembly in the middle as shown in Figure 44. Note that the top platen is made of a series of steel plates welded at the two ends to distribute the load more evenly during compaction. The loading shaft was connected to the upper steel plate rather than extending it to the bottom plate so that an arch effect is introduced that would assist in distributing the load more uniformly. In addition, it was found that if the bottom surface of the

bottom plate is machined to be slightly concave upward, it would counter balance any bending that might occur during compaction and produce more uniform air void distribution.

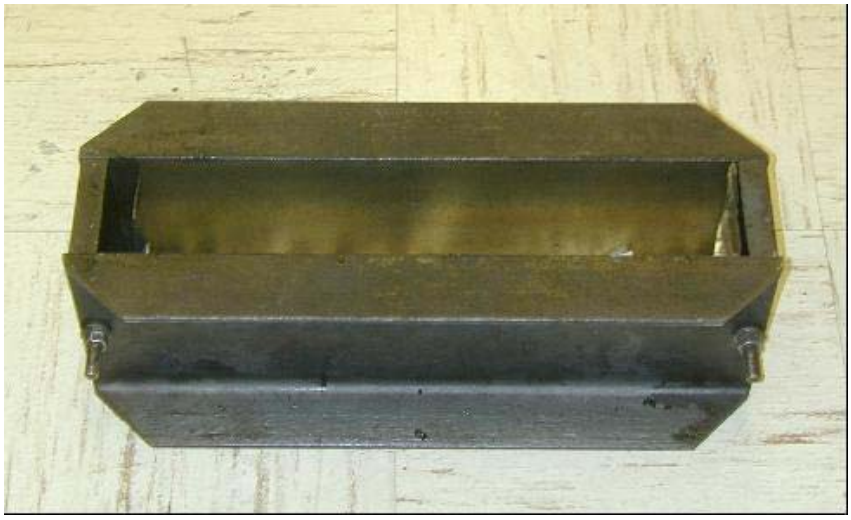

Figure 43 Manufactured Mold for Beam Compaction

Figure 44 Top Loading Platen

7.4.3. Specimen Preparation

The FORTA mixture was heated at 295 ^{o}F (146 ºC). The mold was heated separately for one hour at the same temperature as the mix. The mixture was placed in the mold in one load. The mold was then placed on the bottom plate of the loading machine and the top platen was lowered to contact the mixture.

A small load of 0.2 psi (1.4 kPa) was then applied to seat the specimen. A stress-controlled sinusoidal load was then applied with a frequency of 2 Hz and a peak-to-peak stress of 400 psi (2.8 MPa) for the compaction process. Since the height of the specimen after compaction was fixed, the weight of the mixture required to reach a specified air void value was pre-calculated. Knowing the maximum theoretical specific gravity and the target air voids, the weight of the mixture was determined. During compaction the loading machine was programmed to stop when the required specimen height was reached.

After compaction, specimens were left to cool to ambient temperature. The specimens were brought to the required dimensions for fatigue testing by sawing 1/4 inch (6 mm) from each side (Figure 45). The specimens were cut by using water cooled saw machine to the standard dimension of 2.5 in. (63.5 mm) wide, 2.0 in. (50.8 mm) high, and 15 in. (381 mm) long. Finally, the air void content was measured by using the saturated surface-dry procedure (AASHTO T166, Method A).

Figure 45 Specimen sawing

7.5. Testing Factorial

One load mode (control strain) using 6 to 10 levels of strain, one replicate each was used for testing at 40, 70, and 100 ºF (4.4, 21, and 37.8 ºC). One of the most difficult tasks is to compact beams from field mixes so that they all have the same or tight range of air void levels. This may be possible, but would require a large amount of materials and many trials. Because of the variable strain levels selected and consequent regression analysis conducted, the air void variation was relaxed to accept samples that are within 1% range.

7.5.1. Test Conditions

In summary the following conditions were used:

- Air voids: 7%.
- Load condition: Constant strain level, 5 levels of the range (50-550 μ strain).
- Load frequency: 10 Hz.
- Test temperatures: 40, 70 and 100 ^{o}F (4.4, 21, and 38.8 ^{o}C).

The tests were performed according to the AASHTO TP8, and SHRP M-009 procedures. Initial flexural stiffness was measured at the 50^{th} load cycle. Fatigue life or failure under control strain was defined as the number of cycles corresponding to a 50% reduction in the initial stiffness. The loading on most specimens was extended to reach a final stiffness of 30% of the initial stiffness instead of the 50% required by AASHTO TP8 and SHRP M-009. The control and acquisition software load and deformation data were reported at predefined cycles spaced at logarithmic intervals.

7.6. Test Results and Analysis

Tabular summaries of the fatigue test results and regression coefficients are presented in Tables 28, 29 and 30. Table 31 shows summary of regression coefficients for the fatigue relationships at 50% of initial stiffness for FORTA Evergreen mixtures. The relationships obtained were good to excellent measures of models accuracy as indicated by the coefficient of determination (R^2). Fatigue relationships (flexural strain versus the number of loading cycles) for each mixture are shown in Figures 46, 47 and 48. Figure 49 shows a relationship between each of the FORTA Evergreen mixtures at 70 ^{o}F and 50% of the initial stiffness values.

Table 28 Control Strain Beam Fatigue Test Results for FORTA Evergreen Control Mixture

Beam #	Temp [°F]	Air Void %	Width (mm)	Ht. (mm)	Strain Level (μ)	Initial Stiffness (10^3psi)		50% of Initial Stiffness				30% of Initial Stiffness			
						50 cycles	100 cycles	Stiffness (ksi)	Cycles	Phase Angle	Cum. Energy (psi)	Stiffness (ksi)	Cycles	Phase Angle	Cum. Energy (psi)
FEC06	40	6.63	66.0	51.4	50	1511.1	1487.7	754.9	1,298,170	6.1	1391.1	--	--	--	--
FEC10	40	6.92	64.3	51.2	100	1695.6	1687.0	846.4	47,610	14.7	259.5	507.8	87,990	25.4	411.8
FEC05	40	7.01	64.9	52.5	150	2005.7	2018.1	1001.6	12,020	5.5	149.0	601.6	30,660	0.3	334.8
FEC04	70	6.92	64.0	51.6	100	1083.4	1099.5	540.9	3,066,660	24.4	31337.6	317.8	3,328,290	28.4	33220.2
FEC15	70	6.93	63.4	50.8	125	1079.9	1078.3	539.2	508,940	25.8	8245.4	323.0	640,710	28.8	9677.7
FEC03	70	6.77	66.1	52.3	150	1152.4	1141.7	573.9	249,260	27.2	6000.6	341.5	329,860	26.8	7350.4
FEC13	70	6.88	64.9	50.7	200	899.0	884.4	449.0	62,390	27.8	2104.7	270.0	134,890	29.7	3843.2
FEC01	70	6.93	65.3	52.9	250	813.1	782.9	406.3	45,590	31.2	2143.2	240.9	85,110	27.6	3552.0
FEC14	70	6.90	63.7	50.2	300	984.0	908.0	492.0	3,380	26.2	217.0	295.0	7,010	27.8	475.9
FEC02	70	6.85	64.8	51.9	350	740.0	718.2	370.0	7,630	31.6	698.3	223.0	9,590	31.1	830.1
FEC29	100	7.01	63.8	51.1	200	536.1	517.9	267.9	276,480	31.9	5737.8	160.3	951,330	32.9	17612.1
FEC28	100	6.90	64.9	49.4	225	444.2	422.3	222.1	217,930	42.2	5747.8	129.5	240,800	37.1	6225.0
FEC25	100	6.72	66.7	50.3	250	380.0	363.5	189.9	104,710	39.7	3043.5	113.9	220,460	43.0	5560.2
FEC32	100	6.81	65.9	49.7	325	585.7	549.9	293.0	19,900	22.0	969.0	176.0	162,180	19.7	6996.6
FEC31	100	6.88	64.8	49.8	400	503.2	466.2	251.4	6,250	40.5	617.6	150.6	30,190	42.9	2341.9
FEC22	100	6.97	66.2	49.9	450	249.9	236.3	125.0	22,790	39.9	1545.2	75.0	28,320	24.4	1808.3
FEC26	100	6.81	64.1	49.2	500	363.7	337.5	182.0	5,430	43.7	659.2	109.0	14,340	44.7	1484.1

Table 29 Control Strain Beam Fatigue Test Results for FORTA Evergreen 1 lb/Ton Mixture

Beam #	Temp [°F]	Air Void %	Width (mm)	Ht. (mm)	Strain Level (me)	Initial Stiffness (10^3psi)		50% of Initial Stiffness				30% of Initial Stiffness			
						50 cycles	100 cycles	Stiffness (ksi)	Cycles	Phase Angle	Cum. Energy (psi)	Stiffness (ksi)	Cycles	Phase Angle	Cum. Energy (psi)
FE142	40	6.98	66.9	51.9	100	1585.71	1564.85	790.23	4,986,290	5.6	35570.00	474.76	7,432,090	10.9	49294.86
FE139	40	6.89	64.8	50.4	125	2303.91	2302.92	1148.13	360,300	10.0	5131.59	691.08	549,540	18.2	7340.04
FE137	40	7.04	64.1	49.8	150	1875.84	1861.29	937.11	232,630	10.1	3963.62	557.52	416,860	16.6	6553.13
FE138	40	6.89	65.0	50.1	175	1605.22	1621.84	797.35	64,070	6.8	1324.12	476.03	97,470	10.1	1820.15
FE135	70	7.02	67.1	51.2	125	1191.59	1195.98	595.27	744,160	22.3	10004.33	351.98	800,440	31.4	10535.06
FE128	70	7.30	69.9	50.9	150	1049.36	1036.11	515.13	228,200	24.8	4836.79	307.22	252,150	27.8	5157.58
FE127	70	6.82	68.9	51.3	175	1063.21	1053.53	528.30	229,960	25.8	6833.86	311.66	262,010	26.1	7526.10
FE126	70	7.04	69.0	51.3	250	970.50	946.30	485.00	8,580	25.2	437.91	291.00	12,390	21.0	571.11
FE129	70	6.81	70.2	50.7	300	1196.24	1163.79	598.00	5,310	19.0	368.58	358.90	7,300	18.8	476.84
FE114	100	7.17	67.5	50.0	100	419.05	413.70	195.26	3,082,390	33.8	15586.85	125.65	3,211,190	33.4	15970.80
FE124	100	6.92	70.0	50.7	150	208.20	206.30	102.42	418,470	50.8	2982.72	58.21	437,430	42.0	3068.92
FE115	100	7.03	69.1	50.0	175	317.96	304.66	158.87	346,730	39.0	4283.42	94.34	398,100	34.9	4674.65
FE110	100	7.22	70.2	53.4	200	295.09	279.75	146.87	217,100	44.3	3212.96	84.33	245,470	39.5	3495.86
FE111	100	7.31	68.2	51.2	250	216.33	214.30	108.03	198,000	42.8	3891.13	64.82	284,000	30.7	4868.47
FE122	100	7.11	66.9	50.8	350	138.15	135.18	69.05	39,700	35.7	924.71	41.40	82,110	42.1	1407.43
FE121	100	7.37	71.9	51.4	450	143.29	139.34	72.00	19,200	50.1	880.55	43.00	237	46.3	1022.95
FE107	100	6.84	63.9	52.6	550	274.73	255.01	137.00	4,490	48.8	541.87	82.00	14,490	46.2	1345.66

Table 30 Control Strain Beam Fatigue Test Results for FORTA Evergreen 2 lb/Ton Mixture

Beam #	Temp [F]	Air Void %	Width (mm)	Ht. (mm)	Strain Level (me)	Initial Stiffness (10^3psi)		50% of Initial Stiffness				30% of Initial Stiffness			
						50 cycles	100 cycles	Stiffness (ksi)	Cycles	Phase Angle	Cum. Energy (psi)	Stiffness (ksi)	Cycles	Phase Angle	Cum. Energy (psi)
FE224	40	7.17	66.6	50.3	100	1699.082	1722.049	837.799	532,920	12.2	4110.267	507.917	713,400	17.6	5151.241
FE222	40	7.41	65.7	53.8	125	2067.535	1994.092	1029.983	211,340	12.1	2725.250	617.162	348,070	16.7	4145.442
FE223	40	7.10	65.0	50.5	150	1879.085	1856.876	938.819	48,230	10.3	926.037	558.986	76,630	7.5	1348.540
FE215	70	7.09	65.9	49.0	150	1123.272	1109.552	561.168	815,950	24.4	15039.487	328.141	1,521,320	25.3	25838.332
FE216	70	7.21	65.3	50.6	175	986.069	968.969	486.888	85,550	23.5	2143.177	292.931	95,980	25.0	2313.114
FE214	70	6.72	64.3	49.8	200	1217.650	1176.881	604.035	43,310	23.7	1613.268	364.831	47,010	28.9	1707.376
FE213	70	6.88	66.5	51.0	250	1104.223	1076.283	552.000	10,410	23.8	536.460	331.000	19,000	22.3	834.260
FE206	100	7.11	67.9	52.5	150	340.886	348.437	170.400	767,360	33.8	6925.240	102.300	1,047,120	34.7	8872.160
FEC05	100	6.72	68.8	50.8	200	303.327	294.575	151.468	208,120	35.7	3068.727	90.761	396,580	31.1	5078.501
FE207	100	6.97	70.4	51.8	250	286.226	279.677	143.032	100,770	39.6	2201.014	85.661	225,590	34.1	4259.336
FE212	100	6.70	66.7	50.9	325	232.766	223.391	116.352	32,190	48.1	1063.855	68.926	45,350	44.3	1376.202
FE211	100	6.81	68.7	51.1	350	168.699	154.423	84.400	5,130	40.2	152.400	50.600	13,180	39.3	308.460
FE208	100	6.80	66.1	50.9	450	238.872	222.809	119.400	3,720	42.5	247.230	71.700	5,560	40.9	331.000

Table 31 Summary of Regression Coefficients for the Fatigue Relationships at 50% of Initial Stiffness, FORTA Evergreen

Mix Type	100 °F			70 °F			40 °F		
	k1	k2	R^2	k1	k2	R^2	k1	k2	R^2
Control	0.0028	-0.2068	0.873	0.0012	-0.1529	0.712	0.0013	-0.2301	0.993
1 lb/Ton	0.0064	-0.2792	0.969	0.005	-0.2649	0.950	0.0007	-0.1278	0.939
2 lb/Ton	0.002	-0.185	0.941	0.0007	-0.116	0.941	0.0009	-0.1646	0.964

* $N_f = K_1 * (1/\varepsilon_t)^{K2}$

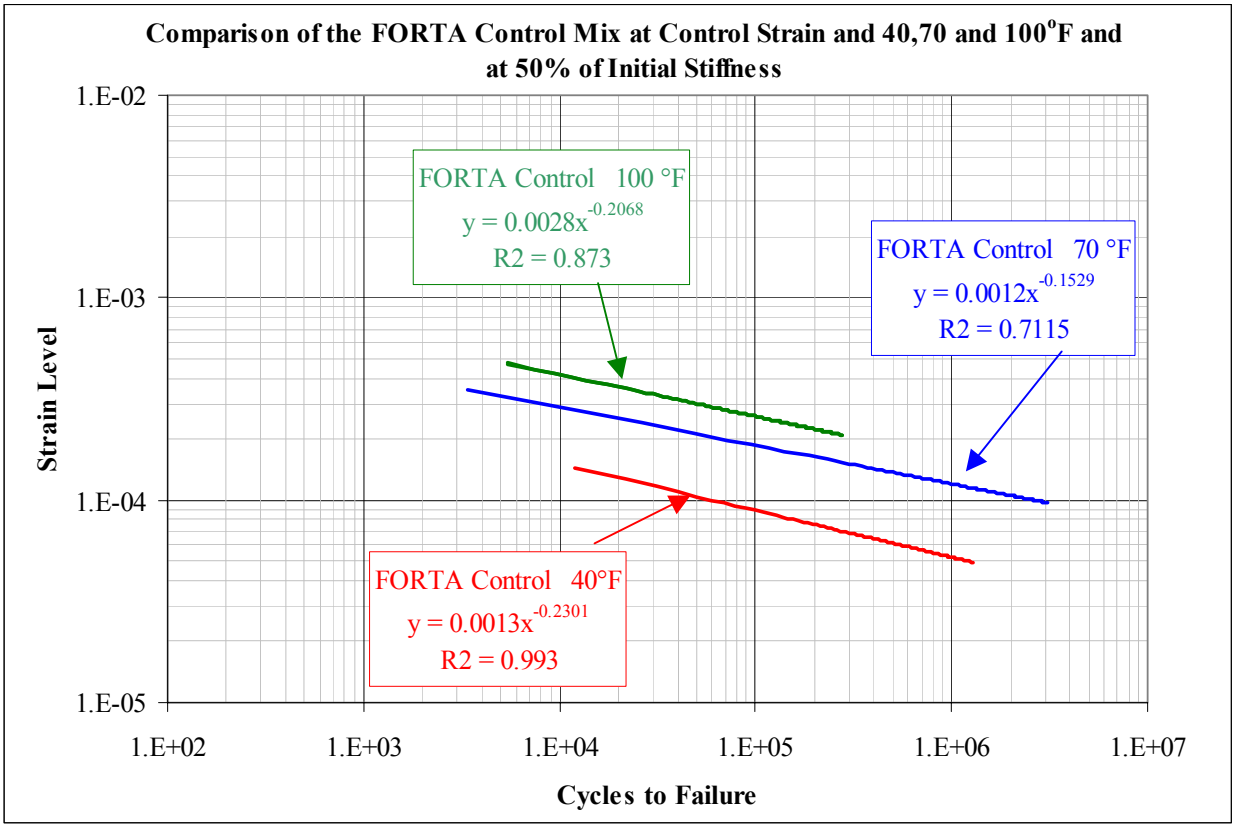

Figure 46 Comparison of Fatigue Relationships for the FORTA Evergreen Control Mixture

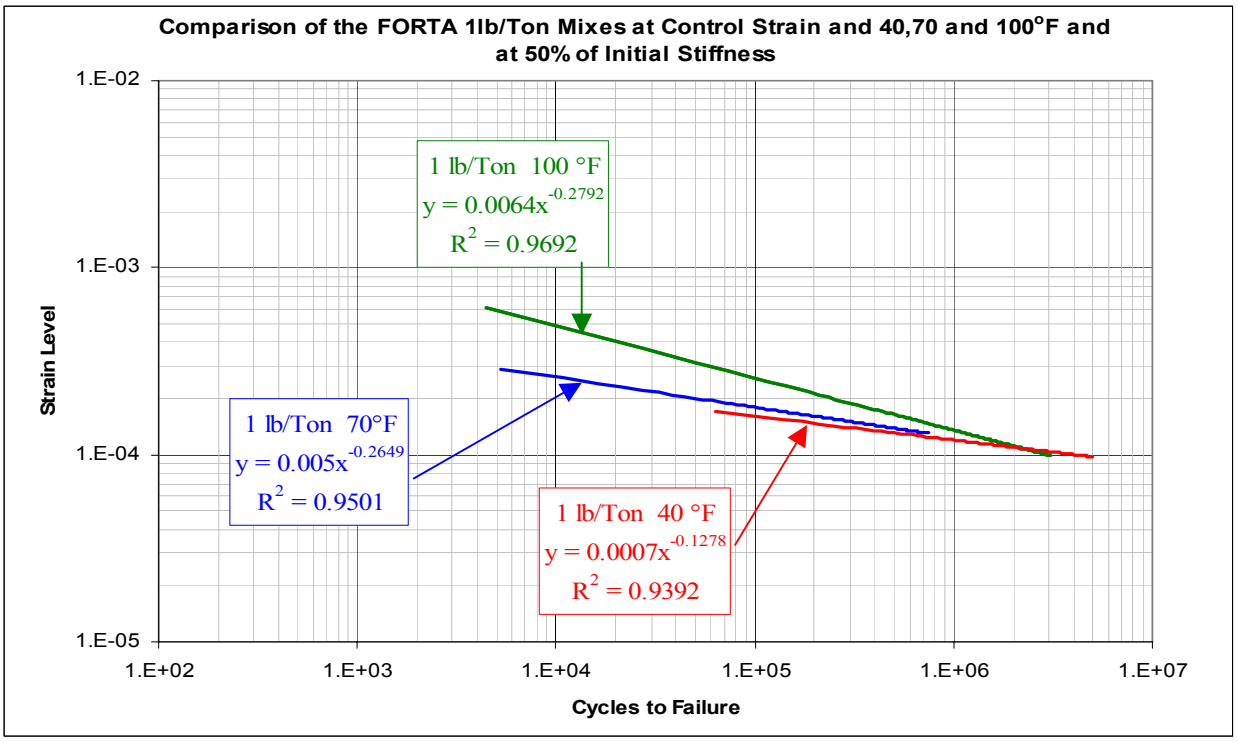

Figure 47 Comparison of Fatigue Relationships for the FORTA Evergreen 1 lb/Ton Mixture

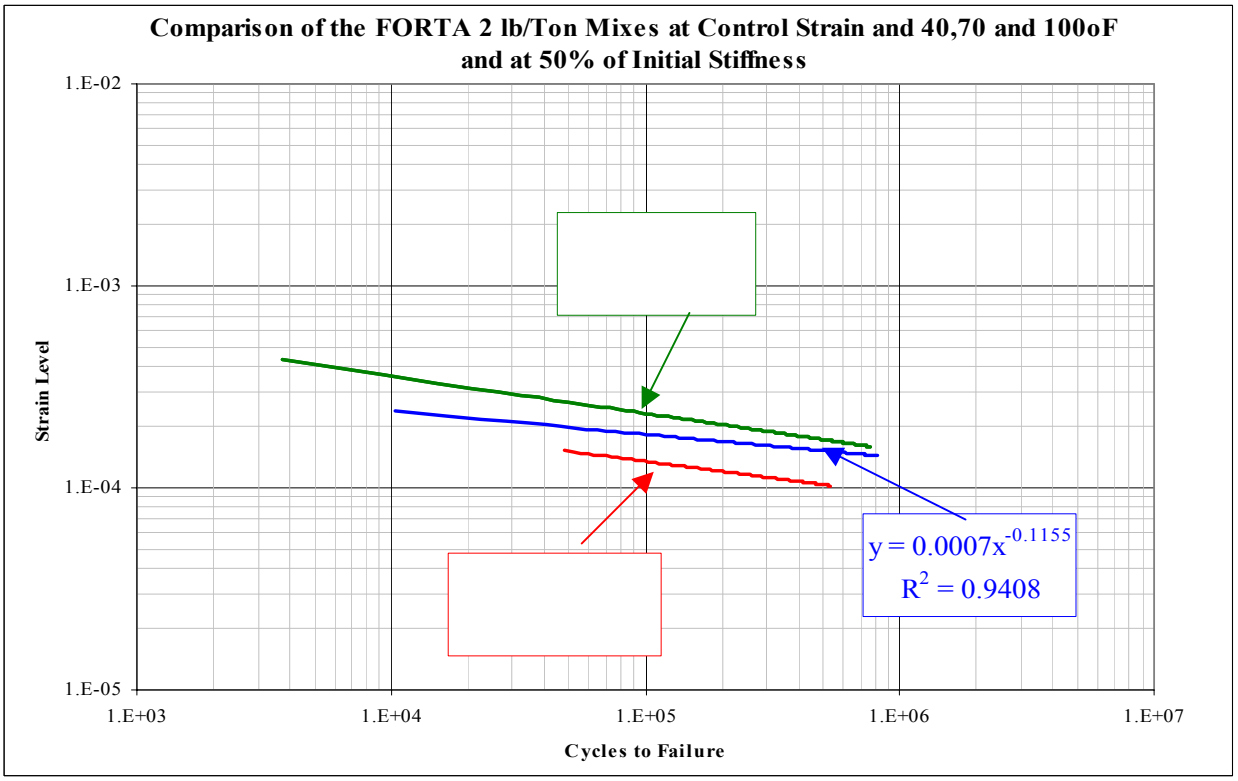

Figure 48 Comparison of Fatigue Relationships for the FORTA Evergreen 2 lb/Ton Mixture

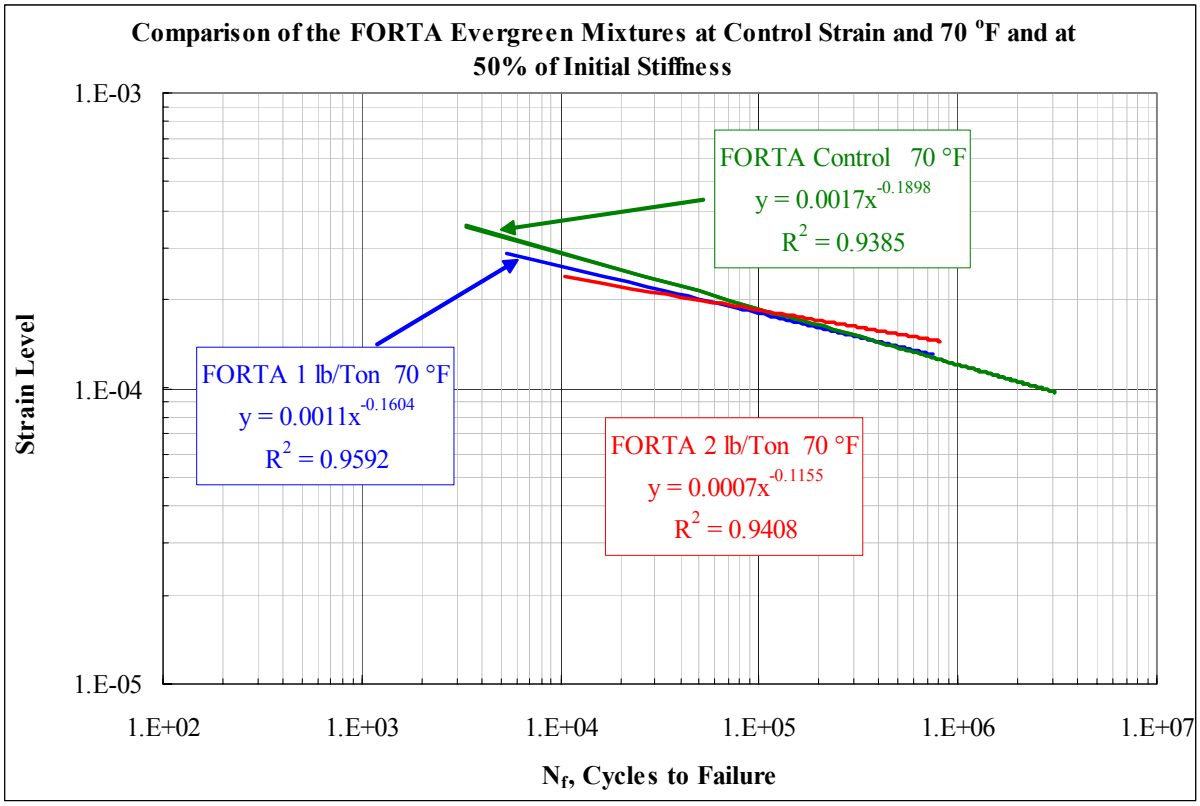

Figure 49 Comparison of Fatigue Relationships for FORTA Evergreen Mixtures

Table 32 summarizes the K_1, K_2 and K_3 Coefficients of the generalized fatigue model for FORTA Mixture (at 50% reduction of initial stiffness). The initial stiffness was measured at N = 50 cycles. These generalized fatigue relationships show excellent measures of accuracy for both control and 1 lb/Ton mixes while the accuracy is lower for 2 lb/Ton mix.

Table 32 Summary of the Regression Coefficients for Generalized fatigue Equation, FORTA Evergreen

Mix Type	50% of Initial Stiffness, So @ N=50 Cycles			
	K_1	K_2	K_3	R^2
FORTA Control	2.3496	2.3601	1.3853	0.914
FORTA 1 lb/Ton	6.48E-22	7.8357	1.0839	0.988
FORTA 2 lb/Ton	5.3E-05	3.24557	0.89885	0.622

* $N_f = K_1 * (1/\varepsilon_t)^{K2} * (1/So)^{K3}$

Figure 50 shows a comparison of Initial Flexural Stiffness for FORTA Evergreen mixtures at different test temperatures. It is noticed that the fiber-reinforced mixtures show slight higher stiffness values comparing with the FORTA Evergreen control mix at 40 and 70 ºF while, for 100 ºF, the control mix shows a about 1.7 higher initial stiffness compared to fiber-reinforced mixtures. An example comparing the fatigue life for FORTA mixtures was predicted using the regression coefficients K1, K2, and K3 at 40, 70, and 100 ºF and for two different strain levels. The results are shown in Figure 51 (a, b). At 150 micro-strains level (Figure 51 (a)), both fiber-reinforced mixture show higher fatigue life compared to the control mixture at different test temperatures especially the 1 lb/Ton mix; while at 200 micro-strains level (Figure 51 (b)), the 2 lb/Ton mixture shows the highest fatigue life followed by the control then the 1 lb/Ton mix. The shift in predicted fatigue life suggests that the fiber-reinforced mixtures will perform better in roads where traffic speeds are higher.

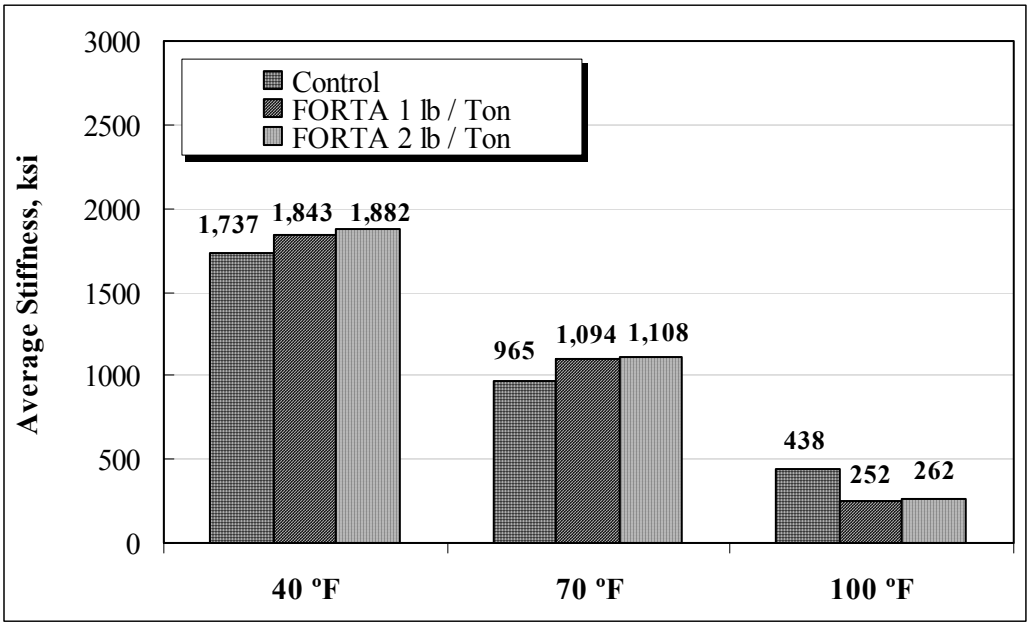

Figure 50 Average Initial Flexural Stiffness Comparisons for FORTA Evergreen Mixtures at Different Test Temperatures

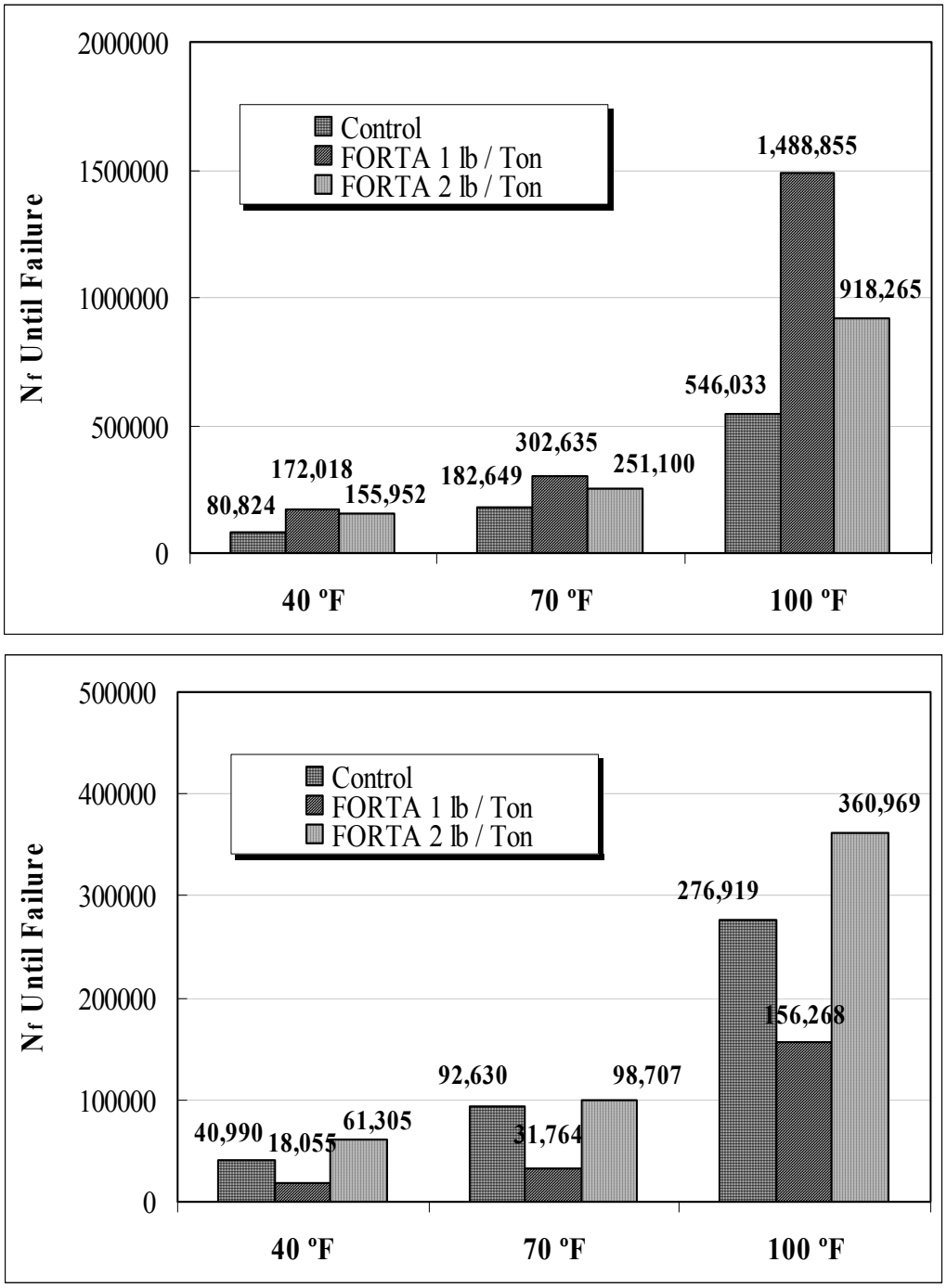

Figure 51 Number of Cycles of Repetition until Failure Predicted by the Regression Coefficients (K_1, K_2, K_3) for FORTA Evergreen Mixtures at All Test Temperature, (a) 150 micro-strains and (b) 200 micro-strains.

7.7 Summary for the Flexural Beam Fatigue Test

Constant strain Flexural tests were performed according to the AASHTO TP8 and SHRP M-009 procedures to evaluate the fatigue performance of the FORTA Evergreen mixtures. Based on the test results and analyses, the following conclusions are made:

- The generalized fatigue models developed excellent measures of accuracy for both control and 1 lb/Ton mix, while the accuracy is fair for 2 lb/Ton mix.
- Comparing the initial stiffness for the FORTA mixtures at all test temperatures, it is noticed that the fiber-reinforced mixtures show slight higher stiffness values comparing with the FORTA Evergreen control mix at 40 and 70 ºF while, for 100 ºF, the control mix shows a about 1.7 higher initial stiffness compared to fiber-reinforced mixtures.
- Comparing the fatigue life for the FORTA mixtures as obtained from the generalized model at lower and higher strain levels; At 150 micro-strains level (lower strain level) both fiber-reinforced mixture show higher fatigue life compared to the control mixture at different test temperatures especially the 1 lb/Ton mix; while at 200 micro-strains level (lower strain level), the 2 lb/Ton mixture shows the highest fatigue life followed by the control then the 1 lb/Ton mix.

7.8. Flexural Strength Test (Special Study)

Fibers contribute to the improvement of the load carrying capacity after the formation of the first crack in the mix. This contribution by means of bridging cracks and pull-out can be noticed by looking at the post peak region of the mechanical response of mixes (load-deformation) (15). Under tensile stress, fibers adsorb energy preventing a dramatic propagation of cracks.

The underlying principles governing the initiation and propagation of cracks in materials is well handled by using fracture mechanics concepts (16). In this special study, flexural strength tests were conducted to evaluate residual strength and energy characteristics of the different mixtures. Since the crack growth in the specimens was not controlled when performing the test, there is a lack of basic test data to evaluate the response of the material by using fracture mechanic concepts. Therefore, an elastic approach was used to analyze the results of the experimental program. Results of flexural strength tests performed on rectangular prismatic beams of conventional and FORTA modified asphalt mixes are reported in this section. The goal is to reflect the improvement on the residual strength of modified mixes imparted by the addition of different dosages of polypropylene and Aramid fibers.

7.8.1 Background

An elastic approach rather than fracture mechanic concepts was used to analyze the results obtained in this study. Common flexural bending test like the one used to evaluate flexural behavior in concrete was performed. The flexural strength of the asphalt beams is defined as the flexural stress applied on the beam at the moment of failure. The following equation was used to assess the flexural strength:

$$FS = \frac{3 \cdot F_{(peak)} \cdot L}{2 \cdot b \cdot d^2} \quad (7.10)$$

Where,

$F_{(peak)}$ = peak load

L = length of the support span

b = width of the beam

d = thickness of the beam

As mentioned before, unlike conventional mixes, fiber-reinforced mix specimen does not break soon after initiation of the first crack. The fibers have the effect of increasing the work fracture which is referred to as toughness and is represented by the area under the load- deflection curve (17). At the cracked section, the matrix does not resist any tension and the fibers carry the entire load taken by the composite. Therefore, in order to include the improvement in the material toughness imparted by the fibers the energy or work of fracture after the peak load should be included when estimating the residual strength. Banthia and Trottier presented a residual strength analysis approach on steel-fiber reinforced concrete that accounts for the toughness improvement imparted by the fibers (18). The same approach is used to estimate the residual strength of asphalt mixes in this study by using the following equation:

$$RS = \frac{E_{(post,0.25)} \cdot L}{\left(0.25 - \delta_{peak}\right) \cdot b \cdot d^2} \quad (7.11)$$

where,

$E_{(post\ 0.25)}$ = post peak energy up to 0.25 in displacement (lb-in)

δ_{peak} = deflection at the peak load

L = length of the support span

b = width of the beam

d = thickness of the beam

The arbitrary deflection value of 0.25 in for calculation of post peak energy was selected since every test reached this point. Once the residual strength was estimated, it was added to the flexural strength for accounting for the improvement in toughness due to the use of fibers.

7.8.2 Testing Program

The purpose of this special study was to evaluate the improvement of residual strength in asphalt mixes reinforced with Aramid and Collated Fibrillated Polypropylene (CPF) fibers and to compare their performance with that of conventional mixes. The dimensions of the beams are 15.5 in length, 2.5 in thickness and 2 in width. Suggested temperatures to perform the test are -5, 5, 15 and 25 °C (19, 20). Due to the lack of controlled temperature chamber, the test is performed at an average room temperature of 24 °C (75 °F). The tests are performed on a closed-loop controlled servo-hydraulic MTS machine.

Both monotonic and cyclic load tests were performed. Cyclic tests are convenient for obtaining the post-peak response of the material. Results from monotonic tests are used to model the load pattern for cyclic tests. A special developed loading fixture useful for eliminating extraneous deformations such as support settlements and specimen rotations is used. A yoke supported by a sort of clamps installed on the specimens automatically eliminates the support settlements from

the gross deflections in such a way that only true-specimen deflections are recorded. A spring loaded LVDT of 0.3 in range is used to measure the deflection of the beams. The test span length is 12 inch. Figure 52 shows the set up for the flexural test.

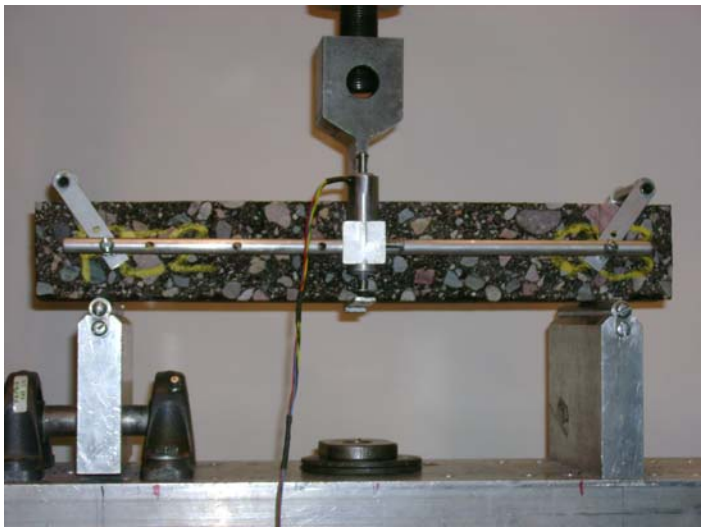

Figure 52 Experimental Set-up

Loading for both monotonic and cyclic load tests is controlled at a constant deflection rate of 0.025 in/min. For cyclic tests unloading is under load control at a rate of 10 lb/sec. The total number of tests performed is 15 for the following factorial:

- Control mix: 3 samples for monotonic test and 3 samples for cyclic test
- 1 lb/Ton mix: 3 samples for monotonic test and 2 samples for cyclic test
- 2 lb/Ton mix: 2 samples for monotonic test and 2 samples for cyclic test

Figure 53 shows a typical load-deflection curve obtained from cyclic load tests.

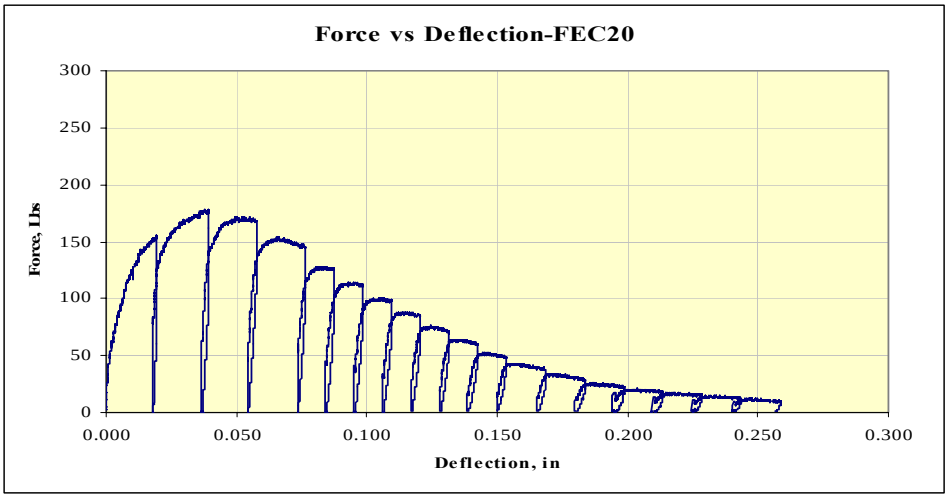

Figure 53 Typical Load-Deflection Results for Cyclic Load Test

7.8.3 Results and Discussion

Results from monotonic load tests are presented in a Table 33. As mentioned before, only the peak load obtained from monotonic test is used to model the load pattern to be used in cyclic load tests. The highest variability is observed for 2 lb/Ton mix (28%). For all mixes, in order to be conservative the sample with lowest peak load value is selected to model the cyclic load pattern. Table 33 presents the monotonic load test results.

Table 33 Summary of Monotonic Load Test Results

Mix	Specimen ID	Peak Load (lb)	Mean	Std. Deviation	Variability
Control	FEC17	290.2	271.4	25.0	0.09
	FEC18	280.9			
	FEC23	243.0			
1 lb/Ton	FE101	190.1	187.6	10.9	0.06
	FE102	197.0			
	FE105	175.7			
2 lb/Ton	FE202	183.4	153.1	42.9	0.28
	FE201	122.7			

Results from cyclic load tests are shown in Figures 54 to 56. Variability on test results as well as difference in the mechanical response among specimens of the same mix for modified asphalt mixes is observed. Results obtained from testing control mix show reasonable consistency.

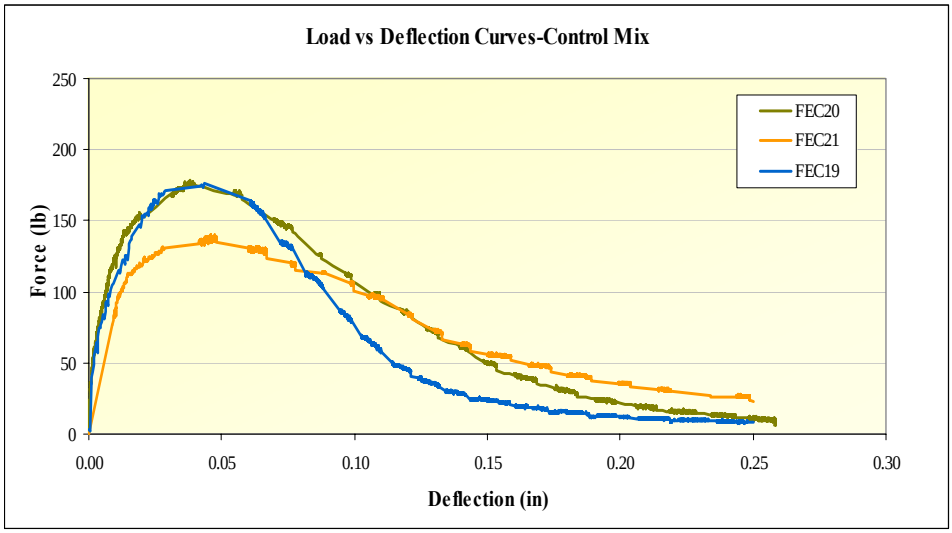

Figure 54 Cyclic Load Test Results for Control Mix

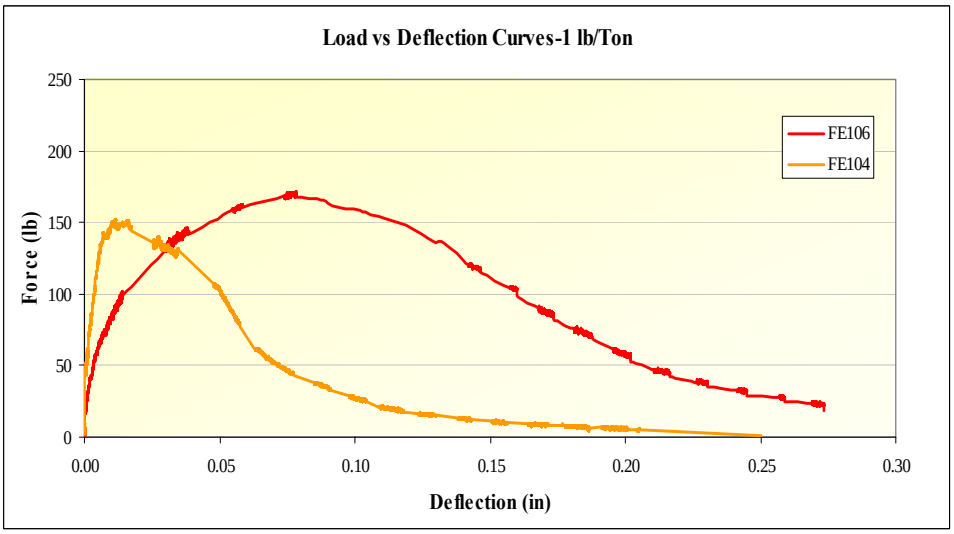

Figure 55 Cyclic Load Test Results 1 lb/Ton Mix

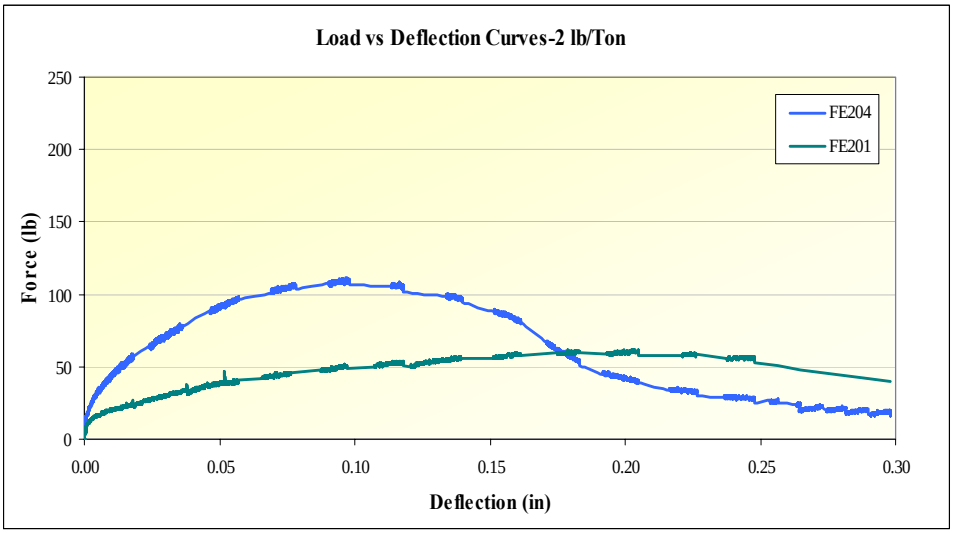

Figure 56 Cyclic Load Test Results 2 lb/Ton Mix

Table 34 shows detailed information about the dimensions of every specimen tested for cyclic load. The listed dimensions are used for computing both the flexural and the residual strength. Variability on the dimensions of the specimens is observed, in special for the width of specimens. It is worth to mention that problems originated by the irregularity of the beam section are issues of concern. None of the samples presented a smooth leveled surface on their faces. This originated instability of the specimens when placed on the supports. These irregularities on the surface can lead to an uneven distribution of load on the top of the specimen. This problem could generate stress concentrations on the specimen. Table 35 summarizes the flexural strength results for cyclic load test. Calculated flexural strength, post peak energy, and residual strength are also included in the table.

Table 34 Dimensions of Specimens Used in Cyclic Load

Specimen Dimensions			
ID	Span Length (in)	Width (in)	Thickness (in)
FEC19	12.00	2.76	2.13
FEC21	12.00	2.70	2.08
FEC20	12.00	2.75	2.13
FE106	12.00	2.77	2.00
FE104	12.00	2.54	2.00
FE204	12.00	2.52	2.05
FE203	12.00	2.46	2.01

Table 35 Summary of Flexural Bending Test results for Cyclic Load

Mix	Specimen ID	Peak Load (lb)	Flexural Strength (psi)	Post Peak Energy (lb-in)	Residual Strength (psi)	Corrected Flexural Strength (psi)
Control	FEC19	176.0	254.2	11.2	52.1	306.3
	FEC21	140.0	215.9	15.0	76.3	292.1
	FEC20	178.7	257.8	16.5	74.8	332.6
1 lb/Ton	FE106	171.4	277.4	17.6	110.8	388.1
	FE104	152.6	270.0	11.5	56.7	326.7
2 lb/Ton	FE204	111.1	188.1	11.2	82.5	270.6
	FE203	61.8	111.5	3.0	75.6	187.1

Similar behavior is noticed for the three specimens of the control mix. The curves exhibit similar response of the material and peak load values are very close among all the specimens. Therefore, in order to make comparisons it would be a good option to take an average value from the three specimens and when comparing curves, the specimen showing calculated parameters closer to mean values can be selected for plotting. Different response between the two specimens for each modified mix can be observed. This difference could be attributed to the variance of the fiber distribution hypothesized for these mixes. Also, the orientation of the fibers plays an important

role in their contribution to improvement of strength. If they are not intersecting the plain of failure, the bridging and pull out effect of the reinforcement will not be effective. For these cases, specimens with curves showing similar mechanical behavior are selected for a reasonable comparison of modified mixes with conventional mix. Because of variability in results between specimens for modified mixes, a statistical analyzes should not be performed. To analyze specimens showing completely different performance by considering them within the same category does not make sense.

Based in the reasons mentioned previously, Table 36 shows comparative results for every mix. The average values of the three specimens tested represents the control mix. The 1 lb/ton mix is represented by specimen FE106 and the 2 lb/ton mix by specimen FE204. Results from table 4 suggest that the overall the flexural response for 1 lb/ton modified mix has been enhanced by fibers and is better than the response of the other mixes. A comparison of load-displacement representative curves is presented in Figure 57. The trends of the curves provide support to the approach used to compare results since all of them show a similar mechanical response. The ratios of 1 lb/ton mix strength to control mix are 1.14, 1.64, and 1.25 for flexural, residual and corrected flexural strength respectively. The enhancement imparted by fibers is noticeable. By performing the same analysis between 2 lb/ton mix and control mix, we can observe that the improvement due to fibers is only reflected in the residual strength. On the other hand, relative strength values for flexural and corrected flexural strength decreased to 0.78 and 0.87 respectively. Figures 58 and 59 show comparative Bar charts.

Table 36 Comparison of Flexural Bending Test Results for Cyclic Load

Mix	Specimen ID	Peak Load (lb)	Flexural Strength (psi)	Post Peak Energy (lb-in)	Residual Strength (psi)	Corrected Flexural Strength (psi)
Control	Average	164.9	242.6	14.2	67.7	310.3
1 lb/Ton	FE106	171.4	277.4	17.6	110.8	388.1
2 lb/Ton	FE204	111.1	188.1	11.2	82.5	270.6

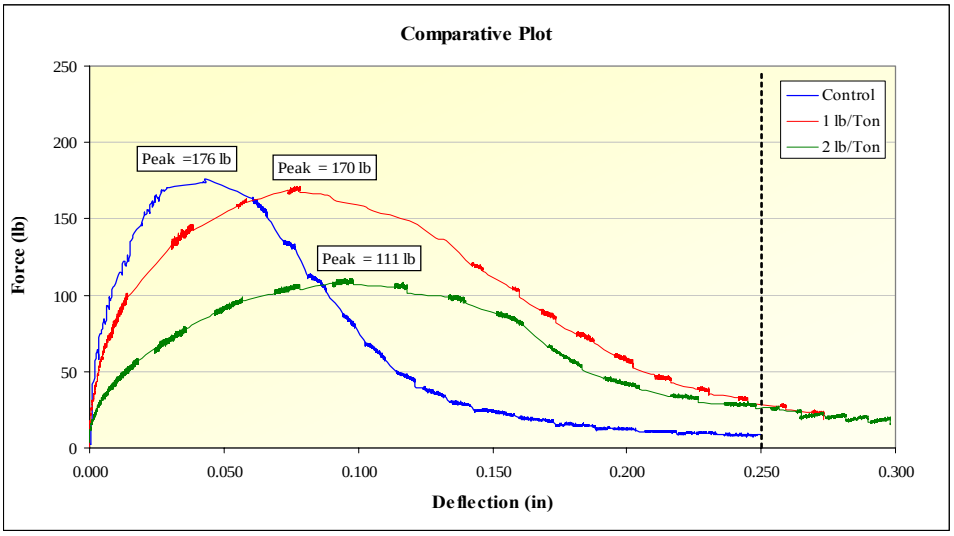

Figure 57 Comparison of Load-Displacement Representative Curves

Figure 58 compares strength results among the different mixes. All results presented in Table 36 are reflected in the figure. Again, the increase in both flexural and residual strength and, as consequence increase in the corrected flexural strength is evident for 1 lb/Ton mix. On the other hand, as mentioned before, Figure 56 shows how the flexural strength of 2 lb/Ton mix is affected may be by the presence of excessive amount of fibers in the beam. Curiously, the residual strength for this mix seems to still being improved by the use of fibers.

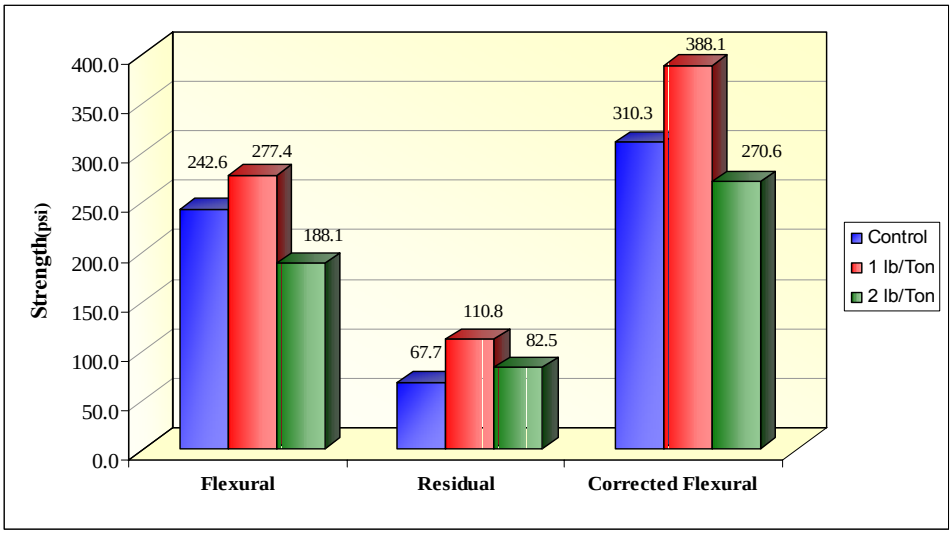

Figure 58 Comparison of Flexural Strength among Different Mixes

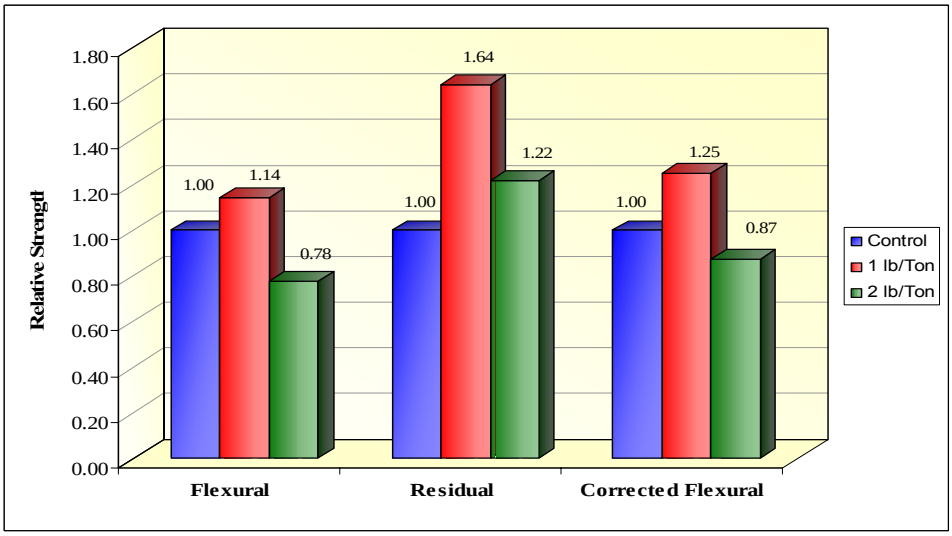

Figure 59 Comparison of Relative Strength among Different Mixes

This misleading result is due to the fact that the residual strength as well as the flexural strength is inversely proportional to the cross sectional area of the specimen. By looking at Table 34, it can be observed that the beam representing 2 lb/Ton mix is the one with lowest cross sectional

area. Therefore, a relatively high residual strength compared to the other two specimens having greater dimensions should be expected. It is not the same case for flexural strength. Besides being function of beam dimensions, the flexural strength is also function of the peak load. In this particular case, the flexural strength of 2 lb/ton does not show improvement since the peak load is too low that the effect of smaller cross sectional area are not reflected. Figure 60 shows another way to deal with the results. Relative strength values are presented in this chart. As discussed before, these strength ratios also reflect the improvement of fibers on 1 lb/ton mix and the detrimental effect that they may cause when used in excessive amounts. All the ideas exposed can lead us to suggest that the ideal optimum fiber content for improving the flexural response of asphalt mixtures is 1 lb/Ton.

Finally Figure 60 shows the energy or work of fracture after the peak load that is accounted for estimating the improvement in the material toughness imparted by the fibers. Again, the improving on 1 lb/ton mix on terms of energy is noticed. A drop of energy of fracture is observed for the 2 lb/ton mix.

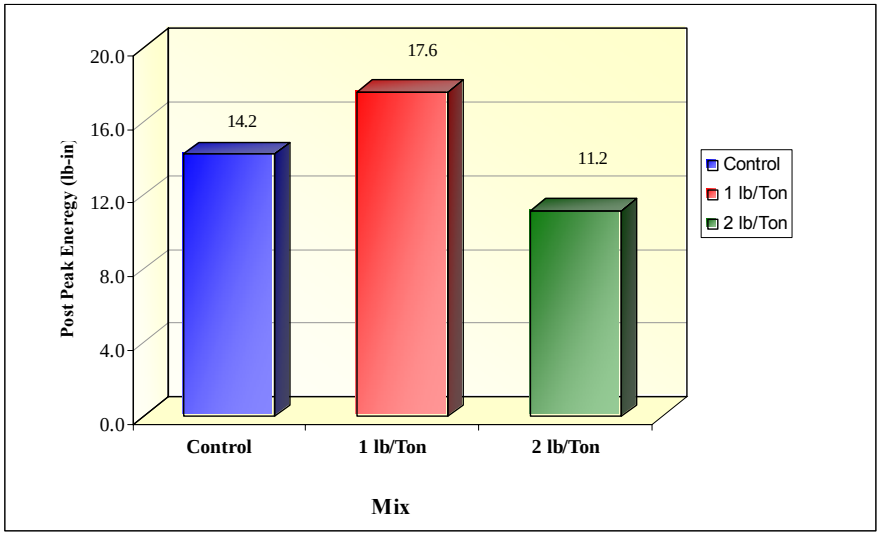

Figure 60 Comparison of Post Peak Energy among Different Mixes

7.9 Summary for the Flexural Strength Test

After analyzing the results of the testing program it can be concluded that the improvement of flexural strength and corrected flexural strength of 1 lb/Ton mix is increased by 14 and 25% respectively. The opposite effect was observed for the 2 lb/Ton mix, the flexural and corrected flexural strength decreased probably due to the excessive amount of fibers in the mix. It can be concluded that in terms of flexural properties, an optimum fiber dosage is 1 lb/Ton.

High variability was observed in the results, especially for the modified mixes. The variability is mainly due to the variance of the fibers distribution and their orientation within the specimens. In order to handle this variability it is recommended to test more samples for future research. The testing program accounted only for one level of temperature (24 °C), it is recommended to perform the test at lower temperature on future research in order to capture the elastic component of the asphalt mix response. The application of fracture mechanics provided that the crack growth is measured during the test could result in a better assessment of what really is happening in the mix.

The technique for preparation of samples should be improved in order to obtain beams with smooth surfaces and constant rectangular prismatic section. The use of beams with uneven surfaces could be leading to inappropriate estimation of the mechanical response of the specimens.

8. THERMAL CRACKING

8.1 Significance and Use

Tensile creep and strength test data are fundamental material inputs required for the Mechanistic Empirical Pavement Design Guide (MEPDG) Level 1 and 2, when a thermal fracture analysis is desired. Thermal cracking predictions are computed using an analysis module called TCMODEL, originally developed under SHRP, which has been modified and recalibrated for inclusion in the MEPDG (21).

One important component of the methodology used in the thermal cracking distress prediction model utilizes the EICM (Enhanced Integrated Climatic Model) as the climatic (temperature) algorithm to determine the temperature-depth profile within the asphalt layer at hourly time interval over the entire analysis period (20-30 years).

Creep compliance data is used to predict field tensile stress development in the asphalt concrete layers as a result of temperature cycling. A fracture mechanics based crack tip model then estimates downward the thermal crack development as a function of time, which is in turn used to compute the amount of thermal cracking versus time based upon a probabilistic crack distribution model (21).

The material inputs required for the fracture model are the tensile strength (at –10 ^{o}C) and the m-value. The tensile strength is directly obtained from the indirect tensile strength test. The m-value is related to the slope of the creep compliance master curve, and is computed in the MEPDG using compliance data obtained from the indirect tensile creep test (21). The creep

compliance and tensile strength values determined with this method are then used in a linear viscoelastic analysis to calculate the low temperature and fatigue cracking potential of the asphalt concrete.

In addition to the MEPDG thermal fracture parameters, there are other potentially important parameters from the indirect tensile strength test that have been correlated to actual cracking values. These parameters include tensile strain at failure (ε_{ff}), total fracture energy (Γ_{fr}), and fracture energy to failure (Γ_{fa}), and will be defined later in this chapter.

8.2 Test Specimen Preparation and Conditioning

All test specimens were prepared according to the Test Protocol UMD 9808, "Method for Preparation of Triaxial Specimens" (22). The compaction temperature was determined using binder consistency test results and viscosity-temperature relationships. The specimens were reheated and compacted with a Servopac gyratory compactor into a 150-mm diameter gyratory mold to approximately 160-mm in height. The test specimen's "ideal" geometry was based on the specimen size and the aggregate effects study that was completed by the Superpave models team (23). Approximately 5-mm was sawed from each end of the compacted specimen, and 3 test specimens approximately 38-mm thick were cut from each compacted specimen.

8.3 Summary of Method

Both indirect tensile cracking tests were carried out based on the procedure developed by Roque et al and described in the draft indirect tensile tests protocol AASHTO TP9-02 (Appendix A). Vertical and horizontal LVDTs were mounted on the specimen for measuring the horizontal and

vertical deformation during the indirect tensile creep test. The tests were conducted using three replicates at three temperatures: 10 ^{o}C (50 ^{o}F), 0 ^{o}C (32 ^{o}F), and -10 ^{o}C (14 ^{o}F). The required nine replicates were obtained from three gyratory compacted plugs. Each group of replicates (according to temperature) contains one specimen from every gyratory compacted plug to ensure unbiased test results.

The tensile creep was determined by applying a static load of fixed magnitude along the diametric axis of the specimen. The horizontal and vertical deformations measured near the center of the specimen were used to calculate tensile creep compliance as a function of time. Loads were selected to keep horizontal strains in the linear viscoelastic range during the creep test.

The tensile strength was determined immediately after conducting the tensile creep test by applying a constant rate of vertical deformation to failure. One specimen per mixture was tested using both vertical and horizontal LVDTs, as recommended in the original Roque et al protocol (1). A modified method of measuring the tensile strength that allows also for determining the energy until failure and total fracture energy was applied using three replicates per mixture. The vertical LVDTs were removed in this method due to the possible damage in the post-failure phase of the test.

8.4 Experimental Plan

The FORTA Evergreen testing program included the complete thermal fracture characterization of one conventional mixture and two fiber-reinforced asphalt mixtures (1 lb/Ton and 2 lb/Ton).

8.5 Test Method: Indirect Tensile Creep Compliance and Strength

8.5.1 Indirect Tensile Tests

The indirect tensile test is the test specified in AASHTO T-283 for evaluating an HMA mixture's susceptibility to moisture damage. Properties that have been used for evaluating moisture damage and fracture-related distresses are the resilient modulus (repeated loadings) and the indirect tensile strength and failure strain (constant rate of loading) (24, 25) Although the reliability of the indirect tensile test to detect and predict moisture damage is questionable, no other test has been found to provide consistent results at a higher reliability.

The indirect tensile method is used to develop tensile stresses along the diametric axis of the test specimen. The test is conducted by applying a compressive load to a cylindrical specimen through two-diametrically opposite arc-shaped rigid platens, as shown in Figure 61. The test specimen is placed with its axis horizontal between the platens of the testing machine.

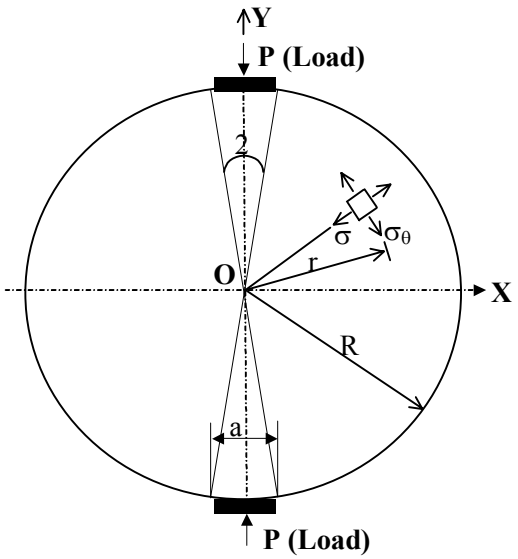

Figure 61 Schematic Diagram of the Indirect Tensile Test

Based on the theory of elasticity, the strain can be expressed in three dimensions. Ideally, the three-dimensional analysis can be reduced to a two-dimensional analysis for special element size and loading conditions. For the case of a circular disk, the two dimensional analysis can be categorized as plane stress (24). The complete protocol for determining the creep compliance and strength of HMA using the indirect tensile test device is reported in Appendix A.

8.5.2 Background for the Indirect Tensile Creep Test

The static creep test in the indirect tensile mode uses a singular load-unload cycle. A constant static load is applied to the specimen for a time of 100 seconds and horizontal deformations are recorded during the loading time. The applied load is a percentage of the horizontal tensile strength of the material. The horizontal deformations are recorded for another 1,000 seconds after the load is removed to measure the recovery of the specimen. Both horizontal and vertical LVDTs are used during the test to measure the deformations under the static load to calculate Poisson's ratio. The Roque et al IDT protocol is now based upon the use of a 100 sec creep test. In general, three replicate specimens are tested at the three temperatures previously noted. Enhanced data analysis techniques (through the new program MASTER) are claimed to provide accurate evaluations of the time-temperature shift factor (a_T) and creep compliance model statistical fitting techniques through Prony and Power Model forms, as well as the development of the Creep Compliance Master Curve (CCMC).

8.5.3 Strain-Time Response Curve

The phenomenon of the static creep test is shown in Figure 62, which illustrates the typical strain-time response of an HMA mixture. The figure shows the salient components of the

load/unload cycle. The total strain (ε_T) can be divided into recoverable and non-recoverable components or time-dependent and time-independent components, just as they are for the triaxial compressive creep test. Equation 8.1 describes the four components composing the total strain.

$$\varepsilon_T = \varepsilon_e + \varepsilon_p + \varepsilon_{ve} + \varepsilon_{vp} \tag{8.1}$$

where:

ε_T = the total strain.

ε_e = the elastic strain, recoverable and time-independent.

ε_p = the plastic strain, irrecoverable and time-independent.

ε_{ve} = the viscoelastic strain, recoverable and time-dependent.

ε_{vp} = the viscoplastic strain, irrecoverable and time-dependent.

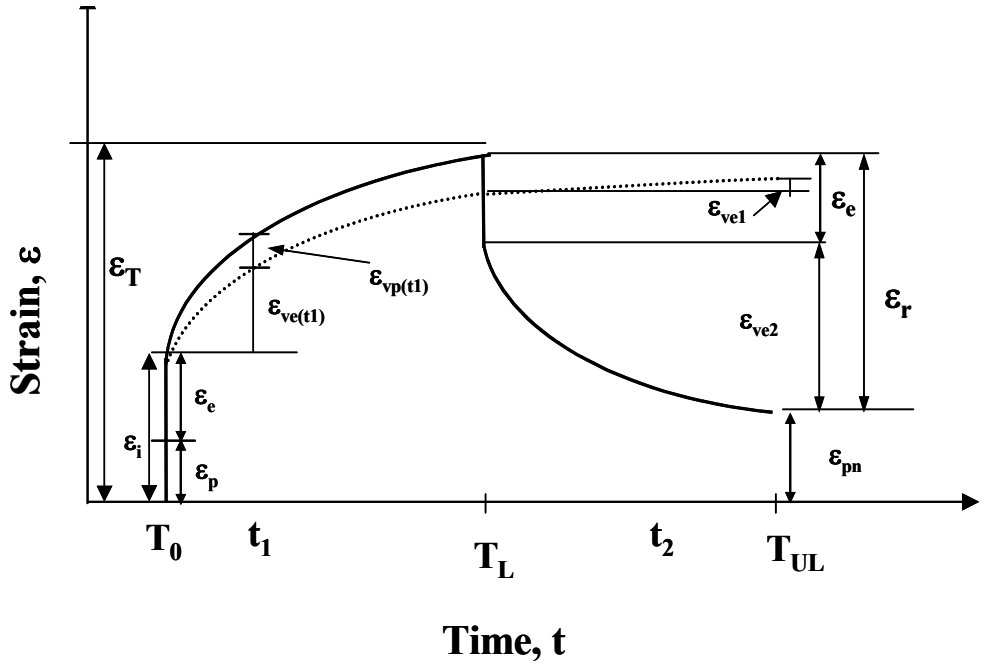

Figure 62 Typical Strain-Time Response for HMA Mixtures for a Static Creep Test

The elastic and viscoelastic strain components exist during both loading and unloading conditions, while the plastic and viscoplastic components exist during the loading portion.

8.5.4 Creep Compliance Parameters

The mathematical form to represent the compliance from the indirect tensile test is similar to the compliance determined from the triaxial compressive creep test and is given by equation 8.2.

$$D(t) = D^*_1 \, t^{m^*} \tag{8.2}$$

where:

D(t) = total compliance at any time.

T = loading time.

D^*_1, m^* = material regression coefficients.

The regression coefficients "D^*_1" and "m^*" are generally referred to as the compliance parameters as shown in Figure 63. These parameters are the general indicators of the creep behavior of the materials.

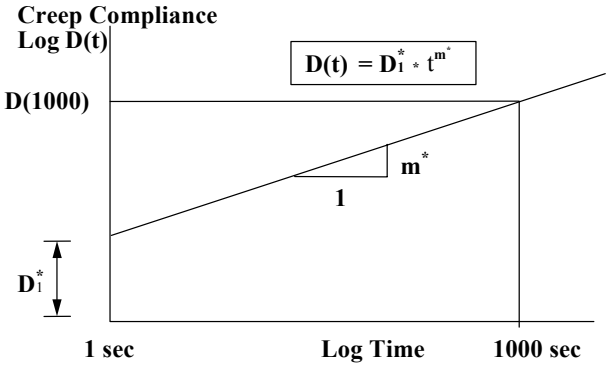

Figure 63 Illustration of Creep Compliance versus Time from a Static Creep Test

8.5.5 Calculations of the Creep Compliance

Tensile creep compliance, D(t), is usually the primary quantity to be obtained from the creep test. The Poisson's ratio that is also obtained is very important because it strongly influences the three-dimensional behavior of the specimen and thus plays an important role in the calculation of creep compliance. Poisson's ratio, by definition, is a function of X/Y, which is equal to the value of the ratio of measured horizontal deflection (x-direction) to measured vertical deflection (y-

direction). Thus, creep compliance adjusted for three-dimensional effects can be expressed as a function of X/Y.

Creep compliance for the biaxial stress state that exists on the specimen face (σ_z =0), is obtained through Hooke's law:

$$D(t) = \frac{\varepsilon_x}{\sigma_x - \nu * \sigma_y}$$

The 3D Final Element Method (FEM) correction factor developed by Roque et al is given by:

$$D(t) = \frac{\varepsilon(t)}{\sigma} = \frac{H_m(t) * D * t}{P * GL} * C_{cmpl}$$

where,

$$C_{cmpl} = 0.6354 * \left(\frac{X}{Y}\right)^{-1} - 0.332$$

With the factor restricted to the limits of:

$$0.20 \le \frac{t}{D} \le 0.65$$

$$\left[0.704 - 0.213\left(\frac{b_{avg}}{D_{avg}}\right)\right] \le C_{cmpl} \le \left[1.556 - 0.195\left(\frac{b_{avg}}{D_{avg}}\right)\right]$$

In these equations:

D(t)	= creep compliance response at time t
H_M(t)	= measured horizontal deflection at time t
GL	= gage length
P	= creep load
t	= specimen thickness
D	= specimen diameter
μ	= Poisson's ratio

The value of X/Y is also used to compute the Poisson's ratio of the material during the test by:

$$\nu = -0.10 + 1.480\left(\frac{X}{Y}\right)^2 - 0.778\left(\frac{t}{D}\right)^2\left(\frac{X}{Y}\right)^2$$

where

$$0.05 \le \nu \le 0.50$$

Other quantities that may be useful in other pavement response or prediction models are presented in the following equations.

The maximum tensile stress, corrected to account for three-dimensional effects, can be obtained by:

$$\sigma_x = \frac{2 * P}{\pi * t * D} * C_{SX}$$

where,

$$C_{SX} = 0.948 - 0.01114 * (\frac{t}{D}) - 0.2693 * (\nu) + 1.436 * (\frac{t}{D}) * (\nu)$$

The maximum compressive stress, also corrected for three-dimensional effects is:

$$\sigma_y = \frac{6 * P}{\pi * t * D} * C_{SY}$$

where,

$$C_{SY} = 0.901 + 0.138 * (\nu) + 0.287 * (\frac{t}{D}) - 0.251 * (\nu)(\frac{t}{D}) - 0.264 * (\frac{t}{D})^2$$

Finally, maximum tensile strain, corrected for specimen bulging and conversion to point, is obtained by:

$$\varepsilon_x = \frac{H_M}{GL} * 1.072 * C_{BX}$$

where,

$$C_{BX} = 1.03 - 0.189 * (\frac{t}{D}) - 0.081 * (\nu) - 0.089 * (\frac{t}{D})^2$$

8.5.6 Description of the Computer Program MASTER

A computer program called MASTER automates the master curve construction using built-in logic capabilities designed to handle the wide variety of measured responses encountered in practice. MASTER was found to closely agree with manually determined shift factors for thirty-six field mixtures investigated. The program was also found to be extremely robust, producing rational shift factors even when used to analyze complicated, thermally-damaged materials (24, 25).

The greatest challenge in creating fully automating TCMODEL involved the construction of the creep compliance master curve and shift factor-temperature relationship (log a_T versus T) required by TCMODEL. The master curve and shift factors are used to obtain a complete viscoelastic characterization of an asphalt mixture at low temperatures with creep data of relatively short duration. However, it is sometimes necessary to extrapolate mixture compliances to longer loading times to provide the required overlap for accurate determination of shift factors (24, 25).

The original extrapolation technique used in Superpave led to errors in shift factors, and consequently, a new procedure was developed. The new procedure involved extrapolating log creep compliance - log time data using a second-order polynomial function to provide the necessary overlap between compliance curves at adjacent temperatures, and visually shifting the data to obtain temperature shift factors. However, visually shifting data, even when performed

by a trained engineer is cumbersome and results are subjective. It was therefore concluded that automated procedure should be developed for the new techniques to be suitable for the Superpave system (24, 25).

The general steps taken by the computer program MASTER to obtain the master curve parameters are:

- Read compliance data from data file
- Fit second degree polynomial to log compliance - log time data at each temperature
- Obtain temperature shift factors for each temperature using fitted compliance - time data
- Discretize fitted compliance-reduced time curves to ten data points per temperature, using an even spacing in the log time domain
- Fit specific rheological models to the discretized master curve data to satisfy TCMODEL formatting requirements for input, and store parameters in data file.

The results of the master creep compliance curve fit to a Power Model defined by:

$$D(\xi) = D_0 + D_1 * \xi^m$$

where,

ξ = reduced time

$D(\xi)$ = creep compliance at reduced time ξ

D_0, D_1, m = power model parameters

8.6 Background for the Indirect Tensile Strength Test

Tensile strength is an important property that is commonly used to evaluate effects of moisture, and to determine the fracture resistance of hot mix asphalt. A method has been developed to

accurately determine tensile strength from indirect tensile test results (24, 25). The tensile strength is determined immediately after determining the tensile creep by applying a constant rate (12.5 mm/min) of vertical deformation (or ram movement) to failure. Failure strength is defined as the stress at which first failure occurs in the specimen. This value is less than or equal to the ultimate stress realized by the specimen and is determined by analyzing deformations on both sides of each specimen.

The tensile strength of the mixture, at the three temperatures noted, is also recommended in the procedure. However, the final TCMODEL only utilizes the strength result at -10^{o}C. Therefore, a special procedure was utilized to determine the "failure load". This is an important modification because the failure load has been found to be less than the maximum load that the specimen can undergo. Thus, once the instant of failure is found (approach uses the deflection measurement difference); the failure load can be defined and the tensile strength computed from:

$$S_t = \frac{2 * P_f * C_{sx}}{\pi * D * t} * C_{SX}$$

where, P_f = failure load

C_{sx} = correction factors (previously defined)

t = specimen thickness

D = specimen diameter

Parameters from the indirect tensile strength test that can be considered for mixture cracking performance include: Indirect Tensile Strength (S_t), Tensile Strain at Failure (ε_{ff}), Fracture Energy to Failure (Γ_{fa}), Total Fracture Energy (Γ_{fr}). The energy approach to thermal fracture analysis has an advantage over the tensile strength evaluation by considering not only the

maximum force that given mixture is able to withstand but also the amount of deformation that the mixture can experience without cracking.

8.6.1 Determining Tensile Strain at Failure

The tensile strain at failure is the horizontal strain corresponding to the failure strength - the stress at which first failure occurs in the specimen. The horizontal strain is calculated as an average deformation measured by the two horizontal LVDTs, divided by gage length, which in this case is equal to 76.2 mm (3 inches). Higher tensile strains at failure are favored as an indication of the mix resistance to thermal cracking.

8.6.2 Determining Energy until Failure

The energy until failure, as shown in Figure 64, is calculated as the area under the load-vertical deformation curve until maximum load occurred. Again, higher energy until failure is favored as an indication of the mix resistance to cracking.

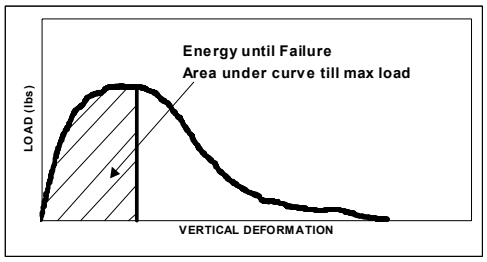

Figure 64 Determination of the Energy until Failure

8.6.3 Determining Total Fracture Energy

The total fracture energy is calculated as the area under the load-vertical deformation curve as shown in Figure 65. Higher total fracture energy is favored as an indication of the mix resistance to cracking.

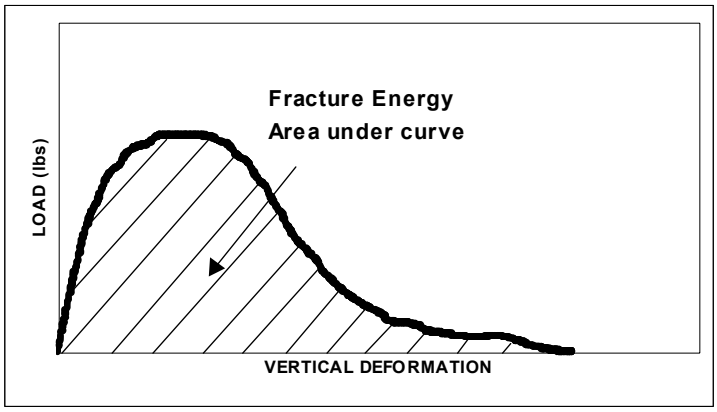

Figure 65 Determination of the Total Fracture Energy

8.7 Modification to the Original IDT Test Protocol

In general, the Indirect Tensile Creep and Strength tests were conducted based on the procedure developed by Roque et al and described in the draft indirect tensile tests protocol AASHTO TP9-02. An important modification to the original protocol was implemented at ASU. The modification consisted of increasing the original LVDT's gage length of 1.5-in into a 3.0-in center-to-center spacing. This modification was applied based on the recommendations from the NCHRP Project 1-28A. It was concluded that a recommended gage length of 3", mounted on a 6" diameter specimen, regardless of the mix type being evaluated; will yield total variance values that are as close to the most likely minimum values possible. In addition, the 3" gage length should have the potential for possessing the minimum amount of possible problems associated with the on-sample measurement system (23).

8.7.1 Determining the Tensile Strength of HMA

8.7.1.1 The Original Roque Method

The tensile strength test was conducted and analyzed using two methods. One specimen per mixture was tested using the original Roque et al procedure reported in Appendix A. The original Roque et al method involves using both vertical and horizontal LVDTs and requires finishing the test immediately after reaching the maximum load in order to preserve the vertical LVDTs. Finishing the test at this point eliminates the possibility of measuring the total fracture energy that is calculated as an area under the deformation - load curve. The vertical LVDTs are used solely to identify which face of the specimen failed first during the strength test. Further analysis of the conducted tests indicated that the difference of the tensile strength between both faces do not exceed 10%.

8.7.1.2 Modified Roque Method

A modified method of measuring the tensile strength that allows also for determining the energy until failure and total fracture energy was applied using three replicates per mixture. The vertical LVDTs were eliminated and tensile strength was calculated as an average value from both specimen faces. The energy until failure and total fracture energy were reported as a promising approach to characterize the fracture properties of the HMA mixtures (1).

8.8 Smoothing Process of the Creep Compliance Data

The data available included test results at 1, 2, 5, 10, 20, 50, 100, 200, 500, and 1000 seconds. However, it was observed that the data at 1 and 2 seconds did not correspond to the trends

expected from the rest of the data and was significantly lower compared to the results from the Roque – Buttlar studies. It was suspected that some errors as a result of insufficient seating load where associated with these two first points. Therefore, it was decided to best fit the data at each test temperature in order to calculate the corresponding test result at 1 and 2 seconds.

The methodology used for this calculation was to apply a power function, using the data points for every test temperature at 5, 10, 20, 50, and 100 seconds as shown below:

$D(t) = D^*_1 * t^{m^*}$

where:

D(t)	= Creep Compliance
t	= Time in seconds
D^*_1, and m*	= regression coefficients

With each D^*_1 and m* coefficient, the corresponding values at 1 and 2 seconds were back-calculated. The correlation found with these power functions was always good to excellent having in average R^2 values higher than 0.95.

8.9 Results and Analysis

8.9.1 Indirect Tensile Creep Test Results

The creep compliance data from laboratory tested temperatures of 0 and -10 ^{o}C, as well as, extrapolated -20 ^{o}C data were used as a MASTER program inputs. The results of the creep compliance for all four temperatures (including –15 ^{o}C) are reported in Table 37.

Table 37 IDT Creep Compliance Results, FORTA Evergreen

	Time [sec]	FORTA Evergreen Control	FORTA Evergreen 1 lb/Ton	FORTA Evergreen 2 lb/Ton
Creep Compliance [1/psi], Low Temp [-10^{o}C]	1	2.46E-07	3.14E-07	3.47E-07
	2	2.83E-07	3.36E-07	3.72E-07
	5	3.42E-07	3.69E-07	3.95E-07
	10	3.94E-07	3.94E-07	4.53E-07
	20	4.54E-07	4.20E-07	4.82E-07
	50	5.48E-07	4.52E-07	4.78E-07
	100	6.31E-07	5.00E-07	5.65E-07
	200	7.27E-07	5.78E-07	6.40E-07
	500	8.78E-07	6.74E-07	7.46E-07
	1,000	1.01E-06	8.27E-07	9.93E-07
Creep Compliance [1/psi], Int. Temp [0^{o}C]	1	3.28E-07	3.77E-07	2.61E-07
	2	3.99E-07	4.63E-07	3.21E-07
	5	5.18E-07	6.17E-07	4.22E-07
	10	6.30E-07	7.54E-07	5.18E-07
	20	7.66E-07	8.94E-07	6.37E-07
	50	9.93E-07	1.16E-06	8.36E-07
	100	1.21E-06	1.54E-06	1.03E-06
	200	1.47E-06	1.90E-06	1.26E-06
	500	1.90E-06	2.60E-06	1.66E-06
	1,000	2.32E-06	3.20E-06	2.04E-06
Creep Compliance [1/psi], High Temp [10^{o}C]	1	5.37E-07	4.81E-07	3.77E-07
	2	6.47E-07	6.17E-07	5.17E-07
	5	8.28E-07	8.56E-07	7.85E-07
	10	9.97E-07	1.10E-06	1.08E-06
	20	1.20E-06	1.41E-06	1.47E-06
	50	1.54E-06	1.95E-06	2.24E-06
	100	1.85E-06	2.50E-06	3.07E-06
	200	2.23E-06	3.21E-06	4.20E-06
	500	2.85E-06	4.45E-06	6.38E-06
	1,000	3.44E-06	5.71E-06	8.75E-06

8.9.2 Creep Compliance Power Model Parameters, FORTA Evergreen

Table 38 summarizes the creep compliance power model parameters calculated using the MASTER program. Temperature shift factors are reported in terms of log ($1/a_{Ti}$). The MEPDG thermal fracture model is using degrees Celsius (SI Units) to characterize the temperature and 1/psi (U. S. Customary Units) to characterize creep compliance. The creep compliance master curve power model is defined by the equation:

$$D(\xi) = D_0 + D_1 * \xi^m$$

8.9.3 Creep Compliance Master Curves, FORTA Evergreen

Figures 66 through 69 present plots of the Creep Compliance Master Curves (CCMC). The CCMC plots include the power model equations and were built based on the results from the IDT creep test and temperature-time shift factors from the MASTER program. High stiffness modulus of the mixture at the low temperature indicates more susceptibility to cracking. On the other hand, low stiffness modulus provides better resistant to low temperature cracking. Since the creep compliance is inversely proportional to the stiffness modulus it is recommended to have high creep compliance asphalt concrete mixtures, at least from the thermal cracking point of view. Traditional analysis has always been to state that the mix with higher creep compliance curve is more resistant to thermal cracking. Comparing the FORTA control and fiber-reinforced asphalt mixtures compacted at the same air void levels, it is observed that FORTA 2 lb/Ton mixture had higher creep compliance compared to both control and 1 lb/Ton mixtures at higher temperatures. Again, the 2 lb/Ton mix had higher creep compliance followed by 1 lb/Ton mix and then followed by the control mixture at lowest temperature zone (left end of the master curve).

Table 38 Creep Compliance Power Model Parameters from MASTER Program, FORTA Evergreen

Mix	Temp Shift Factors		Power Model Parameters		
	0 °C	-10 °C	D_0 (1/psi)	D_1 (1/psi)	m
FORTA Evergreen Control	31.62	6.31	1.48E-07	1.02E-07	0.3640
FORTA Evergreen 1 lb/Ton	56.23	17.78	2.64E-07	3.88E-08	0.4662
FORTA Evergreen 2 lb/Ton	12.59	2.00	3.11E-07	2.18E-08	0.6510

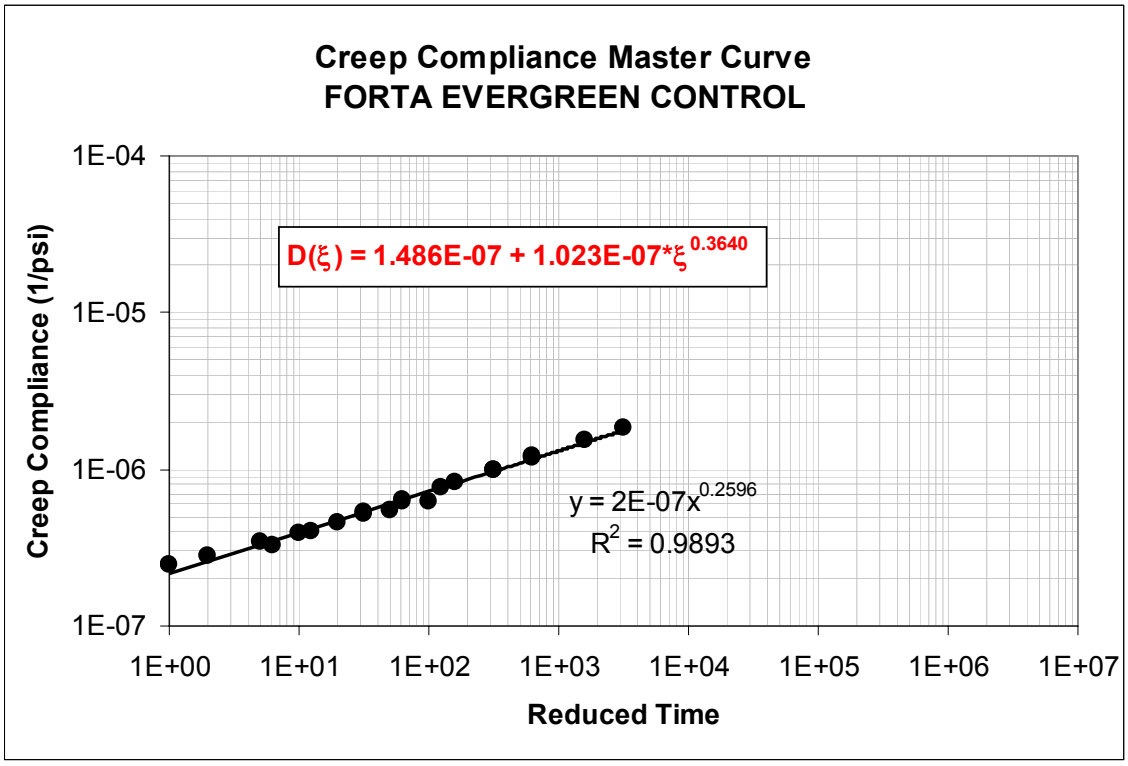

Figure 66 CCMC for the Control Mixture, FORTA Evergreen

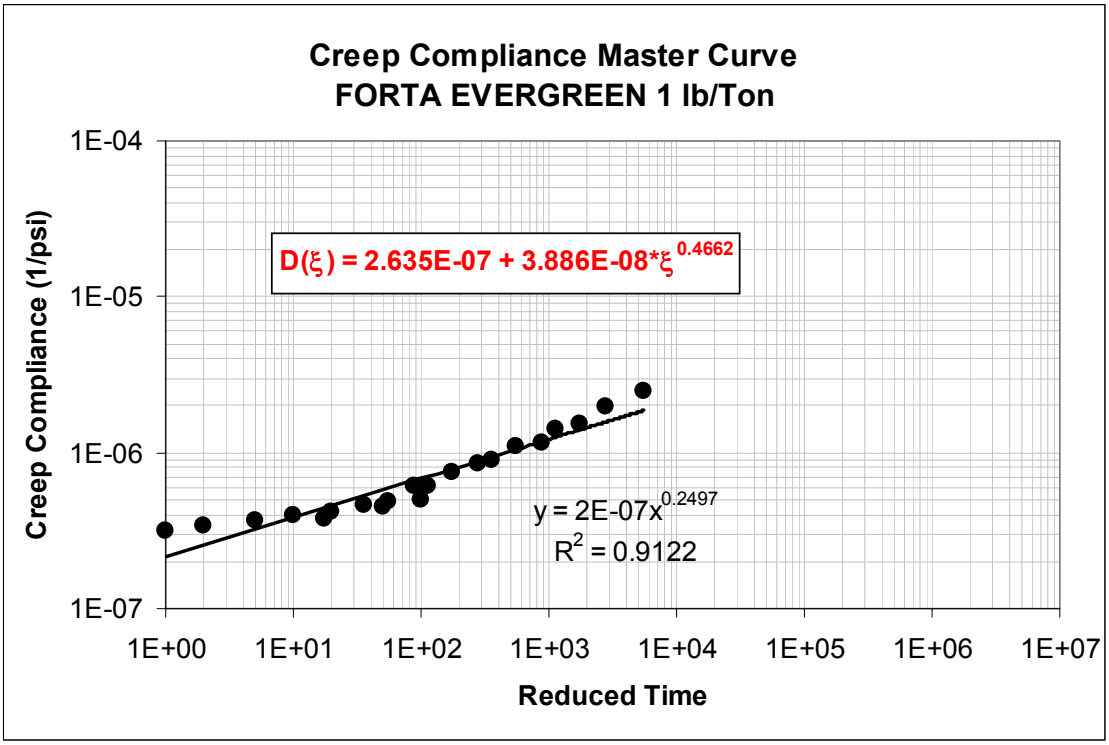

Figure 67 CCMC for the 1 lb/Ton Mixture, FORTA Evergreen

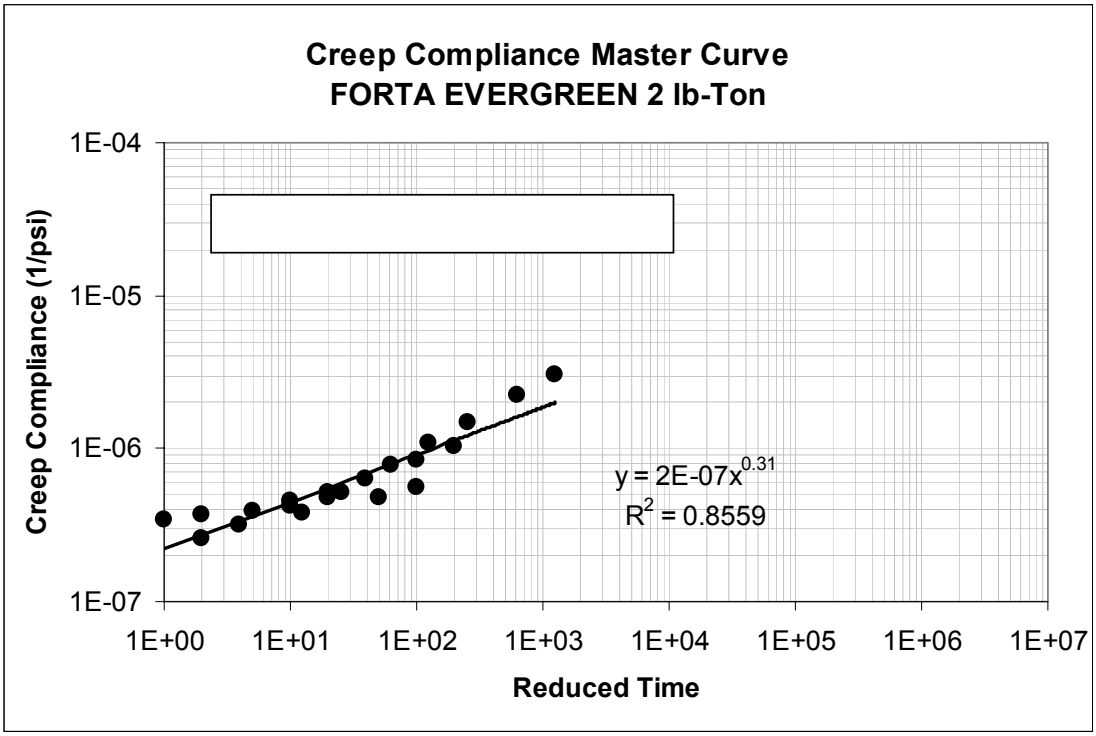

Figure 68 CCMC for the 2 lb/Ton Mixture, FORTA Evergreen

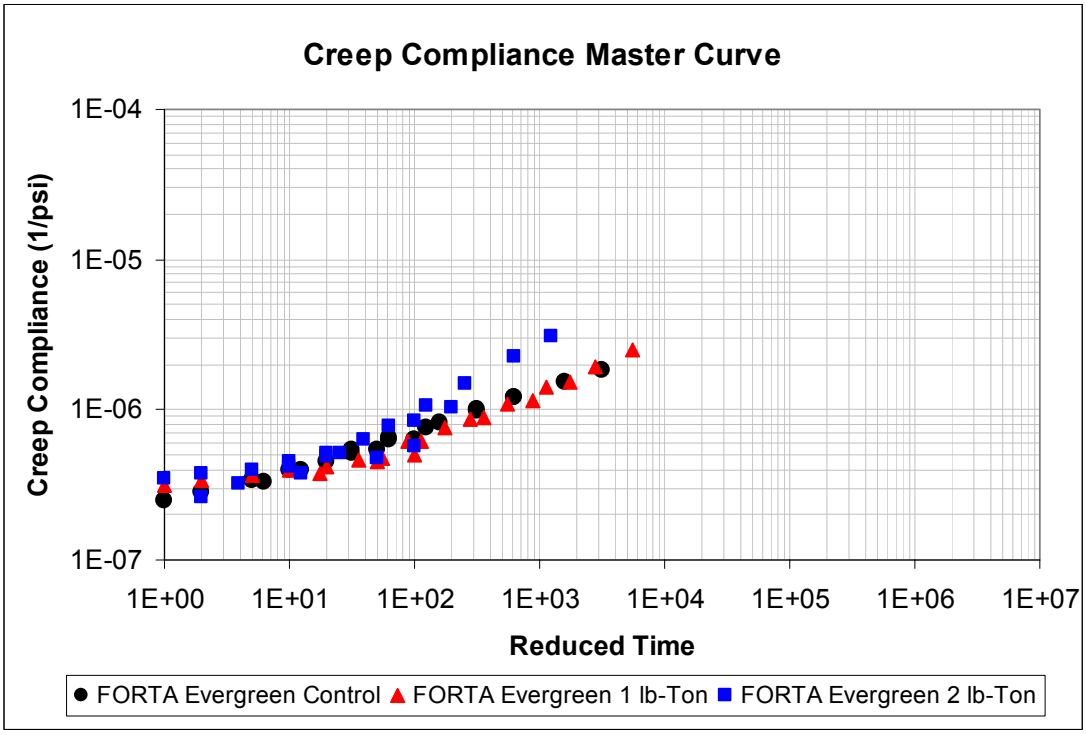

Figure 69 Comparison of the CCMC for All Mixtures, FORTA Evergreen

8.9.4 Indirect Tensile Strength Test Results

8.9.4.1. Tensile Strength

The results of the tensile strength test calculated using modified Roque method are summarized in Table 39. Figure 70 presents the results of the tensile strength for all mixtures.

Table 39 Summary of the Tensile Strength Results, FORTA Evergreen

Tensile Strength (psi)			
Mix	Temp [°C]		
	-10	0	10
FORTA Evergreen Control	410	408	371
FORTA Evergreen 1 lb/Ton	610	571	468
FORTA Evergreen 2 lb/Ton	598	579	467

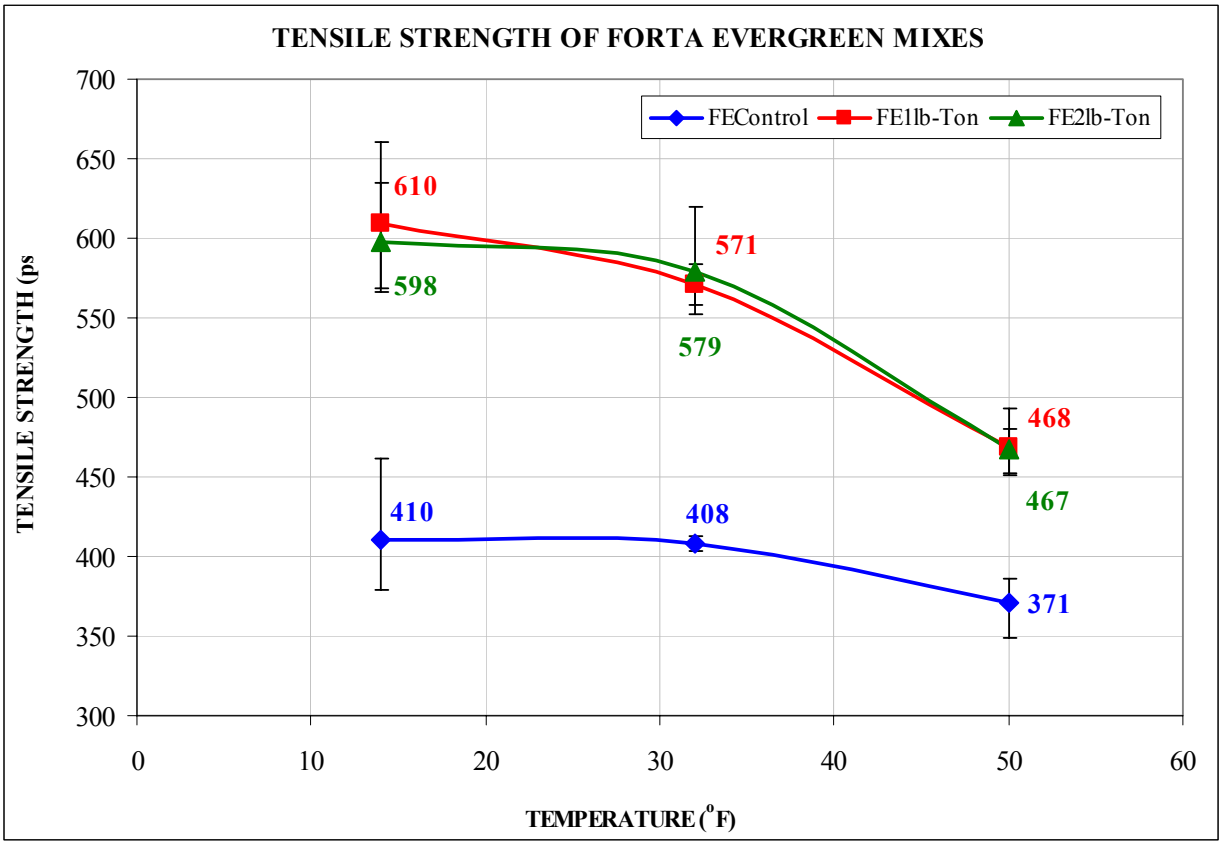

Figure 70 Comparison of the Tensile Strength Results, FORTA Evergreen

Considering the tensile strength results, the following observations are made:

- The tensile strength of all mixtures increased as the temperature decreased.
- Comparing the results of the tensile strength for both the control and fiber-reinforced (1 and 2 lb/Ton) mixtures, it can be observed that both the 1 and 2 lb/Ton fiber-reinforced asphalt mixtures had about 1.5 times higher strength than the control mixtures.
- Traditionally, higher thermal cracking would be expected for mixtures with lower tensile strength values.
- In essence, fibers in the mix play a vital role in resisting thermal cracking in the HMA mixture. However, from the test results, there was not much difference between 1 and 2 lb/Ton mixtures.

8.9.4.2 Tensile Strain at Failure

The results of the tensile strain at failure for the compared mixtures are summarized in Table 40. A graphical representation of the results is shown in Figure 71.

Table 40 Summary of the Tensile Strain at Failure Results, FORTA Evergreen

Tensile Strain at Failure [ε]			
Mix	Temp [°C]		
	-10	0	10
FORTA Evergreen Control	4.20E-04	7.19E-04	1.35E-03
FORTA Evergreen 1 lb/Ton	4.62E-04	6.32E-04	1.39E-03
FORTA Evergreen 2 lb/Ton	3.79E-04	6.28E-04	1.85E-03

Considering the results of the tensile strain at failure, the following observations can be made:

- At 50 °F (highest temperature), the 2 lb/Ton fiber-reinforced asphalt mixture had, as expected, the highest tensile strain at failure than 1 lb/Ton and control mixtures. It can be observed that the 2 lb/Ton mix has about 35% larger strain than the other two mixes.
- At 32 °F, this difference was not significant (~15%) when control and fiber-reinforced asphalt mixtures were compared.
- The difference between the mixtures was about 10 % at the lowest (14 °F) temperature.
- Generally, the higher the tensile strain at failure, the less susceptible the mix to thermal cracking.

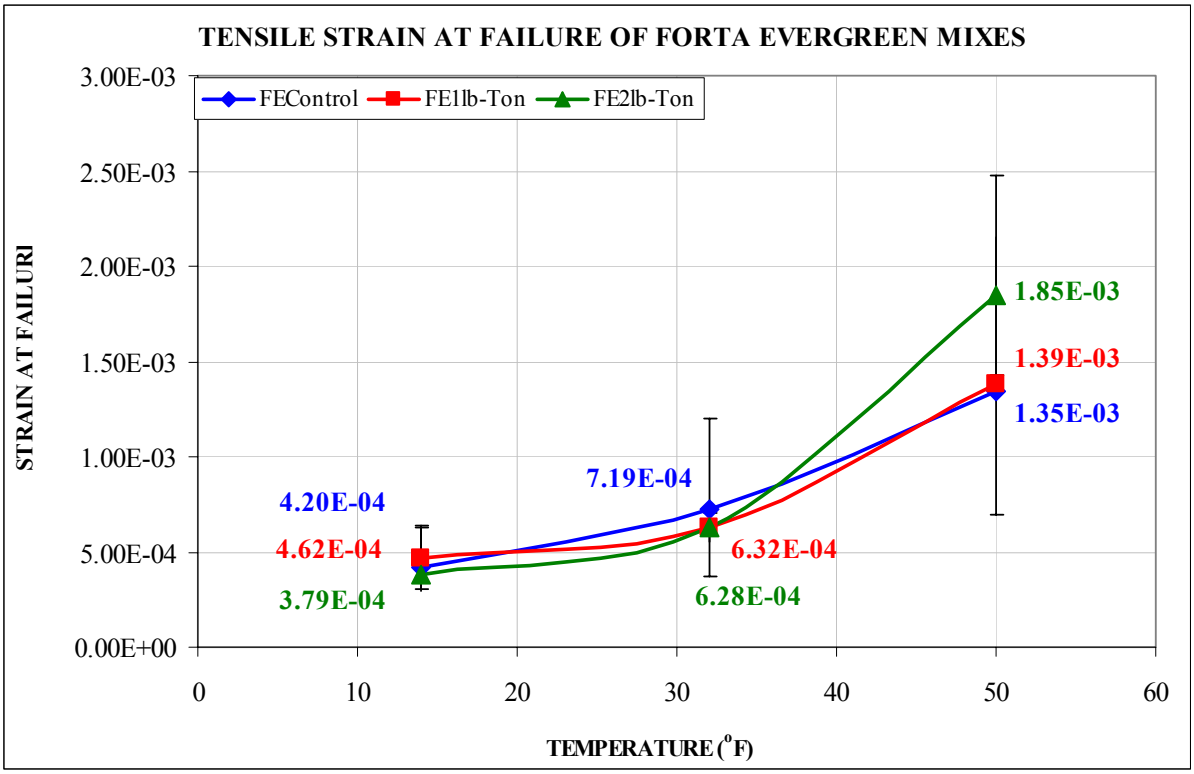

Figure 71 Comparison of the Tensile Strain at Failure Results, FORTA Evergreen

8.9.4.3 Energy until Failure

The results of the energy until failure for the mixtures are summarized in Table 41. A graphical representation of the results is shown in Figure 72.

Table 41 Summary of the Energy until Failure Results, FORTA Evergreen

Energy Until Failure [lbs*in]			
Mix	Temp [°C]		
	-10	0	10
FORTA Evergreen Control	96.7	110.6	178.2
FORTA Evergreen 1 lb/Ton	182.0	213.4	257.0
FORTA Evergreen 2 lb/Ton	180.6	205.3	280.9

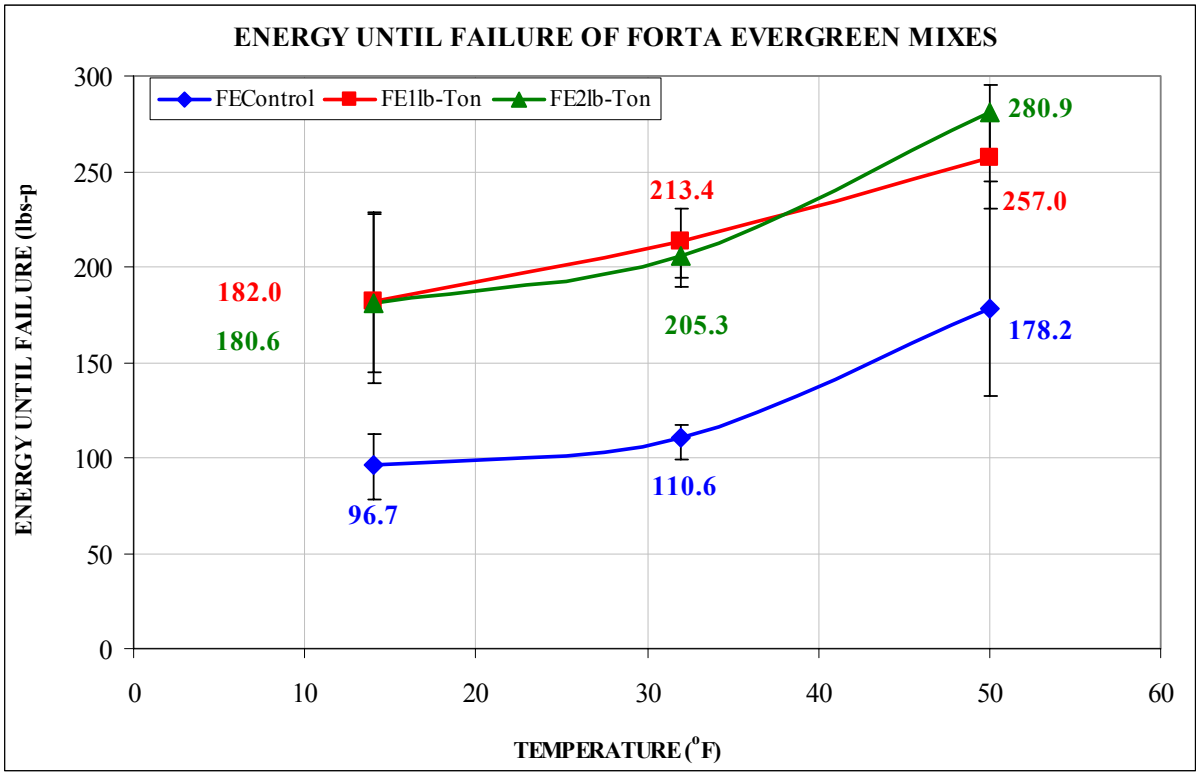

Figure 72 Comparison of the Energy until Failure Results, FORTA Evergreen

Considering the results of the energy until failure, the following observations can be made:

- Both fiber-reinforced asphalt mixtures had very similar trends for the temperature – energy relationship. The peak energy at failure was measured at the highest temperature and the lowest energy was observed at the 14 °F temperature. At the highest temperature (50 °F), the highest energy is exhibited by the 2 lb/Ton mix followed by the 1 lb/Ton mix. At lower temperatures (32 and 14 °F), difference in energies is insignificant for both the fiber-reinforced mixes.
- When fiber-reinforced asphalt mixtures (both 1 and 2 lb/Ton) were compared with control mix, on an average fiber-reinforced mixtures had about 2 times higher energies than control mixes.

8.9.4.4 Total Fracture Energy

The results of the total fracture energy for the all mixtures are summarized in Table 42. A graphical representation of the results is shown in Figure 73.

Table 42 Summary of the Total Fracture Energy Results, FORTA Evergreen

Total Fracture Energy [lbs*in]			
Mix	Temp [°C]		
	-10	0	10
FORTA Evergreen Control	113.0	163.2	279.3
FORTA Evergreen 1 lb/Ton	198.0	284.5	430.4
FORTA Evergreen 2 lb/Ton	206.7	294.3	550.6

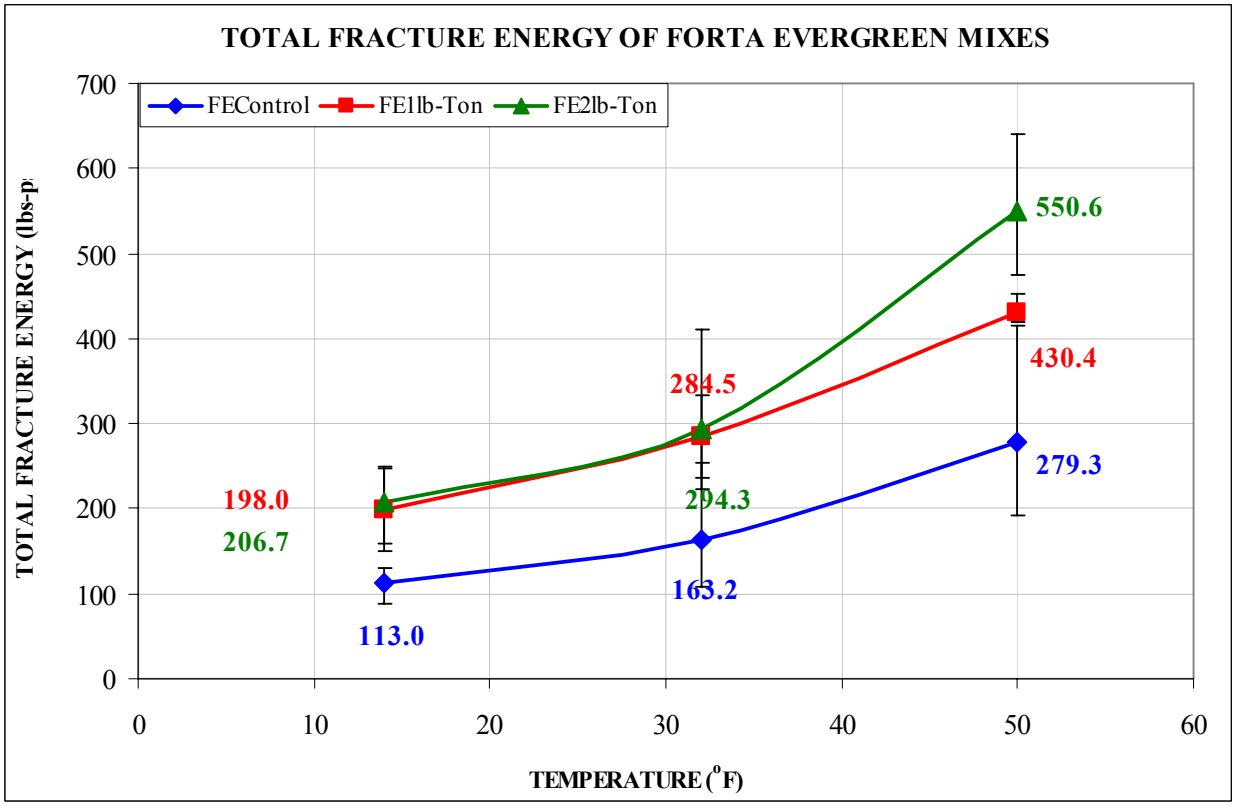

Figure 73 Comparison of the Total Fracture Energy Results, FORTA Evergreen

Considering the results of the total fracture energy, the following observations can be made:

- The fracture energy decreased with increasing temperature for all the three FORTA mixtures. At the highest temperature (50 °F), the 2 lb/Ton mix exhibited the highest

fracture energy followed by the 1 lb/Ton mix and then, followed by control mix.

- At the immediate lower temperature of 32 ^{o}F, both the fiber-reinforced mixtures had very similar total fracture energies but exhibited about 2 times higher energy than the control mix.
- The same trend of fracture energy results were observed at the lowest temperature (14 ^{o}F) as observed at 32 ^{o}F. At the lowest temperature of 14 ^{o}F, where susceptibility of crack initiation and propagation is the highest, it is observed that the fiber-reinforced asphalt mixtures had higher energy values than the control mix.
- Generally, lower thermal cracking should be expected as the energy at failure or fracture energy is increased.

8.10 Summary of Indirect Diametral Tensile Tests

- Both indirect tensile cracking tests (Strength and Creep) were carried out according to the procedure described in the draft indirect tensile tests protocol for the Mechanistic Empirical Pavement Design Guide. The tests were carried out at three temperatures: 50, 32 and 14 ^{o}F.
- The Creep Compliance Master Curve (CCMC) plots include the power model equations and were built based on the results from the IDT creep test and temperature-time shift factors from the MASTER program. Since the creep compliance is inversely proportional to the stiffness modulus it is recommended to have high creep compliance asphalt concrete mixtures, at least from the thermal cracking point of view.
- Comparing the FORTA control and fiber-reinforced asphalt mixtures compacted at the same air void levels, it is observed that FORTA 2 lb/Ton mixture had higher creep

compliance compared to both control and 1 lb/Ton mixtures at higher temperatures. Again, the 2 lb/Ton mix had higher creep compliance followed by 1 lb/Ton mix and then followed by the control mixture at lowest temperature zone.

- The tensile strength of all mixtures increased as the temperature decreased. Comparing the results of the tensile strength for both the control and fiber-reinforced (1 and 2 lb/Ton) mixtures, it was observed that both the 1 and 2 lb/Ton fiber-reinforced asphalt mixtures had about 1.5 times higher strength than the control mixtures. Traditionally, higher thermal cracking would be expected for mixtures with lower tensile strength values. In essence, fibers in the mix play a vital role in resisting thermal cracking in the HMA mixture. However, from the test results, there was not much difference between 1 and 2 lb/Ton mixtures.
- At 50 ^{o}F (highest temperature), the 2 lb/Ton fiber-reinforced asphalt mixture had the highest tensile strain at failure than 1 lb/Ton and control mixtures. It was observed that the 2 lb/Ton mix had about 35% larger strain than the other two mixes. At 32 ^{o}F, this difference was not significant (~15%) when control and fiber-reinforced asphalt mixtures were compared. The difference between the mixtures was about 10 % at the lowest (14 ^{o}F) temperature. Generally, the higher the tensile strain at failure, the less susceptible the mix to thermal cracking.
- Both fiber-reinforced asphalt mixtures had very similar trends for the temperature – energy relationship. The peak energy at failure was measured at the highest temperature and the lowest energy was observed at the 14 ^{o}F temperature. At the highest temperature (50 ^{o}F), the highest energy is exhibited by the 2 lb/Ton mix followed by the 1 lb/Ton mix. At lower temperatures (32 and 14 ^{o}F), difference in energies is insignificant for both the

fiber-reinforced mixes. When fiber-reinforced asphalt mixtures (both 1 and 2 lb/Ton) were compared with control mix, on an average fiber-reinforced mixtures had about 2 times higher energies than control mixes.

- The fracture energy decreased with increasing temperature for all the three FORTA mixtures. At the highest temperature (50 ^{o}F), the 2 lb/Ton mix exhibited the highest fracture energy followed by the 1 lb/Ton mix and then, followed by control mix. At the immediate lower temperature of 32 ^{o}F, both the fiber-reinforced mixtures had very similar total fracture energies but exhibited about 2 times higher energy than the control mix. The same trend of fracture energy results were observed at the lowest temperature (14 ^{o}F) as observed at 32 ^{o}F. At the lowest temperature of 14 ^{o}F, where susceptibility of crack initiation and propagation is the highest, it was observed that the fiber-reinforced asphalt mixtures had higher energy values than the control mix. Generally, lower thermal cracking should be expected as the energy at failure or fracture energy is increased.

9. CRACK PROPAGATION TEST – C* INTEGRAL

9.1 Background

Cracking is a major form of distress in asphalt pavement layers. There are three primary causes of cracking, namely fatigue cracking, due to repetitive nature of traffic loading, reflective cracking, which results from the presence of a defect which may be a crack or joint in other layers of the pavement., and low temperature cracking which is caused by a rapid and large decrease in ambient temperatures (26).

Fracture mechanics discusses the underlying principles which govern\initiation and propagation of cracks in materials. Sharp internal or surface notches which exist in various materials intensify local stress distribution. If the energy stored at the vicinity of the notch is equal to the energy required for the formation of new surfaces, then crack growth can take place. Material at the vicinity of the crack relaxes, the strain energy is consumed as surface energy, and the crack grows by an infinitesimal amount. If the rate of release of strain energy is equal to the fracture toughness, then the crack growth takes place under steady state conditions and the failure in unavoidable (27).

The concept of fracture mechanics was first applied to asphalt concrete by Majidzadeh (28). Abdulshafi (29) has applied the energy (C*-Line Integral) approach to predicting the pavement fatigue life using the crack initiation, crack propagation, and failure. He concluded that two different tests are required to evaluate first the fatigue life to crack initiation (conventional fatigue testing) and second, the crack propagation phase using notched specimen testing under repeated loading. Abdulshafi and Majidzadeh (27) used notched disk specimens to apply J-

integral concept to the fracture and fatigue of asphalt pavements. Various situations such as the effect of load magnitude on fatigue cracking, the length of rest period, load sequence, support conditions, and temperature were included in the testing protocol. Several research studies have also been conducted to apply fracture mechanics principles on asphaltic materials.

9.2 Linear Elastic Fracture Mechanics

Most previous studies assumed a linear elastic material response and used a single load level to relate number of load repetitions to fatigue failure. The assumption of linearity during crack propagation especially at the crack tip is questionable. In addition, the type of laboratory test used by previous researchers does not allow measurement of the crack length and, therefore, does not consider the crack propagation. Additional insight into the laboratory tests and fracture process are still needed to evaluate the number of load repetitions necessary for crack initiation and to evaluate the rate of crack propagation at various stress levels. Once these parameters are determined, the degree of fatigue failure in the material and the corresponding remaining fatigue life of a pavement section can be accurately obtained.

In linear elastic fracture mechanics (LEFM) the intensity of the stress-field in the vicinity of the crack in an opening mode is measured by means of the parameter stress intensity factor, KI. The stress intensity factor depends linearly on the applied stress, and is a function of the geometry of the structure and the crack length. Figure 74 illustrates the process of fracture in different materials. For a perfectly brittle material such as glass, there is no stable crack growth. The energy stored in the material in the vicinity of the crack is a function of the crack length, applied load, and the geometry of loading. It can be expressed using the stress intensity factor, KI, which

can also be related to the available energy for the propagation of the crack by a unit length. When the strain energy release rate is equal to the fracture toughness of the material, KIC, the material fails by unstable propagation of the crack (horizontal line in Figure 74 indicating an unbounded increase in the crack length). Such a failure can be modeled based on LEFM principles using a single parameter (27).

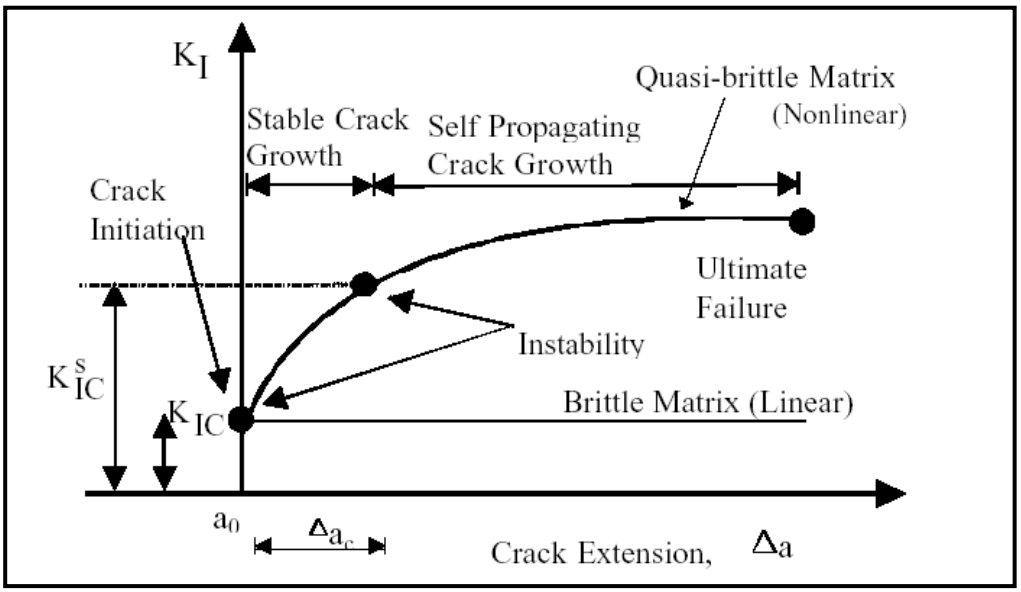

Figure 74 Brittle and Quasi-Brittle Materials (27)

9.3 Nonlinear Fracture Mechanics

Schapery applied the principles of fracture mechanics to viscoelastic materials by considering the kinetics of crack growth as a function of time (30). These approaches were applied to the fracture of HMA by Jenq and Perng (31). One of the characteristics of fracture in quasi-brittle materials is the existence of stable crack growth prior to the crack reaching its critical length (instability) as shown in Figure 72. Such behavior often results in non-linear effects since the crack length at the onset of instability is unknown; therefore, LEFM is not directly applicable. For a granular based material, such as asphalt mixtures, crack growth is heterogeneous and

tortuous; it is accompanied by aggregate interlock, microcracking, and inelastic deformations. Furthermore, the viscoelastic behavior of the matrix results in the relaxation of stresses in the vicinity of the crack tip. These mechanisms give rise to a zone of non-linear deformations (viscoelastic, plastic, and microcracking) generally referred to as the fracture process zone, resulting in the toughening of the material. This response is depicted as the increasing curve in Figure 75 (27). This curve represents the Resistance Curve, or as commonly known the R-Curve response. Since linear elastic fracture mechanics cannot adequately characterize the cracking and failure of materials, several nonlinear techniques have been proposed in which two or more fracture parameters are used. Two approaches have been used to evaluate the nonlinear response, namely the compliance approach and the R-Curve approach. The compliance approach is generally limited to defining the condition of crack instability, while the R-Curve approach evaluates the fracture toughness of the material at different crack lengths providing more insight of the crack propagation phenomenon.

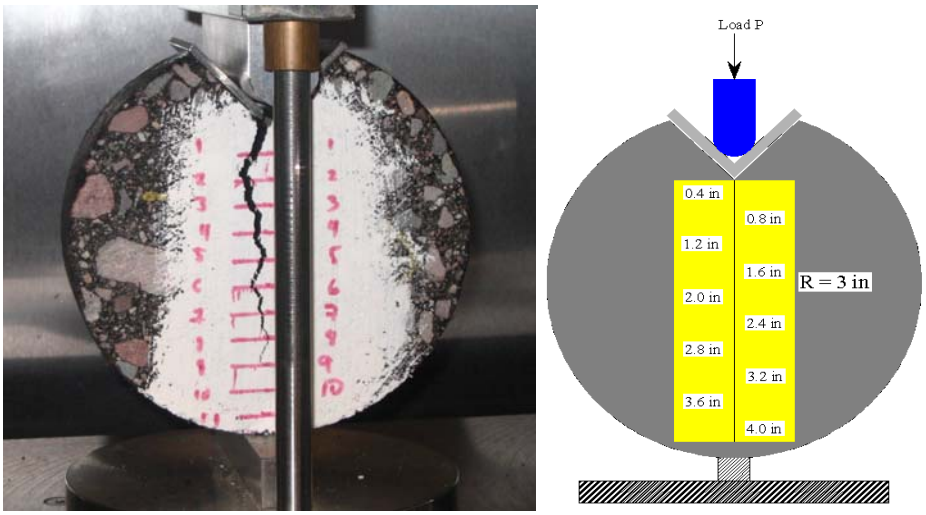

Figure 75 Typical C* Test Setup

9.4 C* Parameters

The relation between the J-integral and the C* parameters is a method for measuring it experimentally. J is an energy rate and C* is an energy rate or power integral. An energy rate interpretation of J has been discussed by Rice (32) and Begley and Landes (33). J can be interpreted as the energy difference between the two identically loaded bodies having incrementally differing crack lengths.

$$J = -\frac{dU}{da}$$

Where

U = Potential Energy

a = Crack Length

C* can be calculated in a similar manner using a power rate interpretation. Using this approach C* is the power difference between two identically loaded buddies having incrementally differing crack lengths.

$$C^* = -\frac{\partial U^*}{\partial a}$$

Where

U* is the power or energy rate defined for a load p and displacement u by

$$U^* = \int_0^u p\,du$$

9.5 Adopted Method for C* Determination

For multiple specimens tested at different displacement rates, the data are collected as load and crack length versus time for a constant displacement rate. The tested samples and adopted displacement rates are shown in Table 43 for conventional and fiber mixtures.

Table 43 Adopted Displacement Rates for Different FORTA Mixtures

Displacement Rate, Δ* (in/min)	Conventional Mix	1 lb/Ton Mix	2 lb/Ton Mix
0.005	FEC22B	FE120T	---
0.01	FEC21B	FE120B	FE222B
0.015	FEC21T	FE121B	FE220M
0.02	FEC22M	FE121M	FE222T
0.025	FEC23M	FE120M	FE222M

The calculation passes through 6 main steps as follows:

1. First, the load value is adjusted to take into consideration the sample thickness by dividing the load value by the sample thickness then the load and crack length versus time are plotted for each displacement rate.
2. The load and the displacement rates are plotted for each crack length.
3. The energy rate input U* is measured as the area under the curve in step 2. Since the value of each displacement rate is required. It was decided to assign an area for each rate as showed in Figure 76. The calculation of these areas can be done by integrating the equation of the trend line that represents this relation. For each area, we will use its boundary in the integration process. To get 5 area values, we extend the trend line for half spacing from the beginning and the end so that each displacement rate represents the center of its area. After that, the U* values are obtained and plotted versus crack length for each displacement rate. The slope of these curves are C* value for each displacement rate.

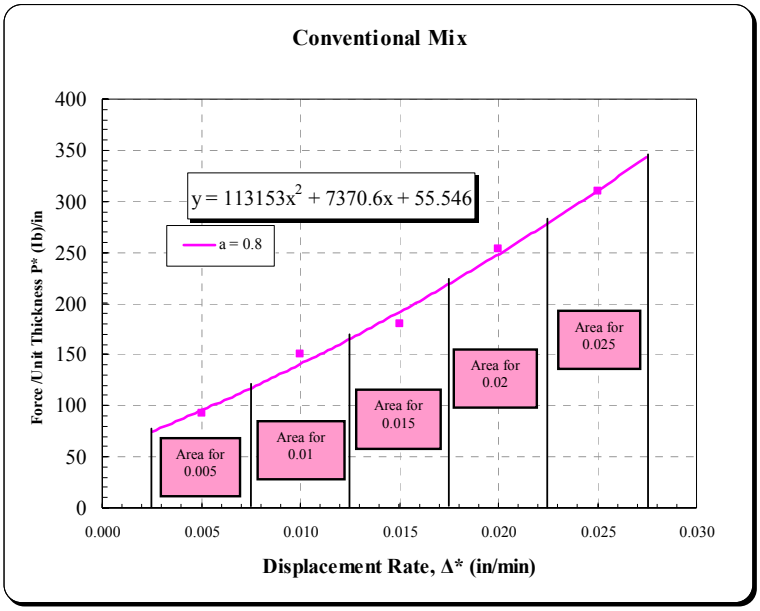

Figure 76 One Example for Method of Area Calculation

4. The C* values versus the Displacement rate are plotted for conventional and fiber mixes.
5. The crack growth rates were calculated for each displacement rate as the total crack length divided by the time. These values also are corrected according to the sample thickness. The crack growth rate versus the Displacement rate values are plotted for conventional and fiber mixes.
6. The crack growth rate versus the C* values are plotted for control and fiber-reinforced mixes to compare the performance of each mix through the slope of this relation ship where the higher the slope the higher the resistance of the mix to resist the crack propagation. The plots for the last step are shown in Figures 77, 78 and 79.

Tables 44, 45 and 46 present summary of test results for all the three FORTA Evergreen mixes.

Table 44 Summary of Test Results for FORTA Evergreen Control Mixture

Sample ID: FEC22B		Average Thickness, b (in): 1.79		Displacement Rate, Δ* (in/min) : 0.005	
Crack Length, a (in)	**Time T, (Min)**	**Force (KN)**	**Force, P (Ib)**	**Force per Unit Thickness P* (Ib/in)**	**Crack Growth Rate, a* (in/min)**
0.40	25.70	0.74	165.50	92.46	
0.80	25.70	0.74	165.50	92.46	
1.20	25.80	0.70	157.40	87.93	
1.60	25.80	0.70	157.40	87.93	
2.00	27.60	0.42	94.20	52.63	
2.40	28.00	0.37	83.20	46.48	**0.364**
2.80	28.50	0.35	78.50	43.85	
3.20	30.00	0.29	64.50	36.03	
3.60	36.40	0.17	38.20	21.34	
4.00	55.00	0.12	27.00	15.08	
Sample ID: FEC21B		**Average Thickness, b (in): 1.92**		**Displacement Rate, Δ* (in/min) : 0.010**	
0.40	4.80	1.32	296.70	154.53	
0.80	4.80	1.28	287.70	149.84	
1.20	5.20	1.07	240.50	125.26	
1.60	5.40	1.03	231.50	120.57	
2.00	5.60	0.97	218.10	113.59	
2.40	5.70	0.93	209.10	108.91	**1.250**
2.80	5.80	0.83	186.60	97.19	
3.20	6.90	0.53	119.10	62.03	
3.60	8.90	0.31	69.70	36.30	
4.00	9.00	0.30	67.40	35.10	
Sample ID: FEC21T		**Average Thickness, b (in): 1.77**		**Displacement Rate, Δ* (in/min) : 0.015**	
0.40	3.38	1.46	328.21	185.43	
0.80	3.40	1.42	319.22	180.35	
1.20	3.43	1.35	303.48	171.46	
1.60	3.47	1.32	296.74	167.65	
2.00	3.53	1.23	276.50	156.21	
2.40	3.67	1.08	242.78	137.16	**2.138**
2.80	3.70	1.05	236.04	133.36	
3.20	4.12	0.77	173.10	97.80	
3.60	5.62	0.37	83.18	46.99	
4.00	8.90	0.12	26.98	15.24	
Sample ID: FEC22M		**Average Thickness, b (in): 1.70**		**Displacement Rate, Δ* (in/min) : 0.020**	
0.40	2.00	3.72	836.26	491.92	
0.80	2.08	1.92	431.62	253.89	
1.20	2.13	1.29	289.99	170.58	
1.60	2.13	1.29	289.99	170.58	
2.00	2.22	1.20	269.76	158.68	
2.40	2.32	1.00	224.80	132.24	**2.277**
2.80	2.47	0.69	155.11	91.24	
3.20	2.60	0.60	134.88	79.34	
3.60	2.75	0.53	119.14	70.08	
4.00	2.93	0.43	96.66	56.86	
Sample ID: FEC23M		**Average Thickness, b (in): 1.83**		**Displacement Rate, Δ* (in/min) : 0.025**	
0.40	2.08	2.32	521.54	284.99	
0.80	2.50	2.52	566.50	309.56	
1.20	3.02	1.76	395.65	216.20	
1.60	3.05	1.69	379.91	207.60	
2.00	3.08	1.63	366.42	200.23	
2.40	3.12	1.51	339.45	185.49	**3.188**
2.80	3.13	1.53	343.94	187.95	
3.20	3.17	1.46	328.21	179.35	
3.60	3.47	1.14	256.27	140.04	
4.00	3.50	0.95	213.56	116.70	

Table 45 Summary of Test Results for FORTA Evergreen 1 lb/Ton Fiber Mixture

Sample ID: FE120T		Average Thickness, b (in): 1.72		Displacement Rate, Δ* (in/min) : 0.005	
Crack Length, a (in)	**Time T, (Min)**	**Force (KN)**	**Force, P (Ib)**	**Force per Unit Thickness P* (Ib/in)**	**Crack Growth Rate, a* (in/min)**
0.40	34.00	1.76	396.08	230.95	
0.80	40.07	0.79	178.27	103.95	
1.20	40.10	0.76	170.62	99.49	
1.60	40.20	0.74	166.13	96.87	
2.00	42.00	0.63	140.95	82.19	
2.40	46.40	0.38	84.30	49.15	**0.107**
2.80	51.00	0.25	56.87	33.16	
3.20	57.50	0.14	31.47	18.35	
3.60	57.60	0.14	30.57	17.83	
4.00	68.00	0.04	8.99	5.24	
Sample ID: FE120B		**Average Thickness, b (in): 1.75**		**Displacement Rate, Δ* (in/min) : 0.010**	
0.40	8.70	3.60	809.28	462.45	
0.80	10.30	3.25	729.48	416.85	
1.20	11.80	2.69	604.71	345.55	
1.60	14.70	1.70	381.04	217.74	
2.00	15.70	1.57	352.94	201.68	
2.40	16.30	1.57	352.94	201.68	**0.156**
2.80	17.50	1.39	312.47	178.55	
3.20	17.70	1.33	298.98	170.85	
3.60	18.90	1.17	263.02	150.30	
4.00	26.50	0.49	110.15	62.94	
Sample ID: FE121B		**Average Thickness, b (in): 1.82**		**Displacement Rate, Δ* (in/min) : 0.015**	
0.40	4.48	4.18	939.66	516.30	
0.80	4.93	4.20	944.16	518.77	
1.20	5.28	4.12	926.18	508.89	
1.60	5.35	4.07	914.94	502.71	
2.00	5.40	4.07	914.94	502.71	
2.40	5.78	3.82	858.74	471.84	**0.586**
2.80	6.73	2.35	528.28	290.26	
3.20	7.77	1.28	286.62	157.48	
3.60	9.00	0.73	164.10	90.16	
4.00	10.17	0.52	116.90	64.23	
Sample ID: FE121M		**Average Thickness, b (in): 1.46**		**Displacement Rate, Δ* (in/min) : 0.020**	
0.40	4.05	3.19	717.95	491.74	
0.80	4.08	3.02	678.84	464.96	
1.20	4.08	3.02	678.84	464.96	
1.60	4.15	2.76	621.56	425.72	
2.00	4.25	2.36	531.51	364.05	
2.40	4.58	1.14	256.75	175.86	**2.529**
2.80	4.70	0.90	201.87	138.27	
3.20	4.72	0.85	190.72	130.63	
3.60	4.75	0.86	193.64	132.63	
4.00	5.62	0.41	91.93	62.97	
Sample ID: FE120M		**Average Thickness, b (in): 1.62**		**Displacement Rate, Δ* (in/min) : 0.025**	
0.40	3.98	4.39	986.87	609.18	
0.80	4.05	4.08	917.18	566.16	
1.20	4.12	3.82	858.74	530.09	
1.60	4.22	3.35	753.08	464.86	
2.00	4.25	3.27	735.10	453.77	
2.40	4.27	3.22	723.86	446.83	**2.694**
2.80	4.53	2.46	553.01	341.36	
3.20	4.58	2.33	523.78	323.32	
3.60	5.37	1.75	393.40	242.84	
4.00	5.95	1.28	287.74	177.62	

Table 46 Summary of Test Results for FORTA Evergreen 2 lb/Ton Fiber Mixture

Sample ID:		Average Thickness, b (in):		Displacement Rate, Δ* (in/min) : 0.005	
Crack Length, a (in)	**Time T, (Min)**	**Force (KN)**	**Force, P (Ib)**	**Force per Unit Thickness P* (Ib/in)**	**Crack Growth Rate, a* (in/min)**
Sample ID: FE222B		**Average Thickness, b (in): 1.78**		**Displacement Rate, Δ* (in/min) : 0.010**	
0.40	8.80	5.64	1267.87	712.29	
0.80	9.00	4.00	898.53	504.79	
1.20	9.20	3.38	759.82	426.87	
1.60	9.50	2.69	604.71	339.72	
2.00	9.70	2.34	526.03	295.52	
2.40	10.10	1.76	395.65	222.28	**0.684**
2.80	10.20	1.68	377.66	212.17	
3.20	11.10	1.14	256.27	143.97	
3.60	12.50	0.78	175.34	98.51	
4.00	16.50	0.39	87.67	49.25	
Sample ID: FE220M		**Average Thickness, b (in): 1.67**		**Displacement Rate, Δ* (in/min) : 0.015**	
0.40	8.20	5.09	1144.23	685.17	
0.80	8.37	4.87	1094.78	655.56	
1.20	8.63	4.39	985.75	590.27	
1.60	8.92	3.69	829.51	496.71	
2.00	9.40	2.23	500.18	299.51	
2.40	9.82	1.54	346.19	207.30	**0.719**
2.80	10.20	1.23	276.50	165.57	
3.20	11.48	0.74	166.35	99.61	
3.60	13.57	0.46	103.41	61.92	
4.00	14.95	0.36	80.93	48.46	
Sample ID: FE222T		**Average Thickness, b (in): 1.76**		**Displacement Rate, Δ* (in/min) : 0.020**	
0.40	5.10	7.00	1573.60	894.09	
0.80	5.10	7.00	1573.60	894.09	
1.20	5.20	4.20	944.16	536.45	
1.60	5.20	4.20	944.16	536.45	
2.00	5.30	2.24	503.55	286.11	
2.40	5.30	2.24	503.55	286.11	**1.278**
2.80	5.30	2.24	503.55	286.11	
3.20	5.40	1.64	368.67	209.47	
3.60	5.60	1.26	283.25	160.94	
4.00	6.70	0.63	141.62	80.47	
Sample ID: FE222M		**Average Thickness, b (in): 1.65**		**Displacement Rate, Δ* (in/min) : 0.025**	
0.40	3.08	7.40	1663.52	1008.19	
0.80	3.65	6.01	1351.05	818.82	
1.20	3.68	4.87	1094.78	663.50	
1.60	3.73	2.68	602.46	365.13	
2.00	3.77	1.98	445.10	269.76	
2.40	3.80	1.60	359.68	217.99	**2.519**
2.80	3.82	1.50	337.20	204.36	
3.20	3.83	1.42	319.22	193.46	
3.60	3.85	1.33	298.98	181.20	
4.00	5.20	0.37	83.18	50.41	

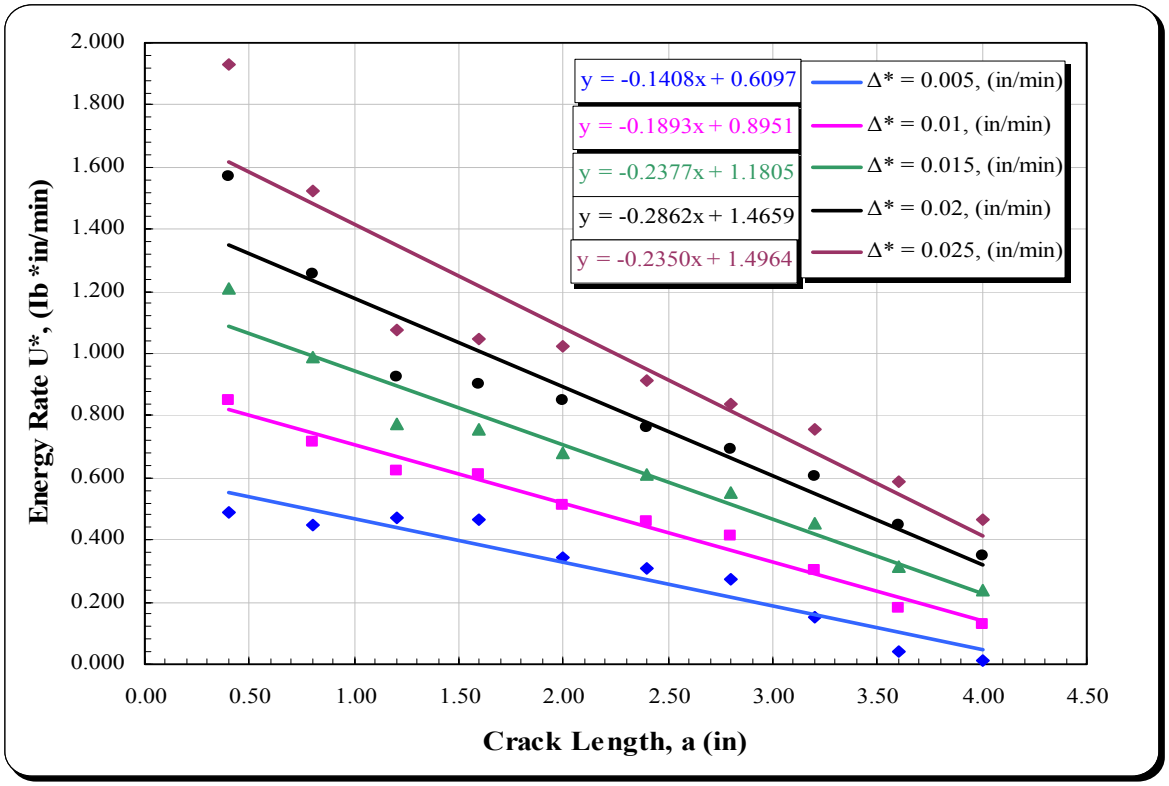

Figure 77 Crack Lengths versus Energy Rate for FORTA Control Mixture

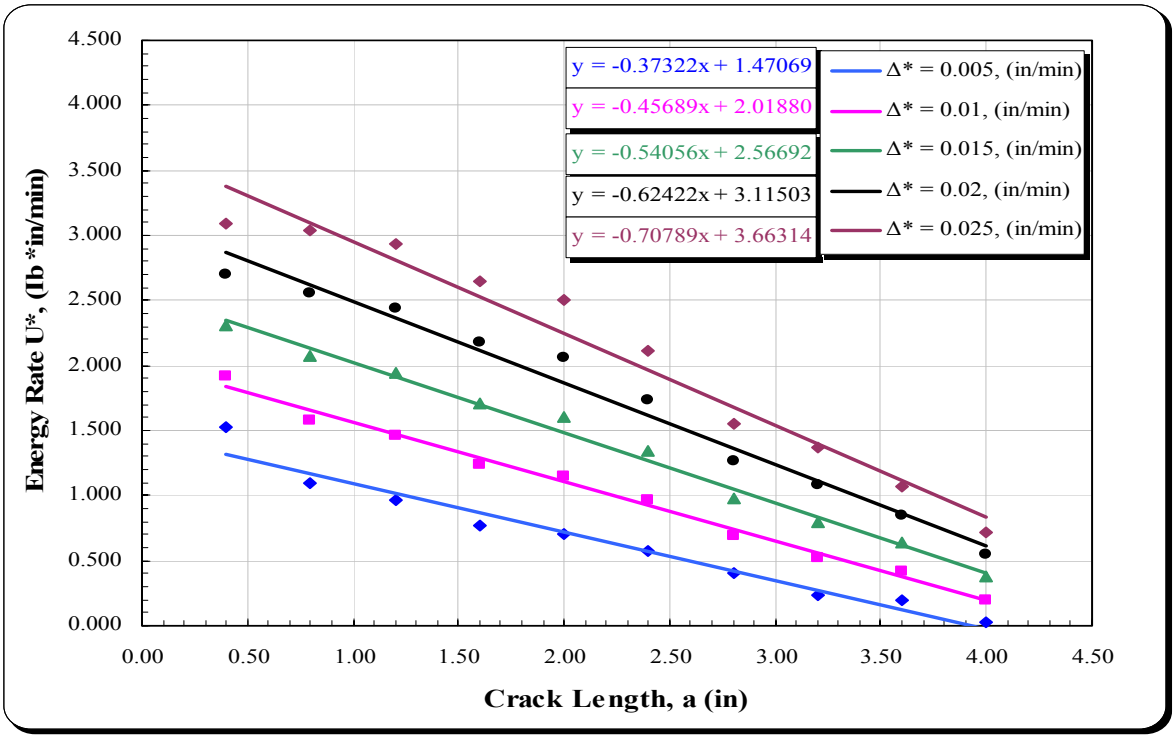

Figure 78 Crack Lengths versus Energy Rate for FORTA 1 lb/Ton Mixture

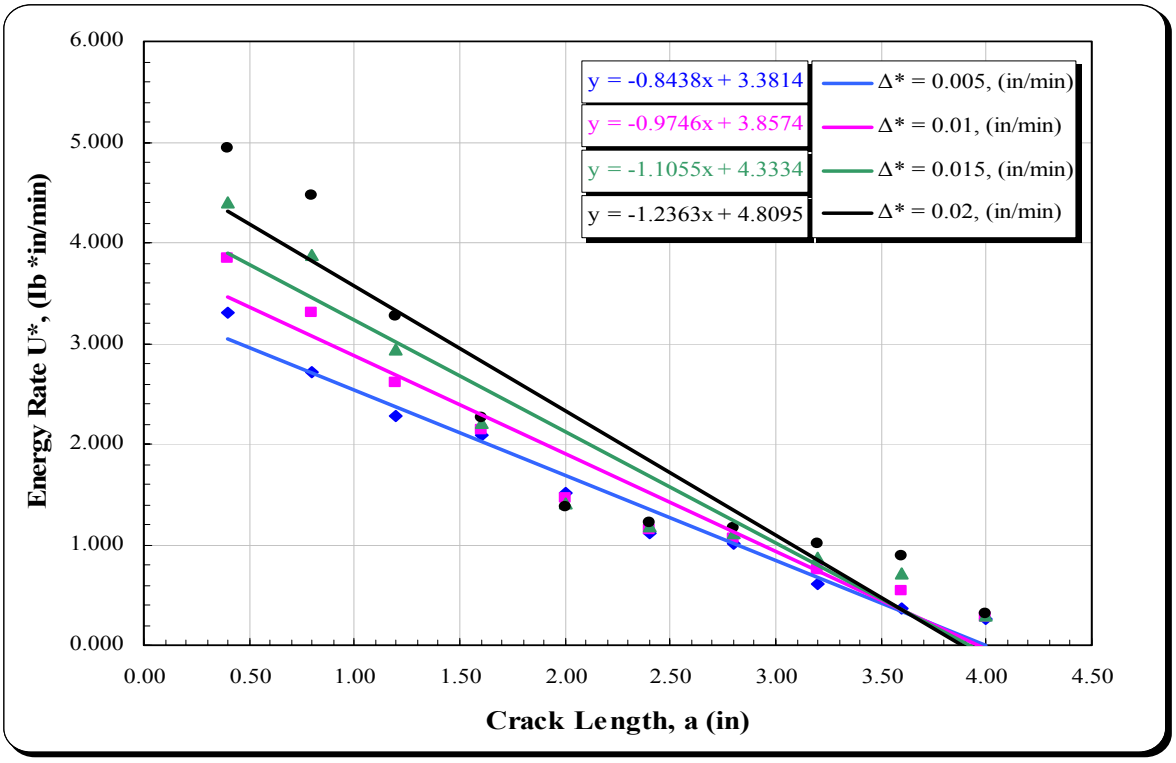

Figure 79 Crack Lengths versus Energy Rate for FORTA 2 lb/Ton Mixture

Figure 80 shows relationships between crack growth rates and C* values for all the three mixtures of FORTA Evergreen project. In addition, slope values of crack growth rates for control and fiber-reinforced asphalt mixtures are shown in Figure 81. From both the figures, it is noticed that the fiber-reinforced mixes, especially the 2 lb/Ton mix has higher slope value when compared to the control mix and also higher C* values. So, fiber-reinforced mixes have the highest potential to resist crack propagation owing to the reinforcement effect of the Aramid fibers. Also, with increase in the fiber percentage, resistance to crack propagation further increases.

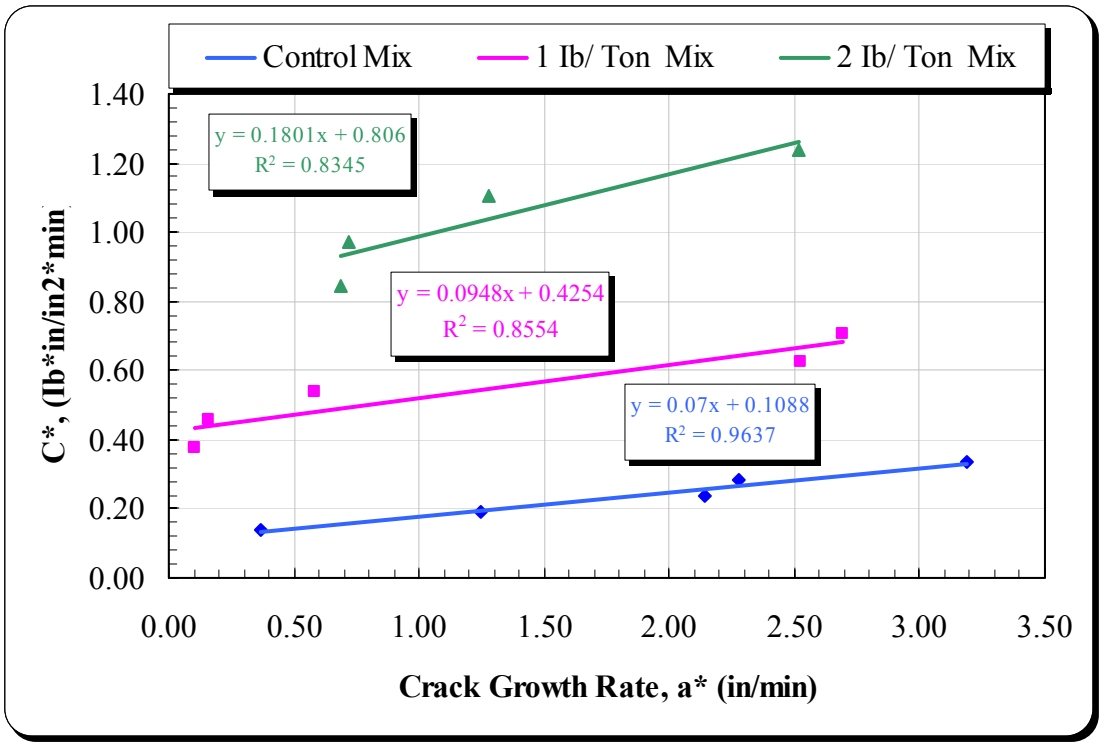

Figure 80 Crack Growth Rate versus C* Values for Control and Fiber-Reinforced Mixes, FORTA Evergreen

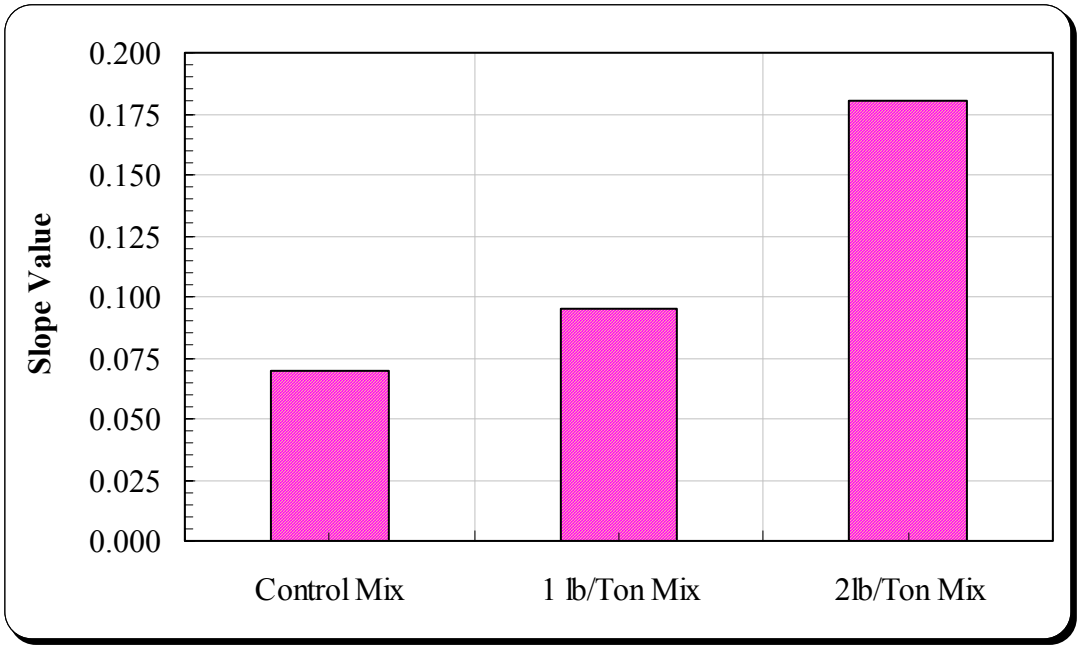

Figure 81 Slope Values of Crack Growth Rate -C* Relation for Control and Fiber-Reinforced Asphalt Mixtures, FORTA Evergreen

9.6 Summary of C* Integral Test

Relationships between crack growth rates and C* values as well as slopes of crack growth rates for all the three mixtures of FORTA Evergreen project were developed. It was noted that the fiber-reinforced mixes, especially the 2 lb/Ton mix had higher C* and slope values than the control mix. This means that the fiber-reinforced asphalt mixtures have higher potential to resist crack propagation because of the reinforcement effect provided by the Aramid fibers; also, the higher the percentage of fibers, the better is the resistance of the mix to crack propagation.

10. EXTRACTION OF FORTA FIBERS FROM ASPHALT MIXTURES

10.1 Introduction

Because of the large variability in test results for the FORTA modified mixtures, a special study was undertaken to evaluate if this variability is due to the quantity of fibers actually present in each test specimen. This might have occurred during HMA mixing and production. The orientation and spatial distribution of the fibers inside the sample may be another reason for such high variability in the test results.

10.2 Objectives of this Special Study

The purpose of this task was to investigate the reasons for the high variability in test results, focusing on specific material characterization tests. Tested specimens were selected from Repeated Load Flow Number and Triaxial Shear Strength tests. Two samples were chosen from 1 lb/Ton mixture (represented as Sample No. 1 and 2 in this section), which were used for Flow Number testing; and one sample was chosen from the 2 lb/Ton mixes (represented as Sample 3) that was used for Triaxial Shear Strength testing.

This effort focused on a method of extracting fibers from the tested samples of FORTA fiber-reinforced asphalt mixtures. The scope of work of this mini-study includes computation of the fiber content, binder content and also, the determination of aggregate gradations after separating out the binder and fibers from the mix. The differences in the actual and calculated values of each parameter was determined and investigated for possible high variability of the material characterization test results.

10.3 Quantitative Extraction of Bitumen from Bituminous Paving Mixtures

The sample is placed in a centrifuge to extract the asphalt from the aggregate (34, 35, 36). Organic solvent is added to the centrifuge to dissolve the asphalt, such that the dissolved asphalt (in liquid form) can be drained out of the centrifuge, through a filter, leaving the bare aggregate in the centrifuge. More solvent is then added to the aggregate to remove the remaining bitumen from the aggregate which is drained out of the centrifuge through a filter. The bare aggregate is removed from the bowl and dried in an oven to remove solvent from the aggregate surface. The aggregate is then weighed. The extracted bitumen is then put into a high speed shear extractor (Swiss extractor) to get the mass of some fine aggregate particles (No. 200 passing) present in the binder. The asphalt-extraction process, in conjunction with the weighing operations enables the determination of the sample's asphalt content. The size range of the aggregates can be determined by passing the bare aggregates through a range of different square mesh size sieves.

10.4 Test Procedure

The ASTM D 2172-95 test procedure covers the quantitative determination of bitumen and gradation of aggregate present in the mix (36). The steps that were followed for the extraction of FORTA fibers from the asphalt mix are as follows.

1. The test procedure requires the addition of solvent for the extraction process. There can be various solvents that can be used but a solvent to which the FORTA fibers are inert must be used. To check the reactivity of various solvents, the fibers were soaked in xylene, toluene and trichloroethylene to choose the best one for the process (Figure 82 a). The fibers did not show any major reactivity to either of them. Trichloroethylene was chosen as the solvent as it is the most common one used in practice.

Figure 82 (a) Fiber Soaked in Different Solvents (b) Disintegration of the Asphalt Sample

2. For preparation of the test specimens, the test specimen was placed in a large, flat pan and warmed to at temperature of 230 ± 9 °F (110 ± 5 °C) only till it could be handled or mixed (Figure 82 b). The material was split with the help of a spatula or trowel. The loose mix was placed in the oven at 230 ± 9 °F (110 ± 5 °C) until the sample lost all its moisture. Then, the weight of the mix was measured.

3. The test portion in the bowl was covered with trichloroethylene and sufficient time was allowed for the solvent to disintegrate the test portion (30-40 minutes). The amount of solvent added was noted down. Later, the test portion and the solvent were placed in the extraction apparatus (Figure 83). The mass of the filter ring was dried and the mass of the filter ring was determined and fitted around the edge of the bowl. The cover on the bowl was clamped tightly and a beaker was placed under the drain to collect the extracted bitumen.

Figure 83 (a) Mix Soaked in Trichloroethylene (b) Mix Bowl (before Keeping in Centrifuge)

4. The centrifuge (Figure 84) was switched on which revolved slowly (400 rpm) and gradually the speed was increased to a maximum of 1000 rpm or until solvent ceased to flow from the drain. The machine was stopped and 200 ml of trichloroethylene was added and the procedure was repeated. Sufficient amount of 200 ml of solvent (not less than three) was added so that the extract was not darker than a light straw color. The number of washes was noted and the extract and the washings were collected in a suitable graduate.

Figure 84 Extraction Apparatus (Centrifuge)

5. The filter ring and washed aggregates along with the fibers were removed from the bowl as shown in Figure 85. Mineral matter adhering to the surface of the ring was brushed off and added to the extracted aggregate. The ring and aggregate were dried in the oven at 230 ± 9 °F (110 ± 5 °C) till it was left with no solvent content and then the weights of aggregates and ring were measured.

Figure 85 Picture Showing Aggregate and Fibers after Bitumen Extraction

6. The amount of mineral matter in the extract was determined by using the centrifuge method (36). The test method employed a Swiss extractor or high speed shear extractor. All of the extract was transferred to an appropriate container or feed suitably equipped with a feed control (valve or clamp, etc.). The mass of a clean empty cone was measured to an accuracy of 0.01 ± 0.005 g and placed in the extractor. The valve was opened to let the extract flow at a rate of 100-150 ml/min. After all the extract had passed through the centrifuge, the feed mechanism (with the extractor still running) was washed. Then, the cone was removed and the outside of the cone was cleaned with fresh solvent. The residual solvent was allowed to evaporate in a steam hood and then dried in an oven at

230 ± 9 °F (110 ± 5 °C). Then, it was allowed to cool in a desiccator. The weight of the cone was measured. Hence, the increase in the mass is the mass of mineral matter.

7. The dried aggregate (containing fibers) was taken and was weighed. 2-3 drops of soap solution with water was added to the aggregate and fiber mix and they were mixed. This was done to remove the bitumen that might have stuck to the aggregate and fibers. Soap solution washed the oil remaining in the aggregates and fibers. A No. 200 sieve was placed with a No. 50 sieve on top of it and the water was drained from the washed aggregates. The washing was performed several times till there was no soap solution left in the washed aggregates and until the water was clear. Most of the fibers floated in water and separated out as they were retained on the No. 200 sieve. If the fibers got clumped to the aggregates, then it was mixed well in water to separate them as the fibers would then float and could be easily separated (Figure 86).

8. The washed aggregates and fibers were dried in oven at 230 ± 9 °F (110 ± 5 °C) and weighed (Figure 86). Sieve analysis of the dried aggregate was performed using the same gradation sieves as used for the original mix preparation. The various aggregates retained were measured and any fibers in the aggregates were manually separated. Then, the fiber weight was measured again on a high precision scale kept in a closed chamber.

Figure 86 (a) Wet Sieving and Retrieval of the FORTA Fibers (b) Retrieved (Dried) Fibers

Originally, the Polypropylene fibers were thought to dissolve under high temperatures and that they were not recoverable. The retrieved sample of fibers indicated otherwise. To verify this, samples of both fiber types were placed in the oven at various temperatures to visually evaluate the effect of high temperatures on the fibers. The Aramid fibers did not show any change in mass or structure up to 200 °C. The Polypropylene fibers also did not show any changes until 110 °C but beyond 160 °C, the fibers started getting flaky and distorted (crumbling up). However, their mass did not show any appreciable change (Figure 87).

Figure 87 Fibers after Exposing to High Temperature (>160 °C)

10.5 Determination of Asphalt Content and the Amount of FORTA fibers in the Mix

Table 47 shows the calculated amount of fibers, theoretically, and based on the mix design and fiber dosage content. These specific samples were chosen because they showed high variability in Flow Number Tests. That is, Sample 1 and 2 should have had similar Flow number results but they were very different. Again, the fiber contents / weights in this table represents only the weights of fiber contents as per the mix design. Tables 48 through 50 present the summary results of the three samples using the fiber extraction laboratory method. The tables include asphalt and fiber content along with the weight of the aggregates. Asphalt contents of the three samples were determined by deducting the dried aggregate weight from the initial sample weight.

Table 47 Calculated Design Fiber Content for Each Selected Sample

Fiber Content per Designed Values			
	Sample 1 (1lb/Ton)	Sample 2 (1 lb/Ton)	Sample 3 (2 lb/Ton)
Weight of Sample, g	2764.4	2841.3	2841.3
Calculated Weight of Fiber, g	1.36	1.39	2.78

Table 48 Laboratory Extraction Results for Sample 1, 1 lb/Ton

a	Weight of filter and Ash, g	37.1
b	Weight of filter, g	33.5
c	Weight of Ash (a-b) , g	3.6
d	Weight of Cone and Ash, g	165.35
e	Weight of Cone, g	142.24
f	Dry weight -#200 (d-e) , g	23.11
g	Total Weight of Ash (c+f) , g	26.71
h	Dry weight of Aggregate, g	2605.5
i	Weight of Aggregate and Ash (g+h) , g	2632.21
j	Initial weight of sample, g	2764.4
k	Weight of Aggregate and Ash (i) , g	2632.21
l	Weight of Extracted Binder (j-i) , g	132.19
m	Binder Content ((l/j)*100), %	4.78
n	Washed Aggregate weight, g	2439.4
o	Number of solvent washes	9
p	Fiber content, g	2.03

Table 49 Laboratory Extraction Results for Sample 2, 1 lb/Ton

a	Weight of filter and Ash, g	36.8
b	Weight of filter, g	33.2
c	Weight of Ash (a-b) , g	3.6
d	Weight of Cone and Ash, g	161.58
e	Weight of Cone, g	142.24
f	Dry weight -#200 (d-e) , g	19.34
g	Total Weight of Ash (c+f) , g	22.94
h	Dry weight of Aggregate, g	2683.1
i	Weight of Aggregate and Ash (g+h) , g	2706.04
j	Initial weight of sample, g	2841.3
k	Weight of Aggregate and Ash (i) , g	2706.04
l	Weight of Extracted Binder (j-i) , g	135.26
m	Binder Content ((l/j)*100), %	4.76
n	Washed Aggregate weight, g	2439.4
o	Number of solvent washes	9
p	Fiber content, g	2.30

Table 50 Laboratory Extraction Results for Sample 3, 2 lb/Ton

a	Weight of filter and Ash, g	38.1
b	Weight of filter, g	33.3
c	Weight of Ash (a-b) , g	4.8
d	Weight of Cone and Ash, g	158.86
e	Weight of Cone, g	140.59
f	Dry weight -#200 (d-e) , g	18.27
g	Total Weight of Ash (c+f) , g	23.07
h	Dry weight of Aggregate, g	2680
i	Weight of Aggregate and Ash (g+h) , g	2703.07
j	Initial weight of sample, g	2841.3
k	Weight of Aggregate and Ash (i) , g	2703.07
l	Weight of Extracted Binder (j-i) , g	138.23
m	Binder Content ((l/j)*100), %	4.87
n	Washed Aggregate weight, g	2560.5
o	Number of solvent washes	10
p	Fiber content, g	2.79

Table 51 shows the design and the actual amounts (recovered) of asphalt and fiber contents determined from fiber extraction process. The design asphalt content was 5.1%. The determined values of asphalt contents for all three samples were found to be lower than the design values (~6% difference). The lower amount is normal for this type of extraction process. A correction factor is usually applied. Of interest, the laboratory determined values of asphalt cement contents were very close, indicating little variation among these specific samples. The laboratory determined fiber content of the 1 lb/Ton mix samples was found to be higher than the design values (for both samples); while the laboratory determined fiber content for the 2 lb/Ton mix sample was found to be almost equal to the design value.

Table 51 Summary of Binder Content and Fiber Content

Mix	Sample 1	Sample 2	Sample 3
	1 lb/ton	1 lb/ton	2 lb/ton
Fiber Content(present), g	2.03	2.30	2.79
Fiber Content(calculated), g	1.36	1.39	2.78
Difference in fiber content, %	49.26	65.47	0.36
Binder Content(present), %	4.78	4.76	4.87
Binder Content(design), %	5.1	5.1	5.1
Difference in binder content, %	6.27	6.67	4.51

10.6 Sieve analysis

Sieve analysis was performed to determine the gradation of the aggregates extracted from each sample and the percent passing values were recorded as shown in Tables 52 through 54. These values were compared to the design gradation of the aggregates found in the mix design. The data show that the sieve analyses results matched the range of aggregates passing per mix design.

Table 52 Laboratory Sieve Analysis Results for Sample 1, 1 lb/Ton

Aggregate Gradation		%passing
Gradation (% passing)	2"	100
	1.5"	100
	1"	100
	0.75"	99.26
	0.5"	93.35
	0.375"	82.16
	No.4	62.84
	No.8	51.91
	No.30	27.52
	No.200	0.45

Table 53 Laboratory Sieve Analysis Results for Sample 2, 1 lb/Ton

Aggregate Gradation		%passing
Gradation (% passing)	2"	100
	1.5"	100
	1"	100
	0.75"	98.86
	0.5"	92.20
	0.375"	82.93
	No.4	63.81
	No.8	52.00
	No.30	27.52
	No.200	0.29

Table 54 Laboratory Sieve Analysis Results for Sample 3, 2 lb/Ton

Aggregate Gradation		%passing
Gradation (% passing)	2"	100
	1.5"	100
	1"	100
	0.75"	98.15
	0.5"	88.98
	0.375"	78.50
	No.4	62.50
	No.8	48.55
	No.30	23.87
	No.200	0.39

10.7 Discussion

The extraction of asphalt cement from the mixture by the centrifuge method is a very common. The research team is not aware of any similar work in the literature to retrieve the fibers. This limited special study demonstrated the successful process of extracting the fibers back from the asphalt mixture.

The asphalt cement contents for both 1 lb/Ton mix samples (1&2) were almost identical but they were lower than the design asphalt content (~6% different). The aggregate gradations were within the range of noted in the mix design.

As far as fiber content in both Sample 1 and 2, (both 1 lb/Ton mix samples), Sample 2 showed a higher fiber content by about 0.3 g than Sample 1. This difference may very well account for the large differences in the Flow Number test results. The Flow Number for Sample 2 was almost 100,000 loading cycles higher than that for Sample 1. The 0.3 g of fibers may not be a large value in terms of weight, but the quantitative difference in terms of the amount of fibers is substantial as shown in Figure 88, (the 0.3 g quantity is compared to a one cent coin).

Figure 88 FORTA Fibers (~0.3 g weight)

Sample 3, 2 lb/Ton mix, showed amazingly no variation between the mix design and determined values of fiber content. This sample was tested for triaxial shear strength test, and the sample test results were found to be more consistent with other tested samples. The different amount of fibers between the 1 and 2 lb/Ton mixes were detectable in this extraction process.

11. SUMMARY AND CONCLUSIONS

11.1. Summary

In coordination with FORTA Corporation and the City of Tempe, Arizona, an asphalt mixture overlay was placed at Evergreen Drive (East of the Loop 101 and North of University Drive) in Tempe. The designated road section within the construction project had three main asphalt mixtures: a control mix with no fibers added; a mixture that contained 1-lb of fibers per ton of asphalt mixture; and a mixture that used 2-lbs of fibers per ton of asphalt mixture. Mixtures for laboratory testing were sampled during construction and brought back to the Arizona State University (ASU) laboratories. Mixture preparation included compaction of 150 mm diameter gyratory specimens for triaxial testing, and beam specimens prepared and compacted according to AASHTO TP8 test protocols. The target air void level for the test specimens were those typically achieved in the field (about 7%). Rice gravities were determined for the loose mixtures, as well as thickness and bulk densities measured in preparation of the testing program.

Laboratory experimental program included: triaxial shear strength, dynamic (complex) modulus, and repeated load for permanent deformation characterization; flexural beam tests along with flexural toughness tests were conducted for fatigue cracking evaluation; Indirect diametral tensile tests to evaluate thermal cracking mechanism; C* Integral test to evaluate crack growth and propagation. The data was used to compare the performance of the fiber-reinforced mixtures to the control mixture.

11.2. Conclusions

11.2.1. Binder Characterization

- Binder consistency tests were conducted to develop information that will complement other mixture material properties such as fatigue cracking and permanent deformation.
- The conventional consistency tests (penetration, softening point and viscosity) were conducted on the virgin binder as well as two FORTA modified binders (the equivalent of 1 and 2 lb of fibers per ton of asphalt mix) to determine whether there were any unique characteristics or difficulties in handling the material.
- The modification process was only done using the Polypropylene fibers. Consistency tests across a wide range of temperatures were conducted according to the accepted American Society for Testing and Materials (ASTM) practices.
- There were no handling problems or difficulties in adding and mixing the Polypropylene fibers. Based on the test results and analysis, the viscosity-temperature susceptibility relationship at lower temperatures showed no changes from the original virgin binder, which is positive and desirable.
- At high temperatures, improved properties were observed in having higher viscosities; therefore, the modified binder is less susceptible to viscosity change with increased temperatures.

11.2.2. Triaxial Shear Strength Test

- Triaxial Shear Strength tests were conducted at 130 ^{o}F (54.4 ^{o}C). These tests provided the standard cohesion and the angle of internal friction parameters of the mixtures.

- When the three mixes were compared, the fiber-modified mixes showed higher values of "c" compared to the control mix. The 2 lb/Ton fiber-reinforced asphalt mix had the highest cohesion value owing to the reinforcing effect of the fibers.
- The 1 lb/Ton fiber-reinforced asphalt mix would yield the best performance based on triaxial shear strength laboratory tests.
- Both fiber-reinforced asphalt concrete mixtures showed higher residual energy compared to the control mix. This indicated that the fiber-reinforced mixes show higher resistance against crack propagation than the mixes without fibers.

11.2.3. Permanent Deformation Tests

Static Creep / Flow Time Test

- Static creep tests were conducted at unconfined test conditions only using at least two replicate test specimens for each mixture. The deviator stress used for loading was 15-psi (105 kPa) for all the test samples. The tests were carried out at 130 ^{o}F (54.4 ^{o}C).
- All tests were carried out on cylindrical specimens, 100 mm (4 inches) in diameter and 150 mm (6 inches) in height.
- Two important characteristics were observed for fiber-reinforced mixes when compared to the control mix. One was the endurance of the secondary stage and the second gradual (less) accumulation of permanent strain beyond tertiary flow for fiber-reinforced asphalt mix. Both were attributed to the presence of the Aramid fibers in the mix, as this behavior is not typically observed in conventional mixes.
- Fiber-reinforced mixes had higher Flow Time values than the control mix (over 9 times for 1 lb/Ton mix and 5 times for 2 lb/Ton mix higher than the control mix). This

indicates that fiber-reinforced mixes have the potential to resist permanent deformation better than the control mix. However, a lot of variability was observed between the FT values of fiber-reinforced mixtures within the same mixture. The reason for this variability perhaps could be due to inhomogeneous distribution and orientation of the fibers in the mixtures.

- The results of the slope parameter of the compliance curve showed that the control mix had 7 times higher slope than the 1 lb/Ton mix and 3 times than the 2 lb/Ton fiber-reinforced mix. Higher slope values are indicative of susceptibility of the mixture to permanent deformation.

Repeated Load Flow Number Test

- Repeated load / Flow Number tests were conducted at unconfined test conditions only using at least three replicate test specimens for each mixture. The deviator stress used for loading was 15-psi (105 kPa) for all the test samples. The tests were carried out at 130 ^{o}F (54.4 ^{o}C).
- All tests were carried out on cylindrical specimens, 100 mm (4 inches) in diameter and 150 mm (6 inches) in height.
- Similar to Flow Time tests, in the Flow Number tests, fiber-reinforced mixes when compared to the control mix showed an endurance of the secondary stage and a gradual (less) accumulation of permanent strain beyond tertiary flow. Both were attributed to the presence of the Aramid fibers in the mix, as this behavior is not typically observed in conventional mixes.

- The FN for 1 lb/Ton mix was 115 times higher than the control mix and 2 lb/Ton was 20 times higher than control mix. Also, between the fiber-reinforced mixtures, 1 lb/Ton mix had about 6 times higher FN than the 2 lb/Ton mix. But, the fiber-reinforced mixtures showed higher variability in the test results than the control mixtures and this perhaps may be due to the inhomogeneous distribution of the fibers in the mix.
- The results of the slope of the permanent strain curve showed that the slope of the control mix is higher than the fiber-reinforced mixtures. Higher slope values are indicative of susceptibility of the mixture to permanent deformation. Both the 1 lb/Ton and 2 lb/Ton fiber-reinforced mixtures had about the same value of the slope parameters.
- The control mix had a higher strain slope compared to the fiber-reinforced mixtures. Also the 1 lb/Ton mix had a higher strain slope than the 2 lb/Ton mix. Lower values of strain slope during the tertiary stage (when the sample has already failed due to higher shear stress) means that the mix has higher potential to resist this shear failure and shows a lower rate of permanent deformation and rutting during this stage.
- The fiber reinforcement, and in particular the Aramid fibers, provide unique resistance to the mix against shear failure beyond the tertiary flow point. This was evident from the monitoring the behavior of the fiber-reinforced mixtures in the tertiary stage of permanent deformation. With lower strain slopes of the fiber-reinforced mixes, the mixes are capable to store more energy than conventional mixes before and during tertiary flow.

11.2.4. Dynamic (Complex) Modulus Test

- The NCHRP 1-37A Test Method was followed for E* testing. For each mix, at least three replicates were prepared for testing. For each specimen, E* tests were conducted at 14, 40, 70, 100 and 130 °F for 25, 10, 5, 1, 0.5 and 0.1 Hz loading frequencies.
- E* master curves of all mixtures were constructed for a reference temperature of 70 °F using the principle of time-temperature superposition.
- The moduli of the 1 lb/Ton mix were higher than the control mix which indicates that fibers enhance the modulus of the mix and therefore its resistance to permanent deformation. However, the 2 lb/Ton mix test results did not show any improvement over control the mix. These results may indicate that the 1 lb/Ton mixture would be best, or optimum, for improved moduli properties.
- The modular ratios of 2 lb/Ton mix with respect to the control mix were all lower. The application of such dosage (2 lb/Ton) may be desirable for low temperature conditions, but it may not provide any additional advantage at the high temperature performance.

11.2.5. Fatigue Cracking Testing

Constant strain Flexural tests were performed according to the AASHTO TP8 and SHRP M-009 procedures to evaluate the fatigue performance of the FORTA Evergreen mixtures. Based on the test results and analyses, the following conclusions are made:

- The generalized fatigue models developed excellent measures of accuracy for both control and 1 lb/Ton mix, while the accuracy is fair for 2 lb/Ton mix.
- Comparing the initial stiffness for the FORTA mixtures at all test temperatures, it is noticed that the fiber-reinforced mixtures show slight higher stiffness values comparing

with the FORTA Evergreen control mix at 40 and 70 ºF while, for 100 ºF, the control mix shows a about 1.7 higher initial stiffness compared to fiber-reinforced mixtures.

- Comparing the fatigue life for the FORTA mixtures as obtained from the generalized model at lower and higher strain levels; At 150 micro-strains level (lower strain level) both fiber-reinforced mixture show higher fatigue life compared to the control mixture at different test temperatures especially the 1 lb/Ton mix; while at 200 micro-strains level (lower strain level), the 2 lb/Ton mixture shows the highest fatigue life followed by the control then the 1 lb/Ton mix.

11.2.6 Flexural Strength Test

- The improvement of flexural strength and corrected flexural strength of 1 lb/Ton mix is increased by 14 and 25% respectively. The opposite effect was observed for the 2 lb/Ton mix, the flexural and corrected flexural strength decreased probably due to the excessive amount of fibers in the mix. It was concluded that in terms of flexural properties, an optimum fiber dosage is 1 lb/Ton.
- High variability was observed in the results, especially for the modified mixes. The variability is mainly due to the variance of the fibers distribution and their orientation within the specimens.

11.2.7 Indirect Diametral Tensile Test

- Both indirect tensile cracking tests (Strength and Creep) were carried out according to the procedure described in the draft indirect tensile tests protocol for the Mechanistic Empirical Pavement Design Guide. The tests were carried out at three temperatures: 50, 32 and 14 ^{o}F.

- Comparing the control and fiber-reinforced asphalt mixtures compacted at the same air void levels, it was observed that the 2 lb/Ton mixture had higher creep compliance compared to both control and 1 lb/Ton mixtures at higher temperatures. Again, the 2 lb/Ton mix had higher creep compliance followed by 1 lb/Ton mix and then followed by the control mixture at lowest temperature zone.
- The tensile strength of all mixtures increased as the temperature decreased. Comparing the results of the tensile strength for both the control and fiber-reinforced (1 and 2 lb/Ton) mixtures, it was observed that both the 1 and 2 lb/Ton fiber-reinforced asphalt mixtures had about 1.5 times higher strength than the control mixtures. Traditionally, higher thermal cracking would be expected for mixtures with lower tensile strength values. In essence, fibers in the mix play a vital role in resisting thermal cracking in the HMA mixture. However, from the test results, there was not much difference between 1 and 2 lb/Ton mixtures.
- At 50 ^{o}F (highest temperature), the 2 lb/Ton fiber-reinforced asphalt mixture had the highest tensile strain at failure than 1 lb/Ton and control mixtures. It was observed that the 2 lb/Ton mix had about 35% larger strain than the other two mixes. At 32 ^{o}F, this difference was not significant (~15%) when control and fiber-reinforced asphalt mixtures were compared. The difference between the mixtures was about 10 % at the lowest (14 ^{o}F) temperature. Generally, the higher the tensile strain at failure, the less susceptible the mix to thermal cracking.
- Both fiber-reinforced asphalt mixtures had very similar trends for the temperature – energy relationship. The peak energy at failure was measured at the highest temperature and the lowest energy was observed at the 14 ^{o}F temperature. At the highest temperature

(50 ^{o}F), the highest energy is exhibited by the 2 lb/Ton mix followed by the 1 lb/Ton mix. At lower temperatures (32 and 14 ^{o}F), difference in energies is insignificant for both the fiber-reinforced mixes. When fiber-reinforced asphalt mixtures (both 1 and 2 lb/Ton) were compared with control mix, on an average fiber-reinforced mixtures had about 2 times higher energies than control mixes.

- The fracture energy decreased with increasing temperature for all the three FORTA mixtures. At the highest temperature (50 ^{o}F), the 2 lb/Ton mix exhibited the highest fracture energy followed by the 1 lb/Ton mix and then, followed by control mix. At the immediate lower temperature of 32 ^{o}F, both the fiber-reinforced mixtures had very similar total fracture energies but exhibited about 2 times higher energy than the control mix. The same trend of fracture energy results were observed at the lowest temperature (14 ^{o}F) as observed at 32 ^{o}F. At the lowest temperature of 14 ^{o}F, where susceptibility of crack initiation and propagation is the highest, it was observed that the fiber-reinforced asphalt mixtures had higher energy values than the control mix. Generally, lower thermal cracking should be expected as the energy at failure or fracture energy is increased.

11.2.8 Crack Propagation Test – C* Integral

Relationships between crack growth rates and C* values as well as slopes of crack growth rates for all the three mixtures of FORTA Evergreen project were developed. It was noted that the fiber-reinforced mixes, especially the 2 lb/Ton mix had higher C* and slope values than the control mix. This means that the fiber-reinforced asphalt mixtures have higher potential to resist crack propagation because of the reinforcement effect provided by the Aramid fibers; also, the higher the percentage of fibers, the better is the resistance of the mix to crack propagation.

11.2.9 Extraction of FORTA Fibers from the Asphalt Mixtures

- This limited special study demonstrated the successful process of extracting the fibers back from the asphalt mixture.
- The asphalt cement contents for both 1 lb/Ton mix samples (1&2) were almost identical but they were lower than the design asphalt content (~6% different). The aggregate gradations were within the range of noted in the mix design.
- The fiber content in both Sample 1 and 2, (both 1 lb/Ton mix samples), indicated higher fiber content in Sample 2 by about 0.3 g. This difference was shown to account for the large differences in the Flow Number test results obtained for both samples. The Flow Number for Sample 2 was almost 100,000 loading cycles higher than that for Sample 1.
- The 0.3 g of fibers may not be a large value in terms of weight, but the quantitative difference in terms of the amount of fibers is substantial.
- The different amount of fibers between the 1 and 2 lb/Ton mixes were detectable in this extraction process.

REFERENCES

Witczak, M. W., Kaloush, K. E., Pellinen, T., El-Basyouny, M., & Von Quintus, H. *Simple Performance Test for Superpave Mix Design*. NCHRP Report 465. Transportation Research Board. National Research Council. Washington D.C. 2002.

AASHTO Designation: T321-03. Determining the Fatigue Life of Compacted Hot-Mix Asphalt (HMA) Subjected to Repeated Flexural Bending.

SHRP Designation: M-009. Standard Method of Test for Determining the Fatigue Life of Compacted Bituminous Mixtures Subjected to Repeated Flexural Bending.

2005 City of Phoenix Supplement to the Maricopa Association of Governments Uniform Standard, Specifications and Details, City of Phoenix, 2005.

Witczak, M.W. and Kaloush, K.E., *Performance Evaluation of CitgoFlex Asphalt Modified Mixture using Advanced Material Characterization Tests*. Department of Civil Engineering, University of Maryland, College Park, Maryland, 1998.

American Society of Testing and Materials (ASTM). *ASTM D2493-01 Standard Viscosity-Temperature Chart for Asphalts*. http://www.astm.org

Monismith, C.L., Ogawa, N., and Freeme, C. *Permanent Deformation of Subgrade Soils Due to Repeated Loadings*. Transportation Research Record 537, Transportation Research Board, National Research Council, Washington, D.C., 1975.

Kaloush, K. E. *Simple Performance Test for Permanent Deformation of Asphalt Mixtures*, Ph.D. Dissertation, Arizona State University, Tempe AZ, May 2001.

Witczak, M. W. and Kaloush, K. E. *Performance Evaluation of Asphalt Modified Mixtures Using Superpave and P-401 Mix Gradings*. Technical Report to the Maryland Department of Transportation, Maryland Port Administration, University of Maryland, College Park, Maryland, 1998.

Biligiri, K. P. *Improved Method to Determine Tertiary Flow for Asphalt Mixtures,* Master of Science Thesis, Arizona State University, Tempe AZ, December 2005.

SHRP-A-404. *Fatigue Response of Asphalt-Aggregate Mixes*. Asphalt Research Program, Institute Of Transportation Studies, University Of California, Berkeley. Strategic Highway Research Program, National Research Council, Washington, D.C., 1994.

Harvey, J., and Monismith, C.L., Effect of Laboratory Asphalt Concrete specimen Preparation Variables on Fatigue and Permanent Deformation Test Results Using Strategic Highway Research Program A-003A Proposed Testing Equipment. Record 1417, Transportation Research Board, Washington, D.C., 1993.

Tayebali, A. A., Deacon, J. A., and Monismith, C. L., *Development and Evaluation of Surrogate Fatigue Models for SHRP.* A-003A Abridged Mix Design Procedure. Journal of the Association of Asphalt Paving Technologists Vol. 64, 1995, pp. 340-366.

Witczak, M.W., Mamlouk, M., and Abojaradeh, M. *Flexural Fatigue Tests*. NCHRP 9-19, Subtask F6 Evaluation Tests. Task F Advanced Mixture Characterization. Interim Report, Arizona State University, Tempe, Arizona, July 2001.

Rodezno, M. C., and Kaloush, K. E., Effect of Different Dosages of Polypropylene Fibers in Thin Whitetopping Concrete Pavements, Presentation at the 87th Annual Meeting, Transportation Research Board, Washington, D.C., 2008.

Mamlouk, M., and Mobasher, B., Cracking Resistance of Asphalt Rubber Mix versus Hot-Mix Asphalt, International Journal of Road Materials and Pavement Design, Volume 5, No. 4, 2004, pp 435-452.

Mehta, P. K., Monteiro, P. J. M., Concrete: Microstructure, Properties and Materials, McGraw-Hill Companies, New York, US, 2005, 121-168.

Trottier, J. F., and Banthia, N., Toughness Characterization of Steel Fiber Reinforced Concrete, Journal of Materials in Civil Engineering, Volume 6, No. 2, 1994, pp 264-289.

Sulaiman, S. J., and Stock, A. F., The Use of Fracture Mechanics for the Evaluation of Asphalt Mixes. Journal of the Association of Asphalt Paving Technologists, v 64, 1995, pp 500-533.

ASTM C1609/C1609M-06, Standard Test Method for Flexural Performance of Fiber-Reinforced Concrete, (Using Beam with Third-Point Loading), 4.02, 2006.

Eres Consultant Inc. Development Of The 2002 Guide For The Design Of New And Rehabilitated Pavement Structures – Stage A Report, NCHRP Project 1-37A Interim Report, ERES Consultants, Inc., Report prepared for the National Cooperative Research Program, Washington, DC, April 1999.

Method for Preparation of Triaxial Specimens (Test Protocol UMD 9808), "Superpave Models Team Inter-Laboratory Testing Manual." University of Maryland, College Park, MD, 1998.

Witczak, M.W., Bonaquist, R., Von Quintus, H., and Kaloush, K., "Specimen Geometry and Aggregate Size Lab Test Study", NCHRP Project 9-19, Task C. Team Report SLS-3, Arizona State University, Tempe, AZ, 1999.

Witczak, M.W., "Harmonized Test Methods for Laboratory Determination of Resilient Modulus for Flexible Pavement Design, Volume II - Asphalt Concrete Material", Final Project Report, NCHRP Project No. 1-28A, May 2003.Witczak, M.W., Roque, R., Hitunen, D.R., and Buttlar, W.G., “Modification and Re-calibration of Superpave Thermal Cracking Model”, Project Report, NCHRP 9-19 Superpave Support And Performance Models Management, Project Deliverable Task B, December 2000.

Roque et al, "Standard Test Method for Determining the Creep Compliance and Strength of Hot Mix Asphalt (HMA) Using the Indirect Tensile Test Device", Draft Test Protocol, AASHTO TP9-02, 2002.

S. J. Sulaiman and A. F. Stock, (1995), “The Use of Fracture Mechanism for the Evaluation of Asphalt Mixes”, AAPT, V64.

M. Mamlouk and B. Mobasher, (2004), "Cracking Resistance of Asphalt Rubber Mix Versus Hot-Mix Asphalt", International Journal of Road Materials and Pavement Design. V.5., 4, pp. 435-452.

Majidzadeh, K., et al.,) 1976), "Application of Fracture Mechanics for Improved Design of Bituminous Concrete," Volumes 1 and 2, Report FHWA-RD-76-91, Federal Highway Administration, Washington, D.C.

Abdulshafi, A.A., (1983), "Rational Material Characterization of Asphaltic Concrete Pavements," Ph.D. Dissertation, the Ohio State University, Columbus, OH, 1983.

Schapery, R. A., (1975), "A Theory of Crack Initiation and Growth in Viscoelastic Media I. Theoretical Development", International Journal of Fracture, Vol. 11, No. 3, 369-387.

Jenq, Y.S., and Perng, J.D., (1992), "Analysis of Crack Propagation in Asphalt Concrete Using Cohesive Crack Model", Transportation Research Record No. 1317, Transportation Research Board, Washington, D.C., p. 90-99.

Rice. J. R., (1968), Journal of Applied Mechanics, American Society of Mechanical Engineers, Volume 35, pp. 379-386.

Begley, J. W. and Landes, J. D., (1972), in Fracture Toughness, Processing of the 1971 National Symposium on Fracture Mechanics. Part II, ASTM STP 514, American Society for Testing Materials pp. 1-20.

Roberts, Freddy L., Kandhal, Prithvi S., Brown, Ray E., Lee, D., Kennedy, Thomas W., National Center for Asphalt Technology, Hot mix asphalt materials, mixture design and construction, second edition(1996).

Behrens, Micheal L., Dvorak, Bruce I., Woldt, Wayne E., Comparison of Asphalt Extraction Procedures: Implications of Hidden Environmental and Liability Costs, J. Transportation Research Board, Volume 1661(1999).

ASTM D 2172-95 Standard Test Methods for Quantitative Extraction of Bitumen from Bituminous Paving Mixtures, Annual Book of ASTM Standards, Volume 04.03.

Synolakis, Costas E., Zhou, Z., Leahy, Richard M., Determination of Internal Deformation Field in Asphalt Cores Using X-Ray Computer Tomography, Transportation Research Record No. 1526, Emerging Technologies in Geotechnical Engineering.

Wang, L.B., Frost J.D., Shashidhar, N., Microstructure study of WesTrack Mixes from X-Ray Tomography Images, J. Transportation Research Board, Issue 1767, 2001.

Masad,E., Jandhyala, V.K., Dasgupta,N., Somadevan, N, Shashidhar,N., Characterization of Air Void Distribution in Asphalt Mixes using X-ray Computed Tomography, Journal of Materials in Civil Engineering, Volume 14, Issue 2, pp. 122-129, March/April 2002.

Appendix A

1. Calculation of percentage of fibers in one FORTA bag

- [redacted]
- [redacted]
- [redacted]
- [redacted]
- [redacted]

2. Calculation of amount of fiber to be added in the Virgin Binder

- [redacted]
- [redacted]
- [redacted]
- [redacted]
- [redacted]